ROLE FOR THE ESCRT COMPLEX IN THE RELATIONSHIP BETWEEN NUTRIENT SIGNALING AND AUTOPHAGY IN *SACCHARYOMYCES CEREVISIAE*

by

Cierra Sing

A thesis submitted to Johns Hopkins University in conformity with the requirements for the degree of Masters of Science

Baltimore, Maryland

April, 2014

Abstract

Nutrient sensing is a vital cellular pathway used by all organisms to synchronize their cellular proliferation to correspond with their nutritional status through TOR (target of rapamycin) regulation. Therefore, when cells sense a low nutrient environment, cellular proliferation is halted and autophagy is initiated. Autophagy is a protective mechanism to allow cells to recycle, self-eat, their expended organelles for energy and survival. The relationship between nutrient sensing and autophagy is imperative for proper cellular growth, and when defective, can result in detrimental onset of various diseases. Results of a high-throughput screening of the yeast knockout collection of *Saccharyomyces cerevisiae* by Teng and the Hardwick lab identified knockout strains that lack components of the ESCRT pathway, which is conserved from yeast to mammals, resulted in a growth phenotype in low amino acid medium. These knockout strains failed to halt proliferation in low amino acid conditions, thus proceeded to outgrow wild type. Yeast screen also revealed a group of strains expressed phenotypes derived from a secondary mutation, rather than the original knockout gene. Although, tetrad dissections I executed on the ESCRT knockout strains confirmed the opposite, phenotypes were derived from the original knockout gene and were not due to a secondary mutations. This knowledge allows for a direct extrapolation of experimental results to be directly related to the gene deletions itself.

ESCRTs dynamic ability to curve membranes and create multivesicular bodies provides exceptional functionality and mobility for various cellular mechanisms. I hypothesize that there are more ESCRT functions to be uncovered. I propose that the multivesicular body biogenesis provides an excellent vehicle to relay nutrient signals to

properly correlate cell growth with its external and internal environments. When correlation is dysregulated improper cell growth occurs under nutrient improvished conditions. My research further investigated the phenotypes of ESCRT strains in relation to TOR and autophagy under nutrient deprivation reveals new insights into ESCRT functions. Evidence show ESCRT protein expression of subcomplexes I and III expressed a defect in TOR kinase regulatory activity due to the maintenance of Tor activity, and or increasing Tor activity during times of nutrient withdrawal. My data suggest new functions of yeast ESCRTs by possibly conveying nutrient signaling through multivesicular bodies. My studies on nutrient signaling emphasizes the critical role of this vital pathway for cellular organisms, and when defective can be detrimental to a cell's ability to effectively sustain life. Defects in TOR can lead to accelerated aging, cancer, and epilepsy. The links between ESCRTs, nutrient signaling, and human health are only just the beginning to be uncovered.

Dr. J. Marie Hardwick, Professor and Thesis Advisor

Dr. Valeria Culotta, Professor

Acknowledgment

I would like to thank the MMI department for giving me this wonderful opportunity to expand my knowledge as a future scientist. This experience has prepared me to succeed in my future endeavors. I personally want to thank Dr. Marie Hardwick. As my PI, she was extremely involved in my projects and provided incredible guidance through my investigation. Through all the conversations with Dr. Hardwick, each conversation opened my eyes to new exploratory experiments I could take and discovered what I am capable of as a scientist. Without her confidence in me, I would not have the courage to continue my scientific career and begin my PhD career. I would like to thank my friends I have made during this journey. Their supports and laughs helped through my lows. The memories created together will last forever. I appreciate the great bonds I have created with my colleagues at Hopkins. Lastly, I would like to thank my family. Through all the lows and all the highs my family has always been there to catch me or to celebrate with me. I appreciate all their hard work they did in order to provide me the opportunity to explore and achieve my academic dreams. I hope one day I can provide and support them as they once did for me. My love for my family runs deep and I can't imagine how I can complete this journey of my life without them.

Table of Contents

List of Tables

List of Figures

Chapter 1

Target of Rapamycin, Autophagy, and ESCRTs

Target of Rapamycin

Introduction

Yeast and mammalian cells have the ability to sense and adapt to the nutrient levels in the external and internal environment, and these process are vital to their survival. The ability and criticality of cells accessing their nutrient levels is important to adjust many cellular physiology processes accordingly such as, metabolism, cell proliferation, cell development, ribosome biogenesis, and transcription[1]. Even though yeast are unicellular eukaryotes, yeast have multiple pathways similar to mammalian cells to sense different types of nutrients including glucose and nitrogen levels[1]. Nutrient sensing abilities are conserved across species[2]. A main sensors of nutrient status is the target of rapamycin (TOR) pathway. TOR monitors both intra- and extracellular parameters and integrates the nutrient signals with cellular physiological signals to properly control its downstream effector pathways such as cell size, proliferation, and life span[3].

TOR was discovered to be the target of a small molecule inhibitor of cell growth, rapamycin, by studying mutations in TOR. Mutations in FKBP-rapamycin complex in TOR-1 and TOR-2 in *S. cerevisiae* resulted in rapamycin growth resistance[4]. Rapamycin, a potent antifungal metabolite produced from *Streptomyces hygroscopius*, was originally identified as macrocyclic lactone, but was later renamed to rapamycin upon the discovery that it inhibits mammalian cell proliferation and has immunosuppressive properties[5].

TOR is part of a conserved group of serine/threonine kinases from the phosphatidylinositol kinase-related kinase (PIKK) family[3].

Although TOR is evolutionary conserved, a remarkable difference occurs between the *S. cerevisiae* and mammals. Yeast encode two TOR genes (*TOR1 and TOR2)*, while higher eukaryotes only have one TOR gene (mTOR)[5–8]. Although structurally similar, TOR1 and TOR2, their functionality is not identical[9,10]. In addition to controlling cellular growth, TOR2 also controls actin organization, endocytosis and lipid biosynthesis[11]. Thereby, TOR2 gene is mainly responsible for TORC2 function allowing TORC2 to be functionally different from TORC1.

However, all TOR genes have similar domain structures, including HEAT repeats, FAT domain, FRB domain, kinase domain, and FATC domain[12]. Heat repeats at the N-terminus provide a binding region for TOR complex subunits[13]. The FAT domain and FATC domain are characteristic of the PIKK family[14–16]. The FRB domain is important because it is the binding region for FKBP-rapamycin, specifically in mammals, the FKBP12-rapamycin complex binds the FRB domain in mTOR[17,18]. Biochemical purification revealed that TOR proteins exist in two distinct protein complexes (TORC1), mTORC1 and TORC2 (TORC1 and TORC2 in yeast)[19].

TORC1

The yeast TORC1 complex consists of KOG1 (mammalian, Raptor), TCO89, LST8 (mLst8), and either TOR1 or TOR2[19–24]. An important characteristic of TORC1 is its sensitivity to rapamycin, although some targets of TORC1 are rapamycin-insensitive,

e.g. phosphorylation of TFEB by mTORC1[25,26]. TORC1 depletion experiments uncovered a role for TORC1 in coupling nutrients with cell growth[5]. TORC1 positively regulates cell growth in response to nutrients by inducing ribosome biogenesis, translation, metabolism, cell survival and nutrient import, thereby increasing biomass accumulation[3,5]. In addition, TORC1 has negative regulators such as stress and starvation, which leads to autophagy induction[3]. Specific amino acids from the media are capable of activating TOR, L-tryptophan, L-phenylalanine, L-arginine, and especially the branched amino acid L-leucine[27,28]. However, it still remains unclear exactly how amino acid sufficiency is sensed. Although speculations can be based off of other known nutrient sensing pathways like nitrogen pathway in yeast[1,29].

The subcellular localization of TORC1 is key in its function as a nutrient sensor. It has been observed that TORC1 is localized on the limiting membrane of the yeast vacuole and mammalian lysosomes[30–33]. The location of TORC1 on yeast vacuoles is logical because the vacuole is a major nutrient reservoir[29]. The location of TORC1 has an enormous influence on its nutrient sensing capabilities.

TORC2

The yeast TORC2 protein complex is composed of AVO1 (Sin1), AVO2, AVO3, BIT61 (Rictor), LST8 (mLST8), and TOR2 (mTOR)[19,20]. Majority of TOR2 is in TORC2 versus TORC1[29]. Unlike TORC1, TORC2 is rapamycin-insensitive due to AVO1 masking the FRB domain in TOR2[29]. In addition, TORC2 is required for actin cytoskeletal organization (mediating spatial control of cell growth), endocytosis, and lipid

biosynthesis[5,19,31]. This function is mostly derived from having TOR2 in this complex and TORC2 location. TOR2 is known to be rapamycin-insensitive and is known to distinct have the distinct ability to control cell growth to control organization of actin cytoskeleton, endocytosis, and sphingolipid synthesis[29]. Multiple studies confirm that TORC2 is near/at plasma membrane[29]. This location is consistent with TORC2 role in controlling the polarization actin cytoskeleton and endocytosis[29]. TORC2 function projects its ability to mediate spatial cell growth by controlling cell-cycle-dependent polarization of the actin cytoskeleton to direct newly made proteins and lipids to the growing daughter bud[29].

AVO1 and AVO3 bind to the HEAT repeats on TOR and are required for TORC2 integrity[5]. AVO2 is a non-essential protein that may recruit additional substrates to TOR[13,34]. However, AVO2 and BIT61 are unique to yeast[5]. Lst8 (Gβ-like propeller protein) binds to the kinase domain in TOR2 and is required for TOR2 kinase activity[13,19]. Unlike TORC1, upstream regulators have not been identified.

TOR is a Central Controller of Cell Growth

In summary, cell growth is heavily dependent on the nutrients for growth stimulation within the cell, and TOR (TOR1 or TOR2) is essential for cell growth. TOR1 primarily upregulates cell growth in nutrient replete conditions and TOR2 regulates the spatial growth via controlling polarization of actin cytoskeleton[29,35]. Cells maintain high rates of ribosome biogenesis, translation, initiation, and nutrient import when TOR is active under nutrient rich conditions[5]. The opposite occurs when cells are starved,

nitrogen depleted, rapamycin-treated, and or depleted of TOR1/TOR2 resulting in a dramatic downregulation of protein synthesis (decreased cell growth) and an upregulation of macroautophagy[5]. In conclusion, depending on cells growth conditions, rapamycin-sensitive TOR signaling can either promote anabolic processes or catabolic processes, and therefore, is influential on life span[3,5].

TORC1 is responsible for correlating nutrient sensing to ribosomal biogenesis. Henceforth, TORC1 promotes cellular growth under nutrient rich conditions. Mammalian and yeast TORC1 regulates translation via phsophorylation and activation of Sch9/S6K1 kinase and phosphorylation and inhibition of 4E-BP[5]. S6K1 belongs to the AGC family kinases, and therefore, requires phosphorylation of two sites to become active[5]. The activated form will phosphorylate a ribosomal protein on S6 to induce protein translation[29].

A well-studied kinase, Sch9, establishes the connection of TOR-dependent nutrient sensing to ribosome biogenesis[1]. Sch9, a kinase from the AGC family kinases, is the closest yeast homolog to mammalian TOR-regulated S6K1[1]. Overexpression experiments of Sch9 reveal its dual capability of inducing ribosome biogenesis genes while repressing carboxylic acid metabolism genes[1]. In response to nutrients, TOR directly phosphorylates Ser/Thr sites on the C-terminus of Sch9[30]. Under rapamycin treatment, carbon, or nitrogen starvation switch leads to the rapid desphosphorylation of Sch9, thus inhibiting translation and cell growth[1]. Therefore, phosphorylation of Sch9 by TORC1, or phosphorylation of S6 by Sch9/S6K1 is the best way to monitor TOR activity. Unfortunately, the exact mechanism used to relay nutrient signals to TORC1 still remains elusive[29].

TOR and its relationship with nutrient sensing

It was found that TOR alteration of yeast physiology was similar to that nutrient starvation, which started TORs relationship with nutrient sensing[36]. However, understanding how TORC1 senses and transduces nutrient signaling remains elusive, but is being actively researched. It was thought that TORC1 was the primary modulator for nitrogen response[1]. Although suggestive, further investigation concluded that TORC1 may respond to the quality of nitrogen source and is not the sole mediator to the nitrogen response pathway due to is difference in reverse recovery from nitrogen deprivation and rapamycin treatment[1]. Therefore, TORC1 nutrient target still remains a mystery. One possibility is through the EGO complex, which shares the same location as TORC1, vacuolar/lysosomal membrane **(Figure 1)**[33].

The yeast vacuole asserts itself as the location for both TORC1 and EGO complex. Since the yeast vacuole is the main nutrient reservoir, EGO complex couples amino acid signals to TORC1[33]. Under unfavorable nutrient conditions, or rapamyin treatment, cells enter a quiescence phase (G0)[29]. For a cell to exit the G0 stage properly requires the EGO complex[37]. In fact, amino acid activates TORC1 through a GTPase heterodimer of Gtr1 and Gtr2, which are found together with Ego1 and Ego3 making up the EGO complex[28]. Gtr1 and Grt2 act in combination to activate TORC1, but Gtr1 interaction with TORC1 dominates over Grt2[33]. Leucine starvation leads to destabilization of Grt1-TORC1 associations and results in reduced phosphorylation of Sch9, which mimics the dephosphorylation of Sch9 during starvation and rapamycin treatment[33].

TOR and autophagy

TOR has the unique ability to link reactions of both cellular proliferation and cellular degradation (autophagy), thereby using its ability to promote both anabolic processes and catabolic processes[3,5]. Its intimate relationship with autophagy promotes cell survival. Autophagy functions to sequester cytosolic material and deliver to lysosome for degradation to provide energy from recycled materials for the cell to survive[38]. In nutrient-improvished conditions autophagy is stimulated to promote cellular survival[5]. Not only is TOR a nutrient sensor and controls cell growth, but it also controls autophagy in yeast and higher eukaryotes[39]. Yeast TORC1 regulates macroautophagy by inhibiting protein kinase Atg1 by phosphorylating Atg13 and preventing Atg13 from interacting with Atg1, Atg17, Atg29, and Atg31, resulting in the inhibition of early activation steps of autophagy[40–42].

Autophagy

Introduction

Autophagy is a pivotal mechanism used to counteract the pressures exerted in hostile environments. This protective cellular mechanism involves sequestering cytosolic material and delivery of cargo to lysosomes for further degradation[38,43]. Stress conditions such as starvation, organelle damage, and microbe invasion, can induce autophagy[43]. Induction is coordinated with the inhibition of cellular proliferation under an autophagy stimulated cellular state. Autophagy is responsible for sequestering a variety of cytosolic materials such as damaged organelles, cytosolic proteins, and invasive microbes[43]. The degradative products of these materials are released back into the cytosol to recycle protein constituents to produce energy in order to maintain cell's viability in conditions of stress and provide protection for cells[44,45].

There are two main types of autophagy macroautophagy and microautophagy. Each type has specific purpose and a different mechanism to sequester its correlating cargo, but both have nonselective and selective properties[46]. In general, non-selective autophagy involves the turnover of bulk cytoplasm under starvation conditions, while selective autophagy involves sequestering specific targets damaged or superfluous organelles (mitochondria and peroxisomes) and invasive microbes[43,47,48]. Unlike macroatuophagy, microautophagy cargo sequestration involves direct invagination of the vacuolar membrane[29,49]. Macroautophagy is the most common autophagy pathway, which is conserved throughout eukaryotes. Macroautophagy involves sequestering cytosolic material into a double-membrane vesicle, autophagosomes[43]. After the formation of the autophagosomes, it is important to distinguish differences between

fungi/plant and higher eukaryotes for the rest of the autophagy pathway[50]. The main difference lies with the fusion of autophaosome. In yeast, the autophagosome fuses with the vacuole, rather than lysosome in higher eukaryotes[50]. An important autophagy feature exclusive to yeast is the fusion of the double-membrane autophagosome with yeast vacuole generating single membrane autophagic bodies (autolyosomes) within the vacuole[50]. Characteristic to yeast, the autophagic bodies can accumulate in the vacuole lumen when the cells have a genetic mutation that causes dysfunction in autophagy genes[50]. It is important to note that only autophagic bodies occur in yeast due to the massive size of a yeast vacuole compared to the higher eukaryote lysosomes. In higher eukaryotes, the autophagosomes move along microtubules, where they will fuse with the lysosome to form autolysosomes[51]. The general macroautophagy proceeds as the following steps phagophore assembly site (PAS), isolation membrane, phagophore, autophagosome, fusion with vacuole/lysosome, protein degradation, and protein recycle **(Figure 2)**. The PAS is a compartment or peri-vacuolar location where the nucleation of the phagophore initiates and exists only in a transient state[43,52–54]. The phagophore is a double-membrane structure that makes up the active component of macroautophagy and is involved in the initial cargo sequestration[55]. Unlike the phagophore, the autophagsome is the product of the completed phagophore extension[56,57].

Over 30 genes were found in yeast to be involved in the autophagy pathway[43]. There are 18 genes that make up the core autophagy proteins[43]. These 18 genes are genes shared amongst the different types of autophagy systems[43]. The core proteins can be furthered categorized into 4 different functional subgroups Atg1, Atg9 complex, PtdIns 3K complexes, and unbiquitin-like protein conjugation complexes[43].

Atg1

Atg1 is the initial autophagy complex responsible for induction of autophagosomal function[43]. The yeast Atg1 complex is composed of Atg1, Atg11, Atg13, Atg17, Atg29, and Atg31[43]. This Atg1 complex is the primary complex that regulates the magnitude of autophagy[40,41,58–60]. Atg1 is a Ser/Thr protein kinase, which functions both in autophosphorylation and phosphorylation of others; although, it's specific substrates are unknown[61]. Atg13 is a regulatory subunit that is required for optimal Atg1 kinase activity[40,43]. Lastly, Atg31, Atg17, and Atg29 exist as a heterocomplex. Specifically, Atg31 bridges the contact between Atg17 and Atg29[61]. Atg17-Atg31-Atg29 complex functions as a scaffold[43].

Atg1 is highly regulated in accordance to nutrient signaling by TOR or PKA phosphorylation[62]. In addition, its characteristic as an autophosphorylator acts as a self-regulator of its own kinase activity[62,63]. Similar to Atg1, Atg13 is regulated by TOR and/or PKA. TORC1 hyperphosphorylates Atg13 under nutrient-rich conditions and is desphosphorylated under starvation induced autophagy[64]. The hyperphosphorylated Atg13 by TORC1 inhibits its ability to bind to Atg1, Atg17, Atg31, and Atg29 **(Figure 3)**[41,42]. Therefore, desphosphorylation of Atg13 of the Atg13-Atg1 complex permits the formation of its complex with Atg17-Atg29-Atg31[43].

Atg17-Atg31-Atg29 complex functions as a scaffold for induction of autophagy by converting the PAS to an autophagy-specific PAS[65,66]. It was proposed that Atg17 may play a role in recruiting Atg proteins to PAS[61]. PAS is constitutively expressed under stable conditions marked with Atg11, but autophagy transition causes the function

of Atg11 to be replaced by the Atg17-Atg31-Atg29 complex[65,66]. Another role Atg1 complex is involved in is the retrieval of Atg9 from PAS[67].

Atg9

Atg9, transmembrane protein, complex exist between the PAS and peripheral sites[43]. This complex is considered the cycling system for membrane delivery to PAS from peripheral sites and is composed of Atg2, Atg9, and Atg18[43]. The Atg9 complex major role involves membrane delivery PAS for expansion into a phagophore after the Atg1 complex assembly to PAS[43]. Atg9 movement from peripheral sites to PAS, anterograde transport, depends on Atg11, Atg23, and Atg27[67–70]. Returning to the PAS from peripheral sites, retrograde movement, requires Atg1-Atg13, Atg2, and Atg18[43].

PtdIns 3-kinase Complex

Phosphoinositide 3-kinase (PtdIns3K) complex is important for staging the vesicle for nucleation[43]. Yeast PtdIns3K is composed of Vps15 (a putative regulatory protein kinase that is required for vps34 membrane association), Vps30/Atg6, Vps34 (the PtdIns3K), Atg14 and Atg38[71–73]**.** PtdIns3K complex is localized on the PAS[71–73]. It is presumed, a key role of this complex, generating PtdIns-3P, is to recruit PitdIns3P-binding proteins (Atg18) to PAS[43] .

Ubiquitin-like Complexes

There are two ubiquitin-like complexes within yeast, Atg8 (Atg3, Atg4, Atg7, Atg8) and Atg12 (Atg5, Atg7, Atg10, Atg12, Atg16)[43]. This ubiquitinated-like conjugated system functions in phagophore expansion[43]. Atg8 is initially synthesized with C-terminal Arginine, but is then cleaved by Atg4 (cysteine protease), exposing the C-terminal Glycine[61]. Agt7 then activates the processed Atg8, promoting the transfer to Atg3[61]. Atg3 is responsible for creating the covalent bond between phosphatidylethanolamine, PE, and Atg8, creating the lipidated form of Atg8 – Atg8PE localizing to the PAS[61] **(Figure 4)**. Atg8 also functions in cargo binding during selective autophagy[74]. However, it can also be recycled by Atg4 cleaving the amide bond between the Atg8 and PE, allowing for Atg8 to re-enter the conjugation process[61]. Atg8 has the greatest change in synthesis during autophagy and the amount of protein produced is correlated to the size of the autophagosome[75–77]. Therefore, Atg8 is a good marker and tracker for autophagic activity in yeast. It is also a good marker for mammalian autophagy activity, but rather, tracking the mammalian homolog of Atg8 – LC3 I and LC3II.

ESCRT complex

Introduction

The study of the endosomal sorting complex required for transport (ESCRT) is an active research field. ESCRT research is constantly uncovering new functions and mechanistic details. Its first molecular insight was discovered in *Saccharomyces cerevisiae*[78]. ESCRT protein form transient protein complexes that are responsible for multivesicular body (MVB) biogenesis from endosomes through the generation of intralumenal vesicles (ILV)[78]. The primary role of the ESCRT machinery is endosomal protein sorting through ILV of the MVB[78]. Sorting proteins in ILVs of the MVB is completed by 4 different subcomplexes (ESCRT-0, I, II, III), ATPase VPS4, and multiple accessory protein factors that assist during disassembly and recycling of ESCRTs[79]. Although the primary role of ESCRT machinery is endosomal trafficking, their functions of the ESCRT machinery extends well beyond [79]. In fact, their functions are dynamic and heterogenic between different species. Their extended function range from cellular signaling regulation to autophagy **(Figure 5)**.

ESCRT functions

ESCRTs are dynamic protein complexes involved in a large array of cellular functions. Sorting proteins in ILV has multiple purposes. ILVs of the ESCRT pathway are known to facilitate the delivery of proteins that are destined to degraded by the lysosome[78]. Most importantly, ESCRT endosomal trafficking is used as a regulatory mechanism for membrane and cytosolic proteins[78]. Thus, enabling its involvement in the

following cellular processes quality like control of misfolded proteins, cellular signaling regulation, apoptosis, TOR, biogenesis and release of exosomes, cytokinesis, and viral budding **(Figure 5)** [78]. Recent research has uncovered the importance of ESCRT in the regulation of cellular signaling.

Cellular Signaling

In general, from *Caenorhabditis elegans, Drosophila melanogaster,* mouse cells and human cells, ESCRT mutant cells fail to sort and degrade components of conserved signaling proteins like receptor tyrosine kinases, g-protein couple receptors (GPCR), transforming growth Beta receptors, Hedgehog receptors, Wnt, t-cell receptor, Toll receptors, and Integrins[80]. Therefore ESCRTs are signaling modulators, both positively and negatively, which occurs through multiple pathways. Signaling regulation is possible through signaling degradation, signaling sequestration, and receptor recycling[78–80]. As a result, failing to sort or degrade these signaling components results in dysregulated signaling in ESCRT mutant cells, which provide strong evidence of the requirement of ESCRT machinery for cellular signaling throughout species[80].

ESCRTs are required to efficiently modulate receptor tyrosine kinase signaling. ESCRTs mutants results in prominent alterations of cellular signaling by leading to receptor accumulation, ending in upregulation of cellular signaling[80]. Therefore, expression of ESCRTs can be negative regulators of receptor tyrosine kinase signaling by sequestering the signaling receptor and directing the receptor for lysosomal degradation, thereby restricting the receptor signaling pool size through MVB-lysosomal

degradation[79]. A common receptor tyrosine kinase that is dysregulated in ESCRT mutant cells is the epidermal growth factor receptor (EGFR). ESCRT-0 (*hrs) D. meleanogaster* mutant embryos, express developmental aberrations during active EGFR signaling by failing to undergo proper morphogenesis within the tracheal cells[80]. More importantly, it was observed down-regulation of ESCRT-1, *tsg101,* led to the reduction of signaling degradation and resulted in a sustained EGFR signaling in response to EGF within cultured mammalian cells[79]. *In vivo* experiments of *D. melangoster* cells with depleted ESCRTs led to increased EGFR activity and enhanced MAP kinases activity[79]. This example is a result of failed signaling degradation by ESCRTs. Failing to attenuate the signal, the active signal accumulates and the active signaling pool is maintained, concluding to a sustained signaling. Therefore, ESCRT-depleted cells result in active accumulation of EGFR signaling causing sustained signaling for cellular proliferation. Extended studies in ESCRT mutant in *D. melanogaster* epithelia revealed the loss of ESCRT function results in a strong non-autonomous cellular proliferation[79]. Meaning ESCRT mutant cells exhibit the mutant phenotype upon surrounding cells. The phenotype of non-autonomous cellular proliferation phenotype provides evidence of a close interactive link with cellular survival function of ESCRT mutant cells, which I will explain shortly. In conclusion, receptor tyrosine kinase, EGFR, signaling will be prolonged in cells with dysfunctional ESCRTs [81]. As a result, cells will have sustained proliferation.

ESCRT-mediated signaling attenuation also occurs in the innate immune system of toll-like-receptor (TLR) signaling. It has been shown that trafficking of intracellular TLRs is important for their signaling[82], especially critical when the endpoint is to activate

NFκB transcription factor[79]. Signaling regulation of TLR occurs in similar fashion of ESCRT modulation of receptor tyrosine kinase, signaling degradation. TLR4 recognizes certain pathogen-associated molecular pattern (PAMPS), such as lipopolysaccharide (LPS) of gram negative bacteria. TLR4 is ubiquitinated upon binding to LPS, which enables recognition by HRS of ESCRT-0 and promotes degredation[83]. ESCRT and its TLR4 signaling regulation is furthered strengthen by the inhibition of endocytosis and endosomal sorting of TLR4 resulting in an increase LPS-induced signaling[79].

Aside from signaling attenuation, ESCRTs have a positive influence on cellular signaling by promoting sequestration rather than degradation in the Wnt pathway. Wnt canonical signaling pathwayknown for its developmental embryonic regulation and its importance in stem cell maintenance[79]. Wnt signaling stabilizes β-catenin[80]. In unstimulated cells, β-catenin is phosphorylated by the cytosolic glycogen synthase kinsase 3 (GSK3) promoting its polyubiquination and proteosomal degradation[78,80]. In Wnt stimulated cells, active wnt signaling binds to its receptor, Frizzled, and co-receptor, LRP6, to inhibit the phosphorylation by GSK3 on β-catenin[79]. This allows β-catenin to accumulate in the nucleus and activate Wnt targeted genes. Until recent studies, Wnt-mediated receptor activation mechanism has been fleeting[79,80]. Studies are discovering in response to Wnt, GSK3 is sequestered within the ILV of MVB in an ESCRT dependent manner[80,84]. Sequestering GSK3 by MVB enables the stabilization of β-catenin permitting its transcription of Wnt targeted genes. However, the crosstalk between Wnt signaling and ESCRT sequestration of GSK3 mechanism remains elusive[79,80]. *In-vitro* experiments of *Xenopus* embryos, have shown GSK3 sequestration requires HRS and Vps4 ESCRT proteins[84].

Cell survival

Not only are ESCRTs involved in EGFR signaling but ESCRTs are also involved in cell survival. As I mentioned before, ESCRT mutant cells in *D. melanogaster* promote a non-autonomous cellular proliferation signaling; meaning that the surrounding cells of the ESCRT mutated cells will proliferate. Mutations in the ESCRT subunits of model organisms result in a prominent phenotype, cell-autonomous death through apoptosis[79]. *In vivo* studies suggest the lack of survival in ESCRT deficient cells is a reflection of cell death program activation upon the dysregulated response of cellular signaling[78]. Apoptosis induced by ESCRT deficiency was observed within the endoderm of the ventral region of HRS-/- mouse embryos[85]. Additionally, apoptosis induced by ESCRT deficiency was demonstrated in cells derived from mice with a conditional knockout of Tsg101[86]. Cells that fail to correct problems or are arrested too long at a cell cycle checkpoint will activate apoptosis and die[79]. Yet again, this prominent phenotype was confirmed by *D. melanogaster* clones of epithelial cells with ESCRT mutations within subunits I, II, or III, which failed to grow in response to active apoptotic pathway induction by caspase activation[87–92].

The mechanism of apoptosis induction in ESCRT-deficient cells remains elusive. There are at least two potential mechanisms to explain the phenotype, dysregulation of the inhibitor survival signal or direct induction of proapoptotic signaling[79]. The fisrt case seems plausible by the down-regulation of DiapI/IAPI, a critical caspase inhibitor, occurs in ESCRT mutant epithelial cells of *D. melanogaster*[91]. The direct proapoptotic induction mechanism can be is observed by the upregulation of proapoptotic regulators such as, Hipp/Mst1/JNK/Hid, in ESCRT mutant *D. melanogaster* cells[79].

Biogenesis and Release of Exosomes

Apart from the role of ESCRTs in cellular signaling, ESCRTs also have an alternative destination aside from lysosome degradation, the biogenesis and release of exosomes. Rather than having ILV of the MVB destined to the lysosome, MVB can fuse with the plasma membrane resulting of the release of ILV into the extracellular space[78]. Now ILV in extracellular space are now called exosomes[78]. Researchers are realizing that all cells have the potential to use the release of MVB-derived exosomes, as a form of intercellular signaling mediator[93]. Exosomes provide a protective pathway for transferring hydrophobic signals and cytoplasmic material between cells[78]. Although, what induces the switch between MVB destinations remains elusive. An example of the MVB destination switch is seen within antigen-presentation among dendritic cells and B-cells[94]. In immature cells, MHC II is targeted to the lysosome for degredation, but within activated cells, MHC II is secreted on exosomes[94]. Additionally, only degradative sorting of MHC II requires ubquitination, giving insight into mechanistic differences among MVB destinations[78]. Another potential molecular difference of MVB destination to exosomes, is the requirement of RAB GTPases, RAB27A and RAB27B, for targeting and docking of MVB to the plasma membrane[78]. Another example supporting a role for MVBs in biogenesis and release of exosome resides in brain-derived oligodendrocytes. In brain-derived oligodendrocytes, myelin membrane protein is known to be stored in MVB and, only upon neuronal contact leads to the induction of MVB exosome secretion[95]. MVB biogenesis and release of exosomes exemplifies ESCRT plasticity.

Viral Budding

ESCRTs also have a role HIV-1 budding. Viruses commandeer ESCRT machinery to assist their release from the host cell[96,97]. HIV-1 Gag proteins contain the same motif as HRS (ESCRT-0) in order to recruit Tsg101 - enabling the virus to bud away from the cell[98–101]. Binding of Tsg101 to gag proteins initiates the engagement of additional ESCRT components to proceed through the canonical ESCRT pathway[102]. The 2nd late domain of viral structural proteins interacts with Alix, which is part of the ESCRT-III accessory proteins[103,104]. Alix binding to 2nd late domain could also happen in conjunction with binding of Tsg101 to gag proteins[78]. It is important to note, not all ESCRT components are utilized in HIV-1 viral budding process. In addition to Tsg101 and/or Alix, only a subset of ESCRT III proteins, CHMP4A/B and Vps4A/B, are recruited during the final stages of budding process in mammalian cells[105].

Not only are ESCRTs important for virus budding, but ESCRTs are critical for the final abscission of virion particles[106]. The action of virus particles pinching off host plasma membrane requires ESCRT assistance. In general, ESCRT machinery is used to bend membranes until the neck can be scissioned[106]. Once HIV-1 gag proteins complete recruiting Tsg101 and Alix, ESCRT-III and Vps4 proteins are then recruited to budding sites within a few minutes, moments before the release of viral particles[106]. The ESCRT machinery is also involved in the abscission process of cytokinesis, but unlike cytokinesis, HIV-1 viral budding uses slightly different ESCRT machinery. For HIV budding, only two ESCRT-III subunits CHMP4 and CHMP2 are required to construct a 50 – 100 nm diameter ring-like structure in the membrane stalk, which connects the viral particle with host cell surface of CHMP4-or CHMP2-depeleted cells[105,106]. CHMP4/2 depletion prevents ESCRT-III filament to fully assemble, blocking viral budding for host

cell surface[106]. For successful membrane scission to release viral particles requires the AAA-ATPase Vps4. Vps4 is responsible for efficiently removing ESCRT-III subunits from the membrane stalk, allowing for the release of the viral particle[106]. However discrepancies remain in how Vps4 is involved in releasing ESCRT-III from membrane stalk. Some researchers proposed that the Vps4 could simply strip ESCRT-III from the membrane. Others have hypothesized that Vps4 progressively remodels ESCRT-III to a disassembly reaction[106].

Cytokinesis

Membrane abscission facilitated by ESCRT machinery also occurs in cytokinesis during the separation of daughter cells from one another. Although the ESCRTs are required for cytokinesis, not all subunits of the ESCRT canonical pathway are required. In fact, only ESCRT-I and ESCRT-III are essential, while ESCRT-0 and ESCRT-II are not involved[80]. This is evident by observing ESCRT-I and ESCRT-III-depleted cells arrest during the final stages of cytokinesis[80]. Proper completion of membrane scission during cytokinesis and ESCRT disassembly from target membrane requires AAA-ATPase Vps4[80,106]. It has been established that ESCRT-III and Vps4 are essential ESCRT components for proper separation of the two daughter cells during cytokinesis[106].

During the separation of the two daughter cells is the formation of a thin membrane stalk, which keeps both daughter cells connected[107]. The middle of the membrane stalk is defined as the midbody. At the midbody of the membrane stalk exists the binding of an

important protein for ESCRT recruitment, CEP55, a centrosomal protein[80,106]. CEP55 recruits ESCRT-I subtunit Tsg101 and Alix to the midbody[80,106]. At the midbody, Tsg101 forms large rings, roughly 1μm, on each side of the midbody[106]. In succession, the recruitment of ESCRT-III subunits (CHMP6/4/3/2/1) results in the formation of a long, ring-like filament along the Tsg101 ring, eventually creating a constriction site at opposing ends of membrane stalk is critical for membrane scission[80,106]. A dynamic characteristic of ESCRT-III filament is profound in its ability to first localize at the midbody Tsg101 ring, but later move towards the constriction zone[106]. The movement of ESCRT-III filament towards the constriction zone at the late stage of cytokinesis creates a 17nm helical filament, which can be observed on electron tomography of high-pressured frozen cells[108]. The top of the helical filament the ESCRT-III subunit CHMP1b recruits AAA-ATPase spastin, which is required to cleave microtubule bundles, severing the membrane abscission at the constriction zone[106,108,109]. The combination of ESCRT-III filaments and spastin and Vps4 are required for proper cytokinesis completion[108].

However, there are multiple models to explain the dynamic movement of ESCRT-III filament towards the constriction zone[108,110,111]. The first model describes the polymerized ESCRT-III subunits to project along the initial assembled ESCRT-III filaments at the midbody to the constriction[106]. As it moves towards the polar end of the membrane stalk, the dynamic ESCRT-III filaments somehow decrease their diameter, creating a gradual constriction of the membrane leading to the formation of the constriction zone[106]. An alternative model is Vps4 mediated. Vps4 remodels or breaks the initial ESCRT-III filament ring to generate a smaller ESCRT-III scission complex to migrate to the constriction zone[106]. ESCRTs involvement in membrane scission during

cytokinesis expresses the importance of ESCRTs in forming structured cellular machinery and displays the dynamic movement by ESCRTs.

Autophagy

ESCRTs may also have a role in autophagy. However, its role in autophagy varies between species. There are no known common ESCRT-autophagy mechanisms shared between all organisms. In fact, mammals and *Drosophila* share many common aspects, unlike *C. elegans*. *C. elegans* is the exception to the rule. They have their own particular ESCRT-mediated autophagy pathway. This displays another level of dynamics ESCRTs hold through the animal kingdom.

Autophagy is a widely used cell survival pathway during times of hardship and exists at a basal level. There are many forms of autophagy, but the main autophagy pathways are known as macroautophagy. To summarize, macroautophagy is responsible for sequestering (damaged) cytosolic components (including organelles) into double membrane vesicles known as autophagosomes. The autophagosome develops from the elongation of the phagophore, which requires the recruitment of Atg8/LC3 (yeast/mammals)[112]. The closure of the phagophore creates the autophagosome, in where a phosphatidylethanolamine (PE) conjugated (lipidated) form of Atg8/LC3II is present[112]. The lipidated form is the universal marker of autophagosomes[112]. There upon the autophagosome will merge with the vacuole/lysosome committing the cytosolic components for degradation. First insights of endosomes involvement with autophagy originally came from observations of ESCRT III mutants and its associations with

neurodegenerative disease, in addition to the discovery of protein aggregates expressing both ubiquitin moiety and p62 autophagic adaptor proteins[113–115]. Thus provides a foundation for the possibility of an alternative autophagy route where autophagosomes fuse with endosomes to generate intermediate vesicles called amphisomes in mammals[80,112]. Evidence that ESCRTs influence autophagy is provided by effects of ESCRT deficiencies in *C. elegans, Drospophila,* and mammals leading to an accumulation of atuophagosomes due to the inhibition of autophagic maturation[80]. Relevant to my studies, ESCRT proteins, which were discovered in yeast, have not found to be associated with starvation-induced macro-autophagy in yeast[80].

It is still unclear how exactly ESCRTs regulate macroautophagy[80]. Research revealed a common theme where ESCRT-0, ESCRT-I, and ESCRT-III are the most influential on the autophagy process[112]. Combined i*n-vitro* experiments of siRNA knockdown of Vps23/Tsg101 (ESCRT-1) or Vps24/chmp3 (ESCRT-III) cultured cells with co-localization, western blots, and electron microscopy images led to the observation of enlarged vesicular structures and their characterization[116]. Characterization of these enlarged vesicles are the appearance of large ubiquitin positive structures associated with endosomal markers, but are also associated with autophagic proteins, p62, and autophagosome marker, Alfy (autophagy-linked FYVE protein), and GFP-Atg8p/LC3[116]. EM images of *VPS23/tsg101* and *VPS24* depleted cells show presences of autophagosomes, amphisomes, but not autolysosomes[112]. Further analysis of autophagy activity results in expression of both the lipidated Atg8p/LC3II form and Atg8p/LC3 form - supporting the idea that ESCRT mutants inhibit the fusion of autophagosome with the lysosome[112]. In conclusions, ESCRT subunit depletion inhibit autophagic maturation,

which results in the accumulation of ubiquitin-positive aggregates in autophagosomes and amiphosomes[112]. Prevention of autophagosome maturation into autophaglyosomes is also impaired in Vps27/Hrs depleted cells[112]. Similarly, mice with mutated *VPS2/chmp2B* or depletion of *VPS32/mSnf7-2* subunits of ESCRT-III results in accumulation of both lipidated and non-lipidated forms of Atg8/LC3 auophagosomes[112]. One can conclude ESCRT-III dysfunction might interfere with fusion between autophagosomes and MVB[112]. The inhibition of autophagosome maturation, inhibiting lysosome fusion, leading to accumulation of autophagosomes with or without the additional accumulation of amphisomes provides one the main hypotheses of how autophagy is defective within ESCRT mutants[112].

The role of ESCRTs in autophagy in *C. elegans* provides further molecular insight of the relationship between ESCRTs and autophagy. Unlike mammals and *Drosophila, C. elegan* ESCRT mutants revealed an increase in the number of autophagosomes, but is not due to fusion blockage, rather it is due to the induction of autophagic flux indicated by western blotting[116]. Induction of autophagic flux is an alternative hypothesis to explain the link between ESCRT deficient cells and their autophagy phenotype**.**

Even though it is unclear how ESCRTs regulate macro-autophagy, ESCRTs involvement in microautphagy, endosomal microautophagy, is easier to comprehend. Endosome microautophagy selective delivers certain cytosolic proteins to vesicles of late endosome during MVB biogenesis[117]. Endosomal microautophagy does not require LAMP2A, lysosomal marker, but rather requires ESCRT-I (Tsg101), ESCRT-II components, and VPS4[117]. My thesis experiment will further explore the possibility of

yeast ESCRTs interaction with autophagy based on the unique phenotype arise from our labs yeast screening.

ESCRT Pathway

Introduction

The first insight of a vesicles containing ILVs was in 1950's by Keith Porter and George Palade. Not until almost 20 years later was the first molecule insight of MVB were uncovered in *Saccharomyces cerevisiae*. In 1980's and 1990's the laboratories of Emr and Stevens first identified "ESCRT" mutants to display a vacuole protein sorting (VPS) defect, classifying them as class E VPS proteins[118–122]. Extensive biochemical studies revealed these class E proteins were distinct from normal class E protein in that these proteins form distinct complexes that directly mediate cargo trafficking and were later named as endosomal sorting complex required for transport (ESCRT). In 1997 Babst and colleagues[123] first identified the AAA ATPase Vps4 as part of the ESCRT pathway. Vps4 is an integral component of disassembly complex (ESCRT-IV) that is responsible for dissociating ESCRT proteins from endosomal membranes[123]. Four years later, in 2001, yeasts ESCRT-I was characterized and was shown to engage in ubiquitinated cargo on endosomes and then sort cargo through MVB[124]. Then ESCRT II and ESCRT-III complexes were discovered and defined as important players of ubquitinated cargo delivery of yeast vacuoles[125]. ESCRT-0 was discovered later than the other ESCRT complexes. ESCRT-0 is critical for MVB biogenesis and functions in recruiting ubiquintinated cargo to endosomal membrane through its of FYVE domain[78].

Combining all findings suggests the ESCRT complexes are only present transiently on the membrane due to disassembly of ESCRT-III proteins by Vps4[126]. Biochemical studies propose the assembly of ESCRT machinery on endosomal membranes occur in a hierarchal fashion[127,128]. Starting with initial recruitment of ESCRT-0 and sequentially ending recruitment with ESCRT-III[127,128]. Multiple studies establish ESCRT proteins are responsible for constructing inward invaginations of the endosomes forming ILVs, which become the defining characteristic of MVB biogenesis. ESCRTs are extensively studied to understand the mechanism ESCRTs use to invaginate the membrane. Now more than 30 genes are involved in the ESCRT pathway (**Table 1)**[128]. Two categories can be used to categorize ESCRTS. Early-acting ESCRT complexes comprised of ESCRT-0, ESCRT-I, and ESCRT-II[128]. Lastly, late-acting modules that specifically function on membranes and is composed of ESCRT-III and ESCRT-IV[128].

ESCRT-0 Complex

ESCRT-0, the primary sub-complex to initiate the binding of ESCRTs to endosomes and recruitment of ubiquitinated cargo to be sorted through MVB. ESCRT-0 is a heterodimeric protein complex of Hrs and STAM1/2 (Vps27 and Hse1 in (**Table 1)**[78,129]. The two ESCRT-0 subunits interact at 1:1 ratio via anti-parallel coiled-coil structured formed by 2 domain-swapped GAT domains (GGAs and *Tom)*[129–131]. The heterocomplex dimer undergoes oligomerization on membranes generating a 2:2 heterotetramer[132]. 2:2 heterotetramer brings the two subunits together to create eight low

affinity ubiquitin binding motifs giving the avidity required for ubiquitin- dependent *in*-vivo cargo sorting[128]. Both subunits contain ubiquitin binding domains[128].

Hrs is the primary subunit involved in recruiting ubiquitinated cargo and localized to the endosome membrane. Hrs subunit contains multiple motifs, a VHS domain, FYVE domain, DUIM, PxxP, CC, and CB[78,128,129]. Each domain has plays a specific role in Hrs subunit function. The ubiquitin binding domain, DUIM, has a higher affinity for ubiquitin than its partner subunit, STAM1/2, because its potential to engage two ubiquitin molecules simultaneously[132,133]. In addition to DUIM domain, Hrs VHS domain also has the potential to bind to ubquitinated molecules, but at a weaker affinity[128]. The difference between the two ESCRT subunits lies within the expression of the FYVE (Fab-1, YGL023, Vps27, and EEA1) domain of Hrs[78,129]. FYVE domain is critical for localizing ESCRT-0 to endosomal membrane and initiating the ESCRT recruitment to the endosomes[78]. FYVE domain of Hrs binds to phosphatidylinositol 3-phosphate (PI(3)P), providing endosomal specificity and membrane recruitment[129,134]. The presence of the FYVE domain in Hrs categorizes ESCRT-0 recruitment to early endosomes[135]. Another primary responsibility of ECRT-0, recruitment of ESCRT-I, is carried out by the PxxP motif in the Hrs subunit[78,128]. The coiled coil domain (CC) is involved in the interface connection between the two subunits, Hrs and STAM[128]. Finally, the Hrs subunit also contains a clathrin-binding motif, CB[78,128]. The clathrin-binding motif enables ESCRT to bind with flat clathrin lattices that assemble on early endosomes[78,134,136].

STAM's motif are similar in that it shares with Hrs are the VHS, CC, and DUIM domains. VHS and DUIM domain associate with ubiquitin molecules, but at a weaker

affinity[137]. However, it does not have a PxxP or FYVE domain. Instead STAM contains SH3 domain that binds to deubiquitinases (DUBs) such as AMSH, USP8 and UBP4[78,128,138,139]. ESCRT-0 is responsible for recruiting ubiquitinated cargo to the endosomal membrane through its various motifs, but it is also important in recruiting ESCRT-1 to the endosome.

ESCRT-1

In subsequent fashion ESCRT-I is recruited in the ESCRT canonical pathway. ESCRT-I was the first complex to be identified in yeast and is a heterotetrameric complex composed of Vps23, VPS28, and VPS37, and Mvb12 (**Table 1**)[124,128,140,141]. Mammalian ESCRT-1 components are slightly different from that of yeast. They consist of Tsg101, Vps28, Vps37, hMVB12 isoforms, and recently discovered UBAP-1 isoforms (Mvb12-like protein)[142–148]. ESCRT-I subunits are in 1:1:1:1 stoichiometry ratio that generates an elongated 20nm long heterotetramer complex[142,143,146,147]. Crystal yeast structure revealed ESCRT-I structure to be composed of three subunits intertwined within a long coiled-coil stalk with a globular head group, which can engage in binding with ESCRT-0 and ESCRT-II[146,149]. However, the structure of metazoan ESCRT-I remains elusive.

Hrs carboxyl-terminus PxxP motif associates with Tsg101 via an ubiquitin E2 variant (UEV) domain of ESCRT-II enabling the recruitment of ESCRT-I to the endosomes[150–153]. Utilizing a different region aside from Tsg101 – Hrs interacting motif of the UEV domain is the region of the motif responsible for binding ubiquitin, but only at a low affinity in mammals[98,124,151,154,155]. Suggests ESCRTs role in ubiquitin-dependent

cargo sorting[128]. Yeast ESCRT-1 contains two ubiquitin binding domains, one in N-terminal of UEV domain of Vps23 and another one in C-terminal of Mvb12; together these contribute to ESCRT-I ability to bind and sort ubiquitin cargo into MVBs[148]. As mentioned before, yeast Mvb12 has been show to bind to ubiquitin and participate in cargo sorting, but, mammalian UBAP1 (Mvb12-like protein) expresses an ubiquitin binding characteristic[142,156,157]. The discovery of UBAP1 confirms the ability of ESCRT-I participation in ubiquitin-dependent cargo sorting.

UBAP1 binds to the central stalk of ESCRT-I through binding to N-terminal UBAP1-MVB12-associated (UMA) domain[158]. At the polar end of UBAP1, its C-terminal region contains three concatermerized ubiquitin-associated (UBA) domains to allow UBAP1 to bind to ubiquitin molecules[148]. UBAP1 depletion studies conclude the importance of UBAP1 to ESCRT-I function in MVB sorting because sorting requires the high affinity of ubiquitin binding activity that UBAP1 can provide, while other ESCRT-I components do not[148]. The discovery of UBAP1 has the potential to explain the structure of mammalian ESCRT-I**.** Lastly, Vps28 subunit of ESCRT-I contains a C-terminal domain (CTD), which functions to recruit ESCRT-I to ESCRT-II[128,129]. Together ESCRT-I and ESCRT-II are necessary requirements for inward budding of vesicles at the endosomal membrane[159].

ESCRT-II

ESCRT-II is next to be recruited to the endosome by ESCRT-1. ESCRT-II subunits forms a stable heterotetramer composed of Vps22 (Snf8, yeast), Vps36, and 2 copies of Vps25[160,161]. A defining characteristic of ESCRT-II is the structure formed by

its subunits. The heterotetramer forms a Y-shaped; Vps22 and Vps36 forms the base of the Y shaped and the two Vps25 form the arms of the Y **(Figure 6)**[128,162,163].

Vps36 subunit is an important ESCRT-II subunit, not only, to bind ESCRT-I, but also important strengthening the localization of ESCRTs to the endosomal membrane. The Vps36 contains Gram-like ubiquitin-binding in Eap45 (GLUE) domain, which is responsible for high affinity binding to PI(3)P[164–166]. A common aspect between both yeast and mammalian GLUE domains is that they share the ability to bind to ubiquitin and phosphoinositide [165,167,168]. The domain structure of yeast Vps36 and mammalian Vps36 differs by the presence of two Np14type zinc fingers (NZF) inserted into the yeast Vps36 GLUE domain[165,167,168]. Each NZF insert of the yeast Vps36 GLUE domain has a distinct function. One NZF insert is responsible for binding Vps36 to ESCRT-1 subunit Vps28 through the C-terminal domain (CTD)[166,168]. The second NZF insert is responsible for binding to ubiquitin, though with low binding affinity[133,165,167]. ESCRT-II would be categorized in the early-acing ESCRT machinery components[133,165,167].

Vps22 of ESCRT-II contains a conserved basic helical domain (HD)[128]. The helical domain associates with acidic phospholipids, and is required for ESCRT-II endosomal targeting[161]. Lastly, ESCRT-III Vps20 is recruited to ESCRT-II by binding to Vps25 two subunits through their winged-helix domain (WH2)[128]. The interaction of Vps20 and Vps25 WH2 domain occurs at a high affinity[128].

ESCRT-III

ESCRT-III has several interesting features. Firstly, it does not form a stable cytoplasmic complex. It creates polymerized filaments and promotes membrane curvature, but the mechanisms of ECRT-III in invagination of the membrane still remains

a mystery. The ESCRT-III complex is made out of four core components Vps20, Snf7, Vps24 and Vps2 [169]. Mammalian homologs of the four yeast core components are denoted as charged multivescular binding proteins (CHPMs), CHMP6, CHMP4, CHMP3, and CHMP2[129].

ESCRT-III monomers are localized in the cytoplasm where they are autoinhibited, which promotes a "closed state" [129]. The recruitment of ESCRT-III subunit Vps20 to endosomes by ESCRT-II induces Vps20 from closed state to active state[129]. When Vps25 forms the arms of the Y-shaped structure, binds the open state of Vps20 in ESCRT-III subunit, which then initiates the recruitment of the rest of ESCRT-III subunits to the endosomes. Vps20 then recruits multiple Snf7 subunits, which homo-oligomerizes[129]. Snf7 polymer formation is important for ESCRT-III to deform the membrane and create membrane invaginations. The Snf7 polymer is then capped by Vps24-Vps2[129]. However, there are multiple theories of the mechanism used by ESCRT-III to create invaginations in the membrane, such as theSnf7 classical oligomerization and dome model[129]. Snf7 also recruits adaptor proteins Bro1/Alix, responsible for stabilizing Snf7 filaments, and Doa4, deubiquitinating enzyme necessary for cargo deubiquitination[170,171]. After the recruitment of all ESCRT-III subunits begins the recruitment of Vps4-Vta1 complex (ESCRT-IV).

Vps4 Complex (ESCRT-IV)

Vps4 is required for ESCRT-III to disassemble properly[129]. The Vps4 complex is comprised of Vps4, Vta1, and Vps60[129]. Vta1 and Vps60 are considered to be "accessory" subunits of ESCRT-IV and they govern the interaction of Vps4 with

ESCRT-IV. ESCRT-III disassembly requires energy to dissociate from the membrane, which is provided by the AAA ATPase activity of Vps4[126]. Vps4 a multimeric enzyme binds to multiple ESCRT-III subunits through its Microtubule Interacting and Trafficking (MIT) domain[123,172]. It is important to note that Vps4 can exist in two states. In an ADP-bound state it exists as a monomer or a dimer, but when fully assembled it multimerizes into a stable dodecamer of two hexameric rings and a supercomplex with Vta1[123,129,173,174]. The multerimization of Vps4 initiates ATP hydrolysis, which is required for removal of ESCRT-III subunits from the membrane[129]. There are multiple theories of how Vps4 complex is involved in ESCRT-III invagination process (membrane scission).

ESCRT-III mechanism in creating membrane invaginations

Like classical vesicle budding, ESCRT-III subunits bind to lipid membranes electrostatically and some subunits can oligomerize[175–177]. When Vps25 recruits Vps20 and Vps20 recruits Snf7, Vps20 then nucleates two Snf7 homo-oligomers creating a ring or spiral that "encircles" the cargo[129]. After recruitment of Snf7, Snf7 oligomerizes to form rings, straight filaments or spirals of varying diameter[129]. However, Snf7 filaments are the best characterized[129]. Together, both Snf7 filaments and Vps24-Vps2 capping work together to deform the membrane surface. However, it still remains unclear about the mechanism used by ESCRT-III to narrow the ILV neck[129]. One theory is that Snf7 oligomers are naturally curving the membrane in favor to the ideal diameter, and as oligomerization processes the filaments narrows the diameter and the diameter is determined by the capping of Vps24-Vps2 subcomplex, which constricts ILV enough to promote scission[129].

The second model is based with the implication that the Vps24-Vps2 subcomplex acts as a central mediator[178]. Lata and her colleagues observed Vps24-Vps2 cylinder staked as rings or spirals; then cylinders form tapered ends decreasing in diameter end ending into a "dome" shape[129,178]. Together, Snf7 filaments followed by Vps24-Vps2 cylinder tapered ring stacking "capping", forms rings or spirals decreasing in diameters inside the neck forming ILV[179]. The dome mediating constriction of the ILV is determined by the protein affinity for the membrane, generating a curved membrane dome, which buckles to facilitate membrane scission[129]. Either theories, the Snf7 classical budding or the dome model, requires the recruitment of Vps4.

Vps4-Vta1 Function in Membrane Scission

Recent studies indicate that Vps4 might have other roles than to "recycle"/disassemble of ESCRT-III subunits after membrane scission[180]. Vps4 has been suggested to also have a role in the membrane scission process. In general, there are two hypotheses. One hypothesis involves Vps4-Vta1 complex to engage ESCRT-III following its assembly and provides the mechanical motor to help generate the constrictive forces needed for scission at the ILV neck[129]. In detail, Vps4-Vta1 oligomers bind to ESCRT-III subunits and mediate a stepwise disassembly motion along the ESCRT-III polymer, which can generate the force needed to mediate the constriction of the polymer into smaller and smaller rings, known as the "purse string" model[181]. The second hypothesis proposes the disassembly by Vps4-Vta1 is more of an explosive dramatic event. Vps4-Vta1 oligomer engages multiple ESCRT-III subunits while

simultaneously mediating a concerted disassembly of ESCRT-III oligomers resulting in a drastic removal of the ESCRT-III complex[129]. The removal of the ESCRT-III complex at once might cause the ILV budding to destabilize the curved membrane leading to buckling and scission[129].

Table 1

ESCRT Complex	Yeast Protein	Mammalian Homolog
ESCRT-0	Vps27	Hrs
	Hse	STAM1/2
ESCRT-I	Vps23/Stp22	Tsg101
	Vps28	hVps28
	Vps37/Srn2	Vps37 A,B,C
	Mvb12	hMVB12 A,B
ESCRT-II	Vps36	EAP45
	Vps22/Snf8	EAP30
	Vps25	EAP20
ESCRT-III	Vps20	CHMP6
	Snf7	CHMP4 A,B,C
	Vps24	CHMP3
	Vps2/Did4	CHMP2 A.B
Vps4 complex (ESCRT-IV)	Vps4	SKD1
	Vps60	CHMP5

Table 1 - Table categorizing all ESCRT components in yeast and mammalian homologues.
A table that categorizes all the components of ESCRT proteins into their prospective complexes. Table lists both metazoan proteins and their yeast homologs.

Figure 1

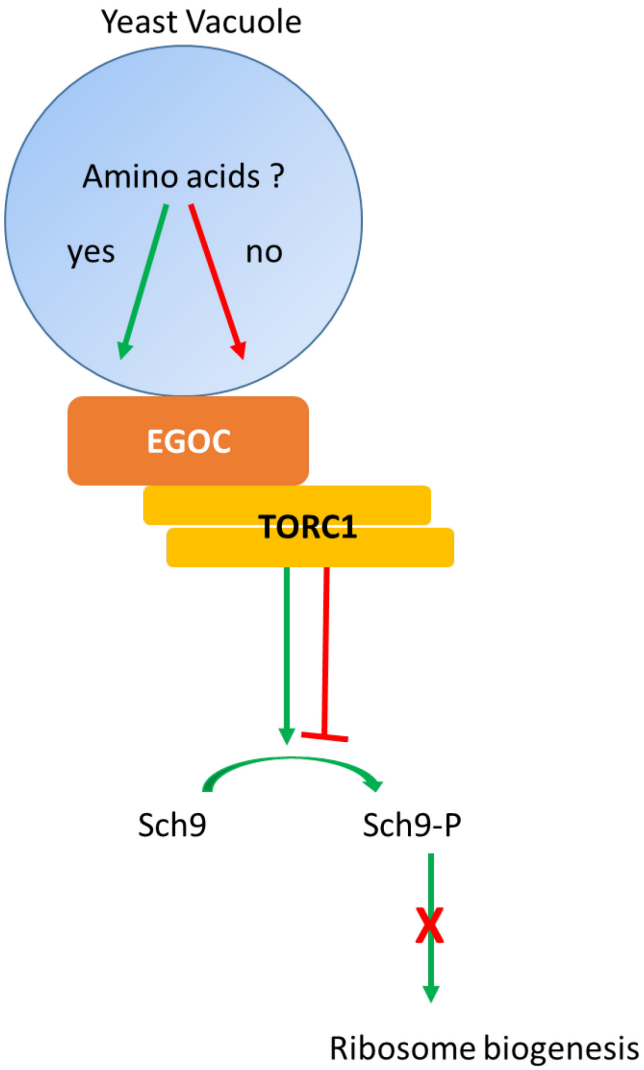

Figure 1 - EGOC and TORC1 interaction schematic
Schematic displaying the potential interaction between EGOC and TORC1 relaying amino acid signaling.

Figure 2

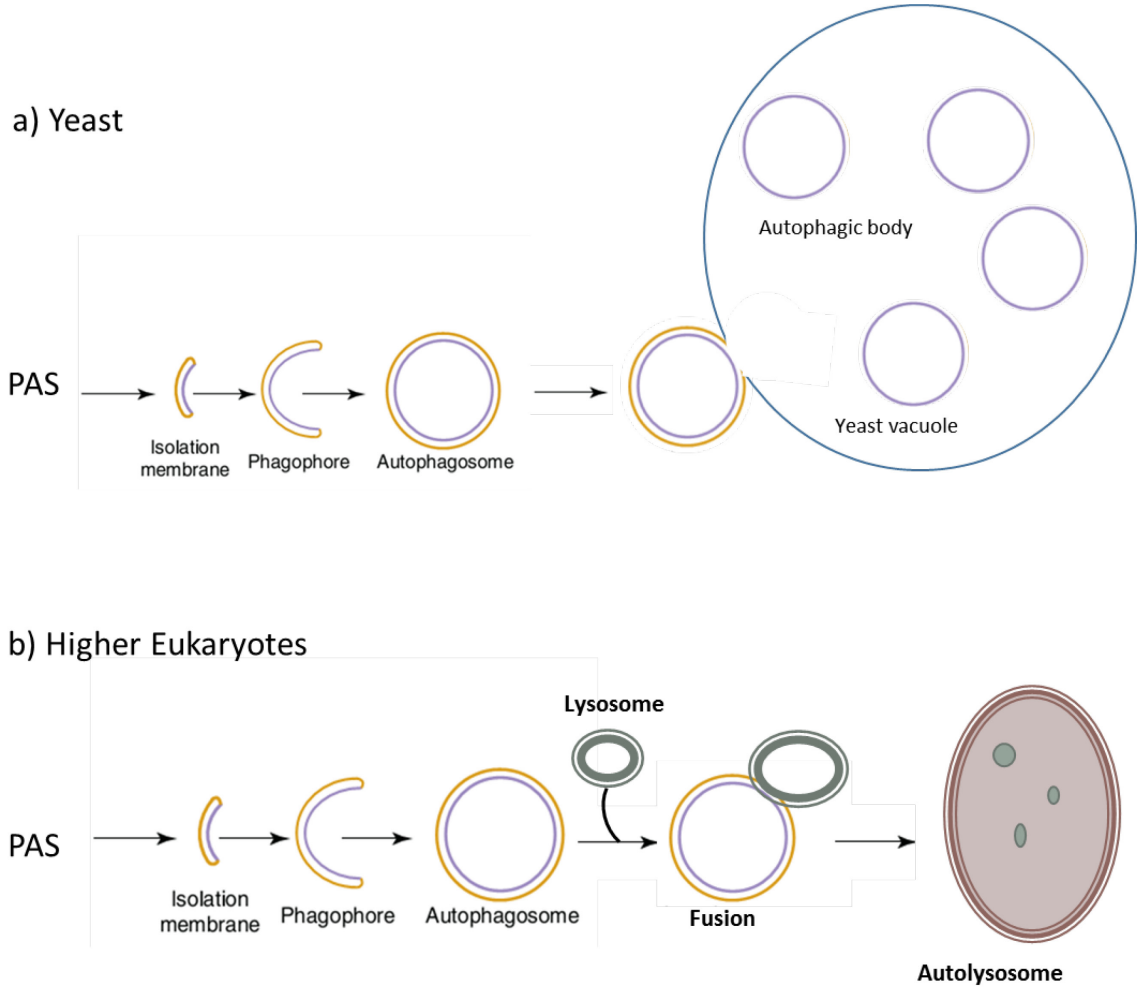

Adapted from McEwan and Dikic, 2011; Klionsky and Eskelinen, 2014

Figure 2 - Macroautophagy schematic
Schematic depicting the overall macroautophagy process.

Figure 3

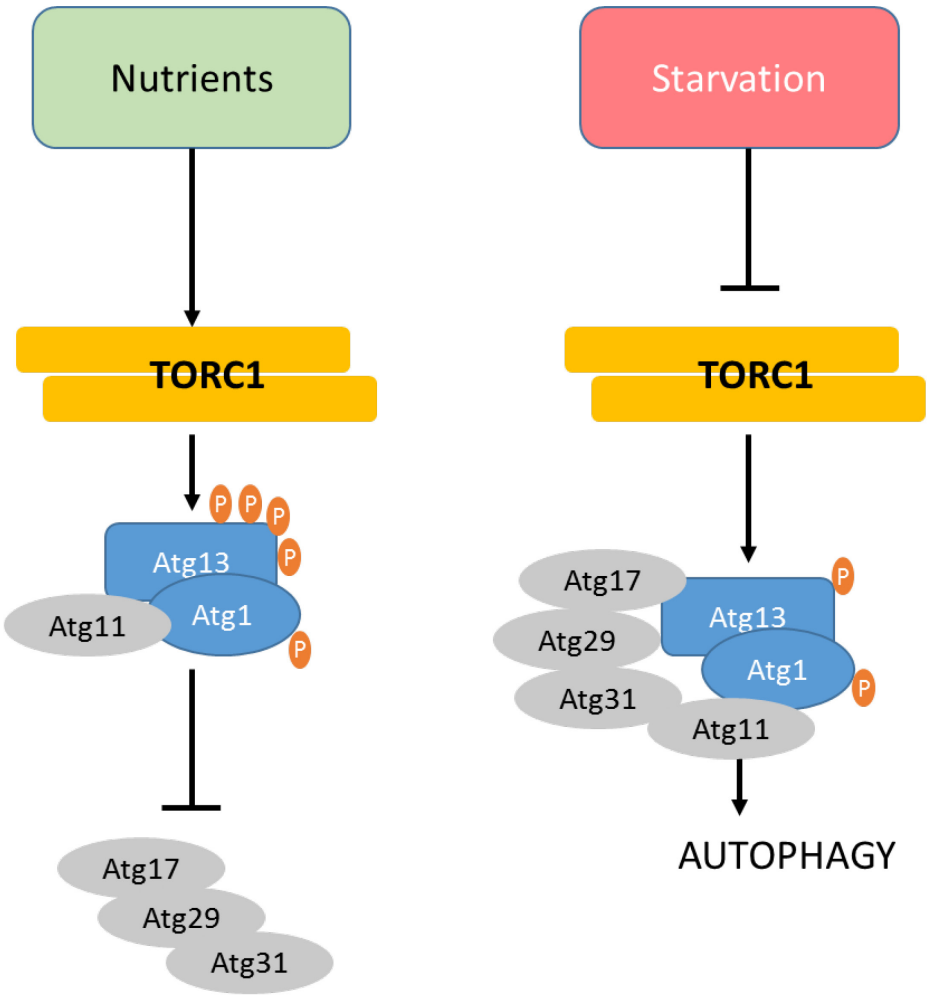

Adapted from McEwan and Dikic, 2011; Klionsky and Eskelinen, 2014

Figure 3 - Nutrient rich vs nutrient poor environment within TOR and autophagy responses.
Nutrient rich environments leads to a negative regulation of autophagy Atg1-Atg13 complex by TORC1 phosphorylation. Phosphorylation on the Atg1-Atg13 complex prevents it interaction with Atg17-Atg29-Atg31 complex; thus, preventing the initial steps of autophagy, autophagosome initiation.

Figure 4

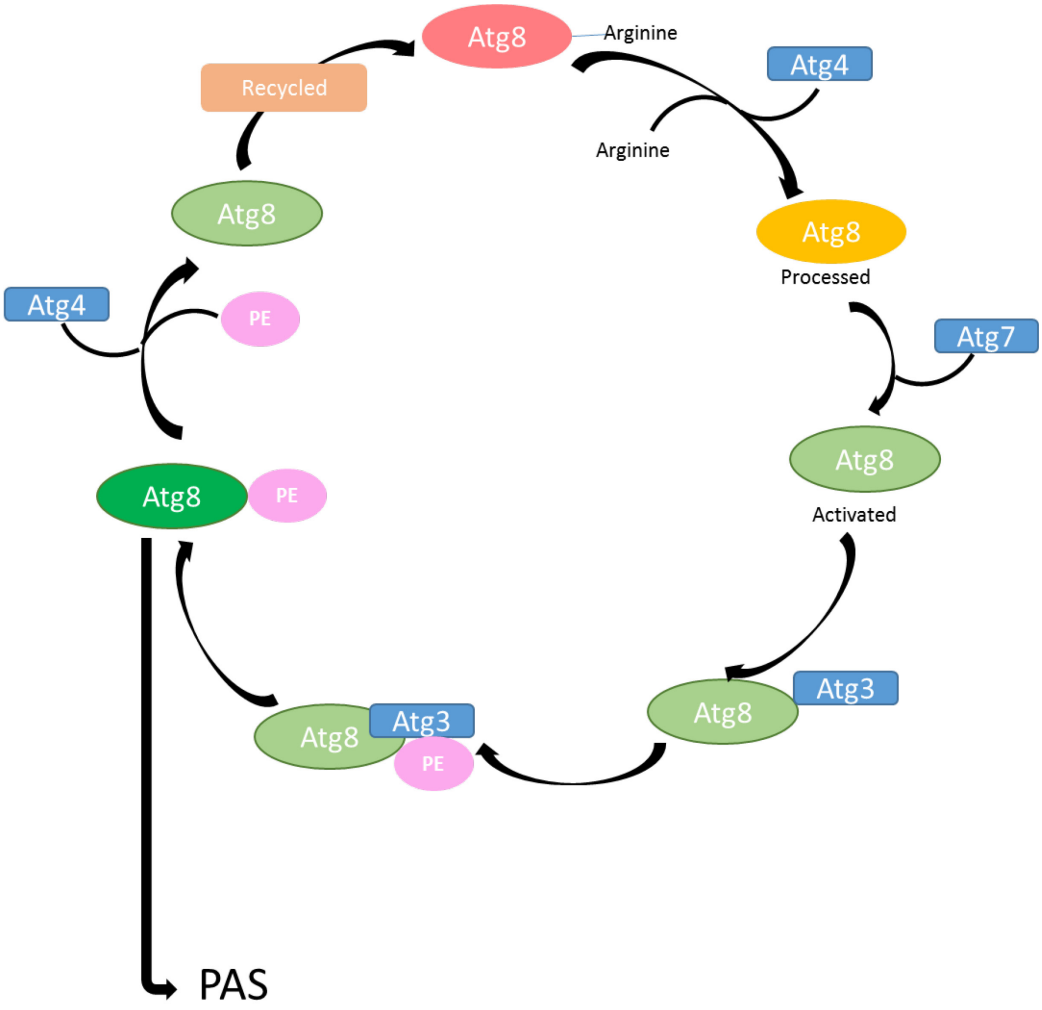

Figure 4 - Lipidated process of Atg8.
Yeast Ubiquitin-like conjugated signaling pathway. Atg8 is initially cleaved by Atg8 resulting in the processed form of Atg8. Active form of Atg8 then binds to Atg7, which activates the process from of Atg8 to initiate the transfer to Atg3. Atg3 is responsible for creating a platform for formation of a covalent bond between PE and Atg8; thus, concluding to a lipidated (conjugated) Atg8 form. This process is yeast representation of the mammalian lipidated of LC3I into LC3II during autophagy.

Figure 5

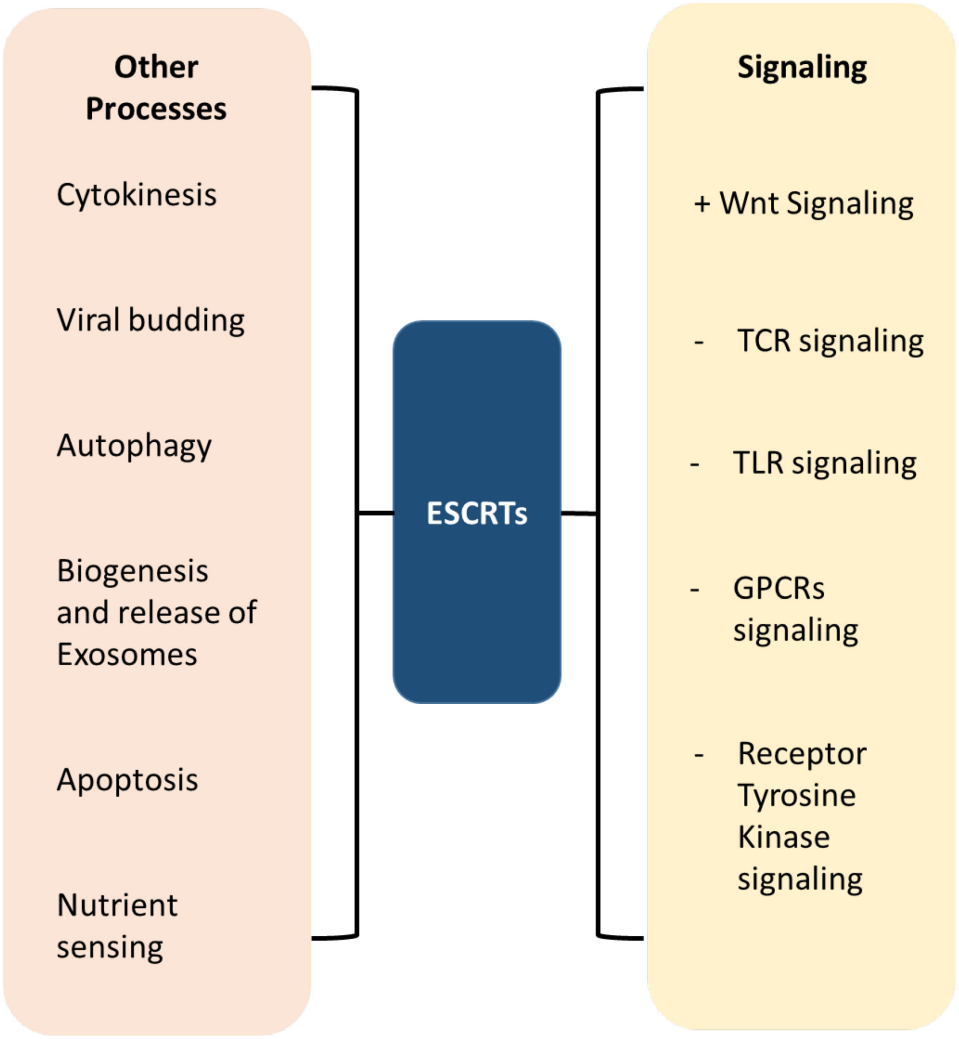

Figure 5 - Summary of all ESCRTs functions.
Summary of ESCRTs dynamic ability in different cellular processes, ranging from signaling to autophagy

Figure 6

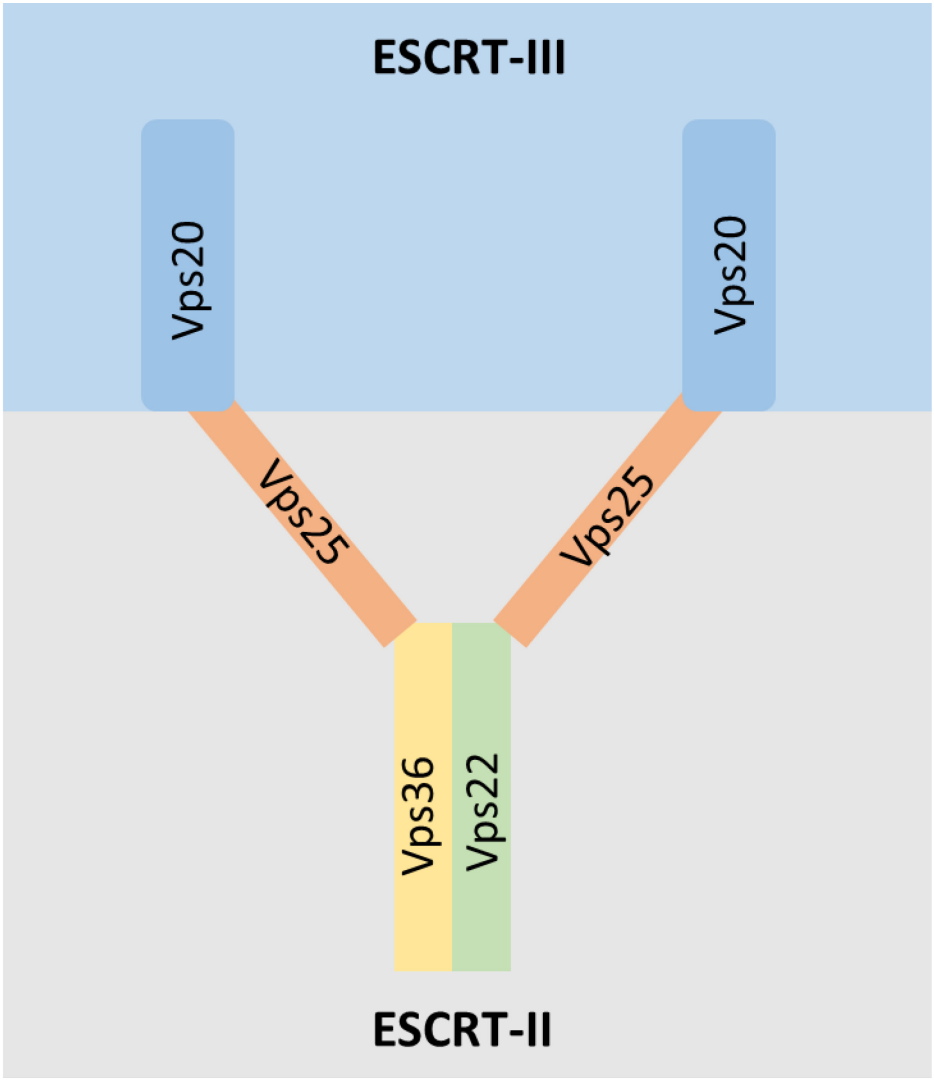

Figure 6 - ESCRT-II diagramed protein structure.
ESCRT-II forms a unique Y-shaped protein structure. Vps22 (hEAP30) and Vps36 (hEAP45) create the base for the Y-structure, Vps25 (hEAP20) create the two arms of the Y-structure that bind to Vps20 of ESCRT-III.

Chapter 2
Evidence ESCRTs may mediate the link between nutrient sensing and autophagy through the TOR pathway

Introduction

My thesis project was derived from the results of a high throughput screen of the yeast knock out collection to identify novel regulators of cell death, amino acid sensing and the TOR pathway by the Hardwick lab[182]. The yeast knockout collection is a collection of about 5,000 yeast strains with single gene deletions (knockouts) of non-essential genes. Earlier studies in our lab revealed that the cell death-sensitivity and amino acid sensing-defective phenotypes of Δ*fis1* strain were not a direct consequence of *FIS1* deficiency, but instead were due to an acquired secondary mutation within *WHI2* gene[182,183]. The phenotype caused by the secondary mutation was over growth in low amino acids conditions compared to wild type[182]. However, three of four independently derived Δ*fis1* strains had also acquired unique secondary mutation in the *WHI2* gene[182,183]. When functioning properly, cellular proliferation should be inhibited under conditions of low amino acids. Low amino acids triggers inactivation of TOR/mTOR, which relieves the suppression by TOR/mTOR on autophagy resulting in autophagy initiation. Therefore, this relationship between autophagy and nutrient-sensing is key for proper cellular function. This overgrowth phenotype and sustained Tor activity of the *whi2* mutant strain implies a role for *WHI2* in either amino acid sensing negative regulation of TOR or induction of autophagy[184,185] suggests that the possible dysfunction is either amino acid sensors or TOR regulators[182]. Therefore, our lab conducted a genome-wide screen for strains that exhibit strong overgrowth phenotypes on low amino

acid medium to search for potential regulators of nutrient sensing. Screening the yeast knockout collection led to the discovery of 751 yeast strains with the overgrowth phenotype[182]. Two additional parameters were included in the same overgrowth screen in yeast cell death (heat ramp assay) and sensitivity of the low amino acid overgrowth to rapamycin[182,186]. They reasoned that the cell death/survival and growth control are perhaps the most important determinants for driving genome evolution. Therefore, they applied heat to yeast strains as a source of stress to induce cell death, and to assess the role of TOR in the overgrowth phenotype, they simultaneously screened with [182]. These studies identified 259 different knockout strains among the 751 that shared all three phenotypes of *WHI2* mutants. The strains with this *whi2-like,* "triple phenotype group", are heat ramp-sensitive, overgrowth on low amino acids, and this overgrowth is rapamycin sensitive[182,183]. Further genetic analysis divided this group of 259 "*whi2*-like" triple phenotypes into two subgroups, those with triple phenotypes due to the knockout gene itself and those with triple phenotypes due to a secondary mutation [182]. The remaining members of the 751 group contains, 492 knockout strains with overgrowth on low amino acids, but without heat sensitivity, and/or rapamycin resistant-overgrowth[182]. Strikingly, these 492 strains were enriched in ESCRT genes, with 13 of the 14 core components of the ESCRT pathway, when deleted, exhibited low amino acid overgrowth **(Figure 7)**. The one ESCRT component that was not captured by the yeast screen, *Δhse1,* which could possibly have its overgrowth phenotype masked by secondary mutations. For example, overgrowth of Δ*atg6* is caused by the loss of *ATG6* itself, but a secondary mutation restores the overgrowth phenotype back to the normal (slower) growth phenotype[182]. The results from this screen are diagrammed in **(Figure 8).**

In conclusion, we know that Whi2 must be necessary for nutrient sensing and/or for responding to low nutrients. Therefore, the other 492 are potential candidates for factors working in the same pathway. It is important to understand the significance of this group by its capturing of 13/14of the ESCRT core components. Therefore, I investigated the role of ESCRTs in nutrient sensing and potentially. It known that there is a link between TOR and autophagy in mammals and yeast. In addition, there is evidence in mammals for the involvement of ESCRTs in autophagy, but this is not yet reported in yeast[112]. However, there have been suggestions that ESCRTs are involved in the TOR pathway, but the evidence thus far is weak[187,188]. My research is based on uncovering ESCRT interaction with TOR pathway and autophagy within yeast.

Material and Methods

Yeast Strains and Media

All yeast strains used have a BY4741 background **(Appendix i)**. YPD liquid medium recipe contained 2% peptone (Peptone-Y, MP Biomedicals), 1% yeast extract (Fisher Scientific) and 2% glucose (Fisher Scientific). YPD agar plate were made by adding 2% agar (BD) in the existing liquid YPD medium recipe.

All low amino acid liquid medium and dropout liquid medium contained 0.67% of yeast nitrogen base without amino acids (MCP), 0.2% glucose (Fisher Scientific), and 0.62 grams dropout mix for SCD $_{ME}$ and 1g amino acid dropout mix for all other dropout, selective, media (**Table 2).** Low amino acid liquid medium and selective media agar plates were made by adding 2% agar (BD) in liquid medium.

Tetrad Dissection and Tetrad analysis

Tetrad Dissection

Tetrad dissections began with a backcross the strain of interest from the yeast knockout collection (*BY MATa*, BY4741 background) with wild type BY4742 (*MAT*α) on rich media agar plates (YPD plates) and incubated at 30°C overnight **(Figure 9)**. The diploids were then selected on a selection plate (SCH_{csh}-MET-CYS-LYS) that incubated at 30°C for 2 days. A single colony from diploid strain was picked to be inoculated in 2ml of YPD liquid medium and incubated at 30°C overnight. The overnight cultures were then diluted to OD_{600} of 0.2 in 2ml of fresh YPD and incubate at 30°C until reach mid-log phase with an $OD_{600} \cong 0.5$ to recover the yeast. Yeast cells were then centrifuged at 13,000 RPM for 1 minute, washed with sterile ddH_2O, and resuspended in 2ml sporulation medium (1g/100ml potassium acetate, 50nM uracil, 50nM adenine, 75nM histidine and 500nM of leucine). Yeast were further incubated on rotator at room temperature for at least 4 days to allow for efficient sporulation. Although, this incubation might vary depending on the sporulation efficiency of the yeast strain. After efficient sporulation, 100µl yeast samples were centrifuged at 13,000 RPM for 1 minute and resuspended in 100µl of 1 M sorbitol. In order to digest yeast cell wall 3µl of zymolyase stock solution (20mg/ml in 1M sorbitol) was added and then incubated in 30°C water bath for 5 minutes. The digested samples were then diluted 1:3 in 1M of sorbitol and streaked on an YPD plate with sterilized metal loop. Tetrads were then dissected using a glass fiber needle under a microscope (Axisoskop 40, 10X objective lens) and 4 spores were placed individually on the same YPD plate. After plating the

individual tetrad spores, the tetrad plate was incubated for 2 days at 30°C to allow the spores to grow into colonies.

The tetrad spores were then genotyped by plating on selective media. First, spores were inoculated in 200µl YPD in 96-well plates for 48 hours. Tetrad verification was completed by spotting 3µl of liquid cultures on the following plates SCD_{csh}-MET-CYS and SCD_{csh}-LYS to assess auxotrophic markers and YPD + G418 plate to verify *KanMX* cassette (knockout gene replacement). Then mating types were then identified by crossing strains with 3µl of tester-*MATa* and tester-*MATα* strains, which were then replica plated on SD plates. Yeast plated on SCD_{csh}-MET-CYS and SCD_{csh}-LYS and YPD + G418 plates were incubated for 1 day at 30°C and scored for growth. Replica plates were incubated for additional day at 30°C and then scored. Then spores were tested for triple assay (Heat Ramp, low amino acids +/- rapamycin) to analyze the genetic linkage between phenotypes and the knockout gene.

Heat-ramp cell death assay

Heat-ramp cell death assay developed my Xinchen Teng was used to ascertain the yeast sensitivity to a death stimulus upon tetrad spores[186]. The tetrad spores were then incubated in YPD for 48 hours incubated and the incubated tetrads liquid culture was diluted 10-fold. After the 10-fold dilution, the culture was then heated by thermocycler at a continuous heat ramp for 20min from 30°C to 62°C. 5µl of the treated cultures were spotted on YPD square plate at 1:1 dilution (the initial 10-fold dilution) and an additional

1:5 dilution. This plate was then incubated at 30°C for 2 days and scored for levels of growth. After the 2 day incubation, images were then obtained of each plate for archives.

Low amino acid +/- rapamycin assay

After the 48 hr incubation of tetrad spores in liquid YPD, the liquid culture was diluted 1:10 and 1:50 with ddH_2O. 5µl of diluted yeast were spotted on low amino acid medium (SCD_{ME}) and low amino acid medium with 2.5nM rapamycin plates. Both plates were then incubate 30°C for 3 days and scored for levels of growth. After the 3 day incubation, images were then obtained of each plate for archives.

Yeast Transformation

ESCRT mutant strains transformed with GFP-Atg8 plasmid was conducted by the following method. First, grew an overnight yeast culture of mutant strain in 2ml of YPD, 14 – 15 hours. Diluted the liquid cultures to OD_{600} of 0.25 OD per sample into 2ml of YPD and incubated at 30°C for 3-4 hours. Then centrifuged 1ml of yeast culture at 13,000 RPM for 1 minute, washed once with 0.1M LiAc, and resuspended with 100µl of LiAc. Next, I prepared denatured salmon sperm DNA (ssDNA) by boiling at 100°C for 5 minutes and then placed on ice. Then added 1-2ug of plasmid DNA to yeast sample. In addition, added 5µl ssNDA to sample. Finally, I added 350µl of transformation plate mix to yeast sample. After mixing all the reagents with the yeast samples, then incubated eppendorf cultures onto rotator for 30 minutes 30°C. After incubation, heat shocked yeast

cultures for 10 minutes at 42°C in water bath. Then centrifuged the yeast samples at 13,000 RPM for 1 minute, resuspended yeast in 100µl of water. Lastly, plated 100µl of yeast onto selective yeast plate and then spread. Incubated plates into a 30°C incubate for 2 days.

Optimized Autophagy Assay

To start the optimized autophagy assay began by inoculating 3 yeast colonies per sample into 3ml of $SCD_{CSH-URA}$ media, which was then incubated overnight for 14hrs – 17hrs, on the rotator in 30°C. Then overnight cultures were diluted into two different sets of yeast cells, set 1 to OD_{600} of 1 and set 2 OD_{600} of 1.2. Set 1 was then centrifuged at 13,000 RPM for 1 minute and stored the pellet at -20°C. Set 1 is labeled as the overnight yeast culture sample. To recover the yeast after their overnight incubation, set 2 yeast samples were also centrifuged set 2 yeasts sample at 13,000 RPM for 1 minute, but then were resuspended with 6ml of $SCD_{CSH-URA}$ and incubated on rotator at 30°C until reached log phase, $OD_{600} \cong 0.5$. After the recovery incubation, required 4 sets per 1 sample and set was calculated to have the volume equivalent to an OD_{600} of 1. Then the sets were centrifuged at 13,000 RPM for 1 minute and the yeast supernatant was aspirated. Out of the 4 sets, set 1 sample was centrifuged and stored pellet at -20°C. However, set 2,3,4 were resuspended in 2ml of SCD_{ME-URA} and incubate on rotator at 30°C for various time points. Set 2 was incubated at 30°C for 1 hour. Set 3 incubate at 30°C for 2 hours. Set 4 incubate at 30°C for 3 hours. After the incubation, the volume of yeast samples were obtained and were equivalent to an OD_{600} of 1 per sample. Each set samples were centrifuged at 13,000 RPM for 1 min; then aspirated the supernatant and froze down the

remaining pellet at at -20°C. The yeast were kept stored at -20°C until the preparation of western blot lysates. Each strain tested will end up having 5 different time points (**Figure 10).**

Preparation of Yeast Cell Lysates

Autophagy assay samples were prepped for western blot by the following cell lysate method. The yeast samples were prepared for lysates at 1:1 ratio of the optical density to SDS page lysis loading buffer. The total amount of lysis buffer was aliquoted during the preparation, which was rounded to the nearest whole number. Then added protease inhibitor and phosphatase inhibitor diluted to 100X to the total volume of aliquoted loading buffer. Next, BME was added to total lysis loading buffer at a final concentration of 5%. The prepared loading buffer was mixed and resuspended each sample with equal amounts of lysis buffer to OD. After adding the prepared lysis loading buffer, half the sample volume with glass beads. Each sample was then vortex sample at max for 4 sets of ON 45 secs and OFF 30-45 secs with resting on ice in between vortexing sets. Then samples were incubated samples at 100°C water bath for 5mins. The finished prepared western lystates were then loaded onto 12% SDS gel with 10µl of sample and 5µl of standard marker. Western blotting procedures were then conducted to ascertain protein expression. The primary antibodies used were rabbit anti-GFP 1:500, rabbit anti-pS6 at 1:1000, and mouse anti-PGK 1:5000. The secondary antibodies' used were anti-rabbit and anti-mouse at 1:20,000.

Results

Tetrad Dissections

A significant portion of yeast knockout strains were found to have a secondary mutation responsible for their overgrowth on low amino acids [182]. However, the evidence also indicates that acquisition of a secondary mutation is a consequence of losing the specific function of the original knockout gene. Nevertheless, to determine if ESCRTs themselves are required for restricting growth on low amino acid medium, it was necessary to perform genetic analyses to identify any potential secondary mutations.

To determine if ESCRT knockout strains fail to appropriately slow their growth on low amino acid medium compared to wild type because of their ESCRT deficiency or because of a secondary mutation, I performed tetrad analyses to segregate any potential secondary loci. One knockout strain for each of the ESCRT complexes was backcrossed to wild type and sporulated. Each tetrad was dissected and analyzed for genotype and phenotype (**Figure 9)**[189]. A dissection is conducted on a single meiotic event by breaking the four haploid spores, therefore two of the four spores will carry the knockout gene (identified based on G418 resistance). After confirming true tetrads based on known markers of the two parental strains, these same spores were then analyzed for three phenotypes of interest (overgrowth on low amino acids, heat-ramp sensitivity/resistance, and the effects of rapamycin on the overgrowth phenotype). To draw firm conclusions, 7-12 tetrads were analyzed for each strain. The results of these tetrad analysis clearly demonstrates that all the ESCRT knockout strains had low amino acid overgrowth that consistently segregated with the knockout locus, indicating that the ESCRT gene deletion was responsible for overgrowth and not a secondary mutation **(Table 3, Appendix i,**

Appendix ii, Appendix iii). Because all tested ESCRT knockout strains behaved similarly, and because each ESCRT is a multimeric complex as explained above, we can reasonably conclude that the low amino acid overgrowth phenotype of the other ESCRT subunit gene knockouts would yield similar results. However, it is interesting to note that the true cell death phenotype of ESCRT knockouts strains is that cause increased sensitivity to heat-ramp treatment **(Appendix iii).** Thus, there is a secondary mutation that confers cell death resistance, explaining why the parental ESCRT knockout stains have heat ramp-resistant phenotype **(Appendix iii)**. Substrains of tetrad spores were relatively heat sensitive phenotype compared to WT, but greater growth than Δ*whi2* heat sensitivity phenotype.

Autophagy Assay

To determine if ESCRTs are important for autophagy induced by low amino acid conditions. I transformed the ESCRT knockout strains with a plasmid expressing a GFP-Atg8 fusion protein **(Figure 11, Appendix i).** This reporter can detect autophagy induction as it is under the control of *ATG8* promoter, which is induced upon activation of autophagy (provided by Jodi Nunnari)[190]. The transformation of this plasmid also allows for the detection of autophagy flux by tracking the degradation of the Atg8 moiety and liberation of the more protease-resistant GFP portion in the yeast vacuole. To induce autophagy in the transformed yeast, an overnight culture of yeast was subjected to nutrient deprivation via incubation in low amino acid medium ($SCD_{ME\text{-}URA}$), known as the autophagy assay. In the same lysates, I also analyzed TOR kinases activity via the phosphorylation of ribosomal protein S6 (pS6). The autophagy assay used in the western

blots was optimized from the original autophagy assay used in our lab because the original autophagy assay used yeast at the post-diauxic growth phase many hours after switching to low amino acid medium. Furthermore, high density cell cultures of different strains could have the ability to consume key nutrients in the medium at different rates which may mimic an autophagy result. Therefore, I optimized this assay to exclude outside influences by restricting the yeast to their log phase and using shorter treatment times. These low density cultures also prevent the yeast depleting the medium.

ESCRT I and II – analysis of Srn2 and Snf8

Tor activity

Nutrient withdrawal was conducted on knockout yeast strains lacking subunits of ESCRT-I and ESCRT-II. *srn2*Δ (ESCRT-I) and *snf8*Δ (ESCRT-II) transformed with the Pro^{ATG}-GFP-Atg8 plasmid. Each transformed ESCRT strain subjected to nutrient withdrawal ($SCD_{ME\text{-}URA}$) (**Figure 10)**. Yeast lysates of $1OD_{600}$ were collected from each time point during the autophagy assay, including the starting overnight (O/N) culture, 4 hr recovery in YPD, then switching to 1, 2 and 3 hr in low amino acid medium ($SCD_{ME\text{-}URA}$), Lysate were prepared for western blots using anti-pS6 (see methods). Tor activity was measured using a phosphorylation-specific antibody directed against mammalian phosphor-S6, which cross reacts with yeast pS6 due to high conservation[185]. pS6 was detected by anti-$pS6_{rabbit}$ and phosphoglycerate kinase (PGK), major glycolysis enzyme, was used as a loading control.

As expected, WT Tor activity during following autophagy induction decreased as time progressed in the low amino acid medium incubation **(Figure 12)**. Deletion of *SNF8*

caused a decline in Tor activity similar to that of WT (**Figure 12A, B)**. Therefore, Snf8 of ESCRT-II does not appears to be a negative regulator of TOR, in contrast to Whi2 [184]. In contrast, the deletion *SRN2* subunit of ESCRT-I exhibited sustained Tor activity in low amino acids (**Figure 12 A, B).** This is based on the pS6 levels during low nutrient conditions. *srn2*Δ sensing low amino acids reaction was slower that the sensing abilities of *snf8*Δ and WTα, represented by the minor decrease in Tor activity. Potentially, resulting in a nutrient sensing defect/TOR dysfunction.

To confirm that the deletion of *SRN2* results in the low amino acid overgrowth and sustained Tor activity, I tested a *srn2*Δ haploid spore from the tetrad dissections described below. This *srn2*Δ haploid tetrad spore has a phenotype of heat sensitive, overgrowth on low amino acid, and has rapamycin-resistant overgrowth. *srn2*Δspore was tested in the autophagy assay against a positive control, *whi2*Δ, and negative control, WTα. *srn2*Δ haploid spore, *whi2*Δ, and WTα were transformed with GFP-Atg8 plasmid. However, this time the WTα did not depict the normal protein profile of pS6 during low amino acid condition (**compare Figure 12 and Figure 13)**. Initially there was a decrease in pS6 levels from 1 hour to 2 hours, but then rises from hour 2 to hour 3. This is not a typical Tor activity in WTα strains. This profile was only seen once in the total of three times the autophagy experiment was run. Although this was the only experiment in my experience where the wild type did not behave as expect, thereby compromising my conclusions for the ESCRT knockout strains, the Western blots results suggest that there is a delay in nutrient-sensing in *srn2*Δ (ESCRT-1) (**Figure 12 A, B and Figure 13 A, B).** In fact, western blots revealed there was an increase of Tor activity through times points with low amino acid incubation (**Figure 12 A, B and Figure 13 A, B)**.

Autophagy activity

WTα, *srn2*Δ and *snf8*Δ yeast lysates of $1OD_{600}$ were collected from each time point during the autophagy assay. Lysate were prepared for western blots using anti-GFP antibody (see methods)**.** Autophagy activity was measured through the protein levels both the conjugated form GFP-Agt8 and free GFP. Western blots revealed that there was a presence of both forms, Atg8-GFP and free GFP, during the autophagy assay (**Figure 12 C, D)**. In addition, there was a high background level. Therefore, the data is inconclusive and results might be an artifact. On the other hand, presences of both forms can be due to an autophagy flux or a lysosome dysfunction.

The second set of transformed yeast WTα, *srn2*Δ tetrad spore, and *whi2*Δ yeast lysates were collected the same way. The autophagy activity was similar to the previous transformed yeast, presences of both GFP forms. But western blots revealed that there was high expression of GFP-Atg8 during time points of WT, but GFP-Atg8 expression was lost in *srn2*Δ tetrad spore and *whi2*Δ (**Figure 13 C, D)**. Although *whi2*Δ lacked expression of GFP-Atg8, there was presence of GFP maybe concluding to an induction of autophagy. It is interesting to note that wild type has expression of both GFP-Atg8 and GFP, both induction and flux is occurring. However, there was a high protein background level. In conclusion, the data still remains inconclusive.

ESCRT-0 and III – analysis of Vps27 and Snf7

Tor activity

Nutrient withdrawal was conducted on knockout yeast strains lacking subunits of ESCRT-0 and ESCRT-III. v*ps27*Δ (ESCRT-0) and *snf7*Δ (ESCRT-III) was transformed

with Pro^{ATG}-GFP-Atg8 plasmid. Each transformed ESCRT strain was subjected to nutrient withdrawal ($SCD_{ME\text{-}URA}$) at three different time points. Yeast lysates of $1OD_{600}$ were collected from each time point during the autophagy assay, including the starting overnight (O/N) culture, 4 hr recovery in YPD, then switching to 1, 2 and 3 hr in low amino acid medium ($SCD_{ME\text{-}URA}$). Lysate were prepared for western blots using anti-pS6 (see methods). Tor activity was using a phosphorylation-specific antibody directed against mammalian phosphor-S6, which cross reacts with yeast pS6 due to high conservation[185]. pS6 protein was detected by anti-$pS6_{rabbit}$ And phosphoglycerate kinase (PGK), major glycolysis enzyme, was used as a loading control.

As expected, wild type Tor activity during the autophagy decreased as time progressed in the low amino acid medium incubation. v*ps27*Δ Tor activity showed the traditional phenotype, decreased of pS6 expression during times in $SCD_{ME\text{-}URA}$ medium like WTα. However, western blots revealed a different protein expression profile for *snf7*Δ. Tor activity, pS6, continued to increase in low amino acid medium up to 2 hrs of incubation **(Figure 14 A, B).** After 2 hours incubation in $SCD_{ME\text{-}URA}$ medium Tor activity begins to decrease. Results are interpreted as a nutrient delay/TOR dysfunction.

Autophagy activity

WTα, v*ps27*Δ, *snf7*Δ yeast lysates of $1OD_{600}$ were collected from each time point during the autophagy assay. Lysate were prepared for western blots using anti-GFP antibody (see methods)**.** Autophagy activity was measured through the protein levels both the conjugated form GFP-Agt8 and free GFP. Western blots revealed that there was a presence of both forms, GFP-Atg8 and free GFP, during the autophagy assay throughout

all the time points. **(Figure 14 C, D)**. However, detection of free GFP was faint in all samples, but was most prominent in overnight samples of v*ps27*Δ and *snf7*Δ, which may present a lack of autophagy induction. Overnight WTα sample expresses only minimal protein expression a sign of autophagy induction. There was high background level within the blot. Therefore, data is conclusive, but the prominent appears of the background from three trials could be a true result. Perhaps there is a lysosome dysfunction, cargo attachment, or that not all the protein is being broken down during lysate preparation.

Table 2

		SCD_{CSH} Media[131]	SCD_{ME} Media[132]
Component	**MW g/mole**	**mg/L**	**mg/L**
Adenine	368.34	18.35	20.00
Alanine	89.00	73.40	0.00
Arginine	174.00	73.40	20.00
Asparagine	150.10	73.40	0.00
Aspartic acid	133.00	73.40	100.00
Cysteine	175.63	73.40	0.00
Glutamine	146.00	73.40	0.00
Glutamic acid	169.10	73.40	100.00
Glycine	97.05	73.40	0.00
Histidine	155.00	73.40	20.00
Inositol	180.16	73.40	0.00
Isoleucine	131.00	73.40	30.00
Leucine	131.00	367.00	30.00
Lysine	182.65	73.40	30.00
Methionine	149.00	73.40	20.00
PABA	137.14	73.40	0.00
Phenylalanine	165.00	73.40	50.00
Proline	115.00	73.40	0.00
Serine	105.00	73.40	400.00
Threonine	119.00	73.40	200.00
Tryptophan	204.00	73.40	20.00
Tyrosine	181.00	73.40	30.00
Uracil	112.00	73.40	20.00
Valine	117.00	73.40	150.00
TOTAL amino acids		**1761.60**	**1240.00**
Percent of CSH		**100.00**	**70.39**
Percent Leu of CSH		100.00	8.17

*2 g of each dry drop out mix was used for all media except SCD_{ME}, which was 1.24 g. Some medium had liquid amino acid mixtures added after autoclaving to the amount indicated

Adapted from Maragret Dayhoff

Table 2. Media recipe for rich media and low amino acid media.
Media recipe for rich media and low amino acid media.

Table 3

ESCRT Complex	Yeast Protein	Mammalian Homolog	Found in Yeast Screen +overgrowth	Heat Ramp (Cell Death)	Rapamycin	Phenotype result from gene deletion
ESCRT-0	Vps27	Hrs	Yes	HS	Rap^R	Yes
	Hse	STAM1/2	No			
ESCRT-I	Vps23/Stp22	Tsg101	Yes	HS	Rap^R	Yes^MDB
	Vps28	hVps28	Yes	HS	Rap^R*	Yes
	Vps37/Srn2	Vps37 A,B,C	yes	HS	Rap^R*	Yes
	Mvb12	hMVB12 A,B	Yes	HS	Rap^R*	Yes
ESCRT-II	Vps36	EAP45	Yes	Not completed	Not completed	Not completed
	Vps22/Snf8	EAP30	Yes	HS	Rap^R*	Yes
	Vps25	EAP20	Yes	Not completed	Not completed	Not completed
ESCRT-III	Vps20	CHMP6	Yes	Not completed	Not completed	Not completed
	Snf7	CHMP4 A,B,C	Yes	HS	Rap^R*	Yes
	Vps24	CHMP3	Yes	Not completed	Not completed	Not completed
	Vps2/Did4	CHMP2 A.B	Yes	Not completed	Not completed	Not completed
Vps4 complex (ESCRT-IV)	Vps4	SKD1	Yes	HS	Rap^R	Yes
	Vps60	CHMP5	Yes	Not completed	Not completed	Not completed

Notes:
Rap^R* - analysis descripencies based on poor growth on 5 nM concentration
MDB – performed by PhD student, Margaret Dayhoff-Branningan [185]

Table 3 - Summary of ESCRT components and correlating phenotypes through tetrad dissections.

Table of ESCRT components that have had the phenotypes of the spore-derived substrains verified as phenotype derived from the single gene mutation through tetrad dissections.

Figure 7

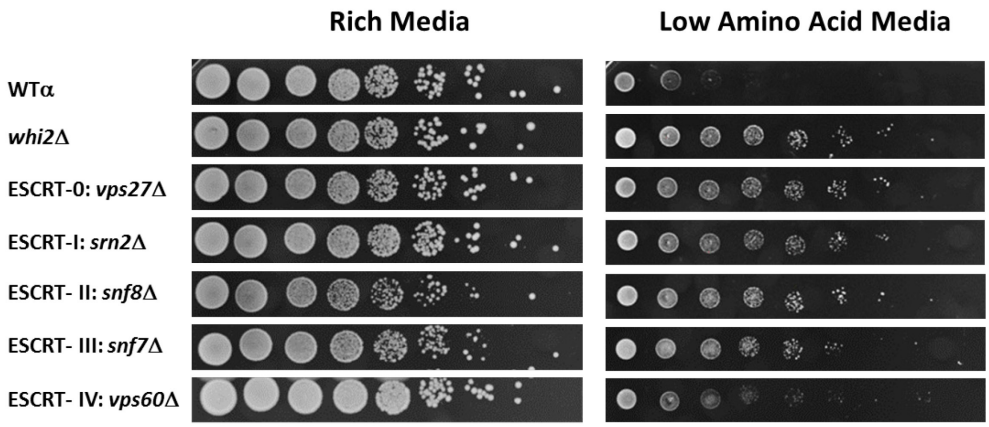

Figure 7 - Overgrowth phenotype in low amino acid conditions.
Overgrowth phenotype on low amino acid medium compared to YPD (rich) medium. 1:4 serial dilutions at 20µl yeast: 80µl dH_2O. Knockout strains are representative of each ESCRT complex are shown. Complied images, same exposures, but rearranged for presentation purpose.

Figure 8

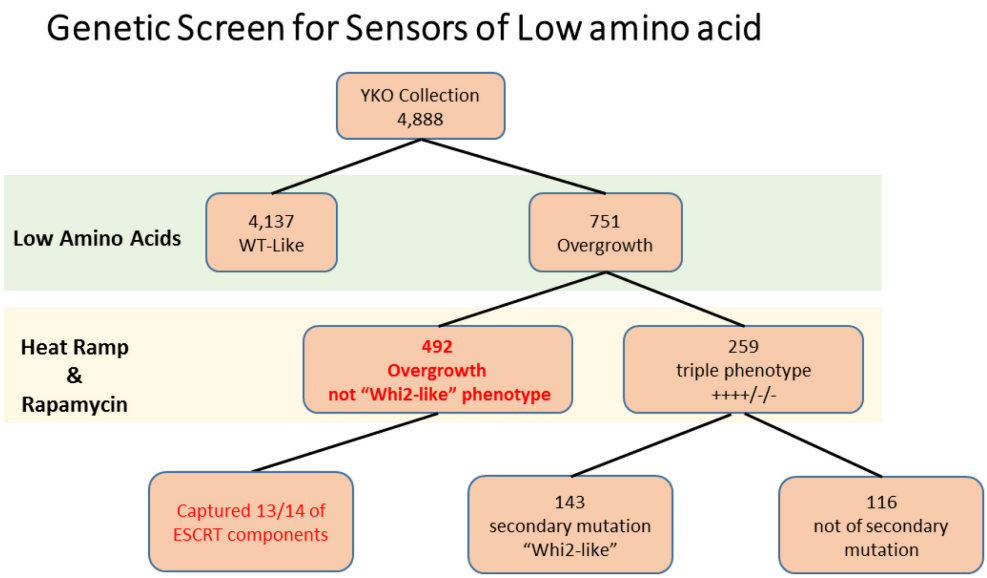

Figure 8 - Flow chart of yeast knockout collection screen.
Schematic of the genetic yeast knockout collection screening results for sensors of low amino acids. Red text indicates the location of ESCSRT knockout strains within the genetic screen flow chart. In red, distinguishes the location of ESCRTs within the genetic screen map.

Figure 9

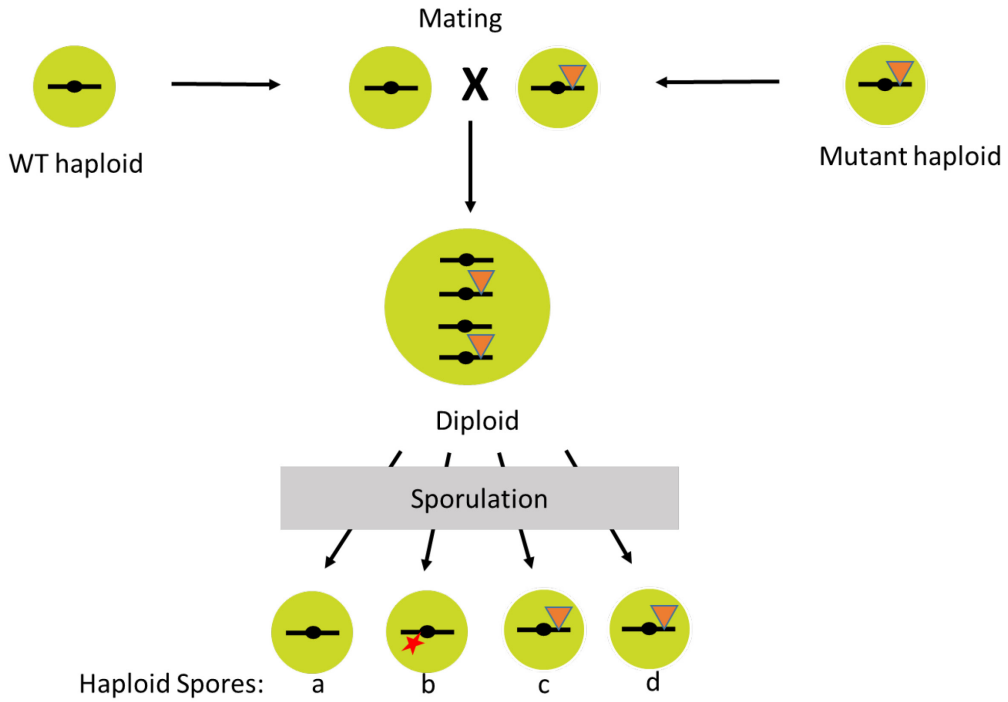

Figure 9 - Schematic of a tetrad dissection.
Schematic of a tetrad dissection genetic process to confirm the origination of the phenotype. Haploid strains are then plated on YPD plates to grow. Haploids are the subjected to heat, low amino acid conditions, and low amino acid conditions with rapamycin and growth analysis is taken.

Figure 10

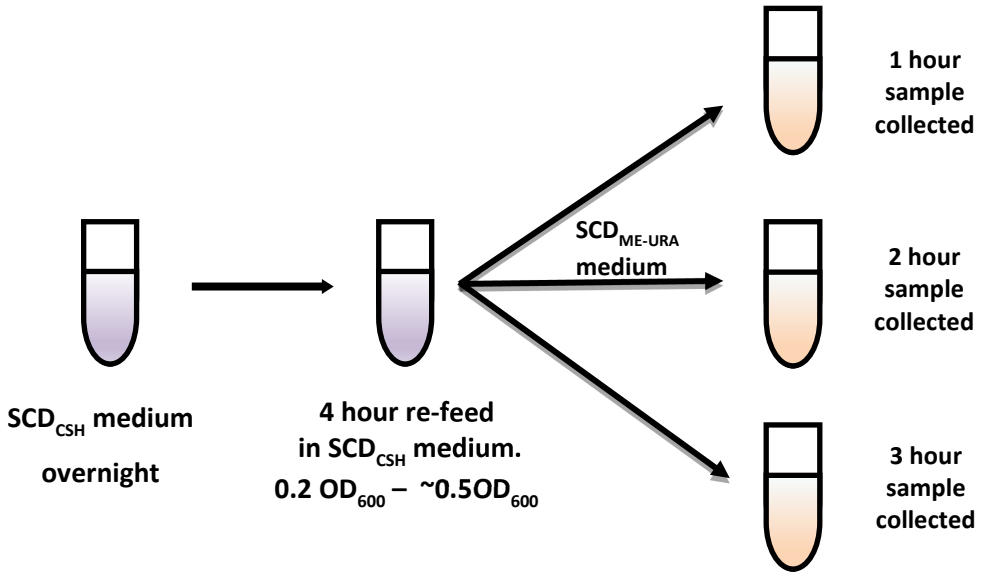

Figure 10 - Schematic of autophagy assay.
Schematic of the log-phase restricted autophagy assay.

Figure 11

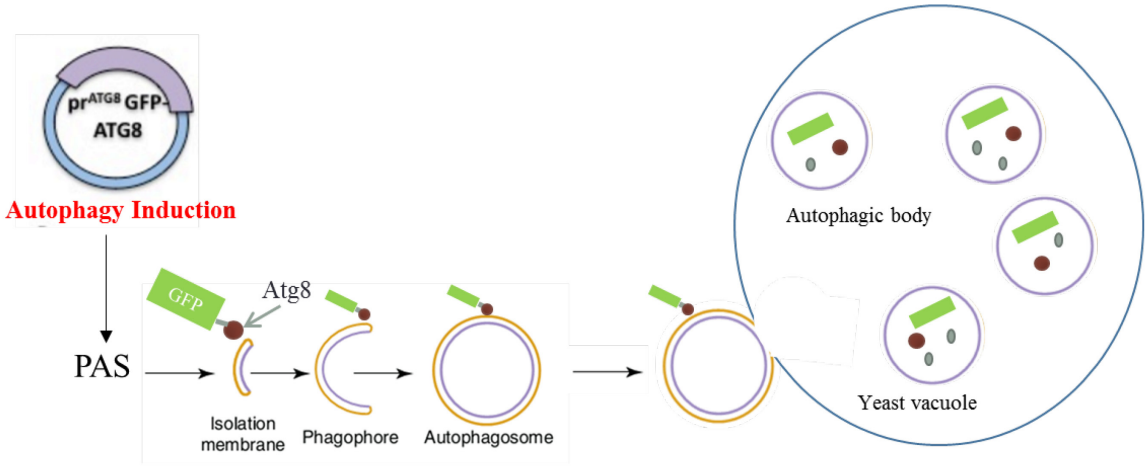

Adapted from McEwan and Dikic, 2011; Klionsky and Eskelinen, 2014

Figure 11 – Plasmid reporter autophagy assay.
Yeast transformed with pr^{ATG8} GFP-ATG8 plasmid to track autophagy activity. Atg8 is a core lipidated autophagy protein marker for active autophagosomes. During autophagy, Atg8-GFP autophagsome will merge with lysosome and degrade Atg8, freeing GFP.

Figure 12

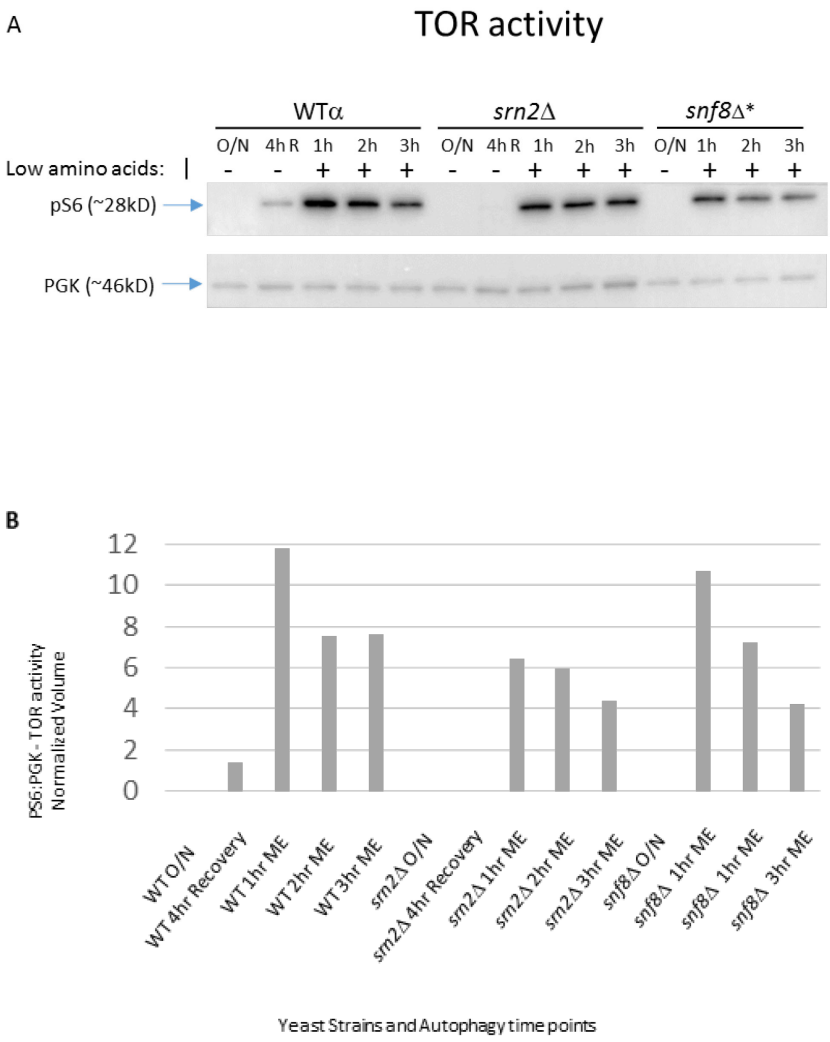
A
TOR activity
WTα
srn2Δ
snf8Δ*
O/N 4h R 1h 2h 3h O/N 4h R 1h 2h 3h O/N 1h 2h 3h
Low amino acids: - - + + + - - + + + - + + +
pS6 (~28kD)
PGK (~46kD)
B
PS6:PGK - TOR activity Normalized Volume
0
2
4
6
8
10
12
WT O/N
WT 4hr Recovery
WT 1hr ME
WT 2hr ME
WT 3hr ME
srn2Δ O/N
srn2Δ 4hr Recovery
srn2Δ 1hr ME
srn2Δ 2hr ME
srn2Δ 3hr ME
snf8Δ O/N
snf8Δ 1hr ME
snf8Δ 1hr ME
snf8Δ 3hr ME
Yeast Strains and Autophagy time points

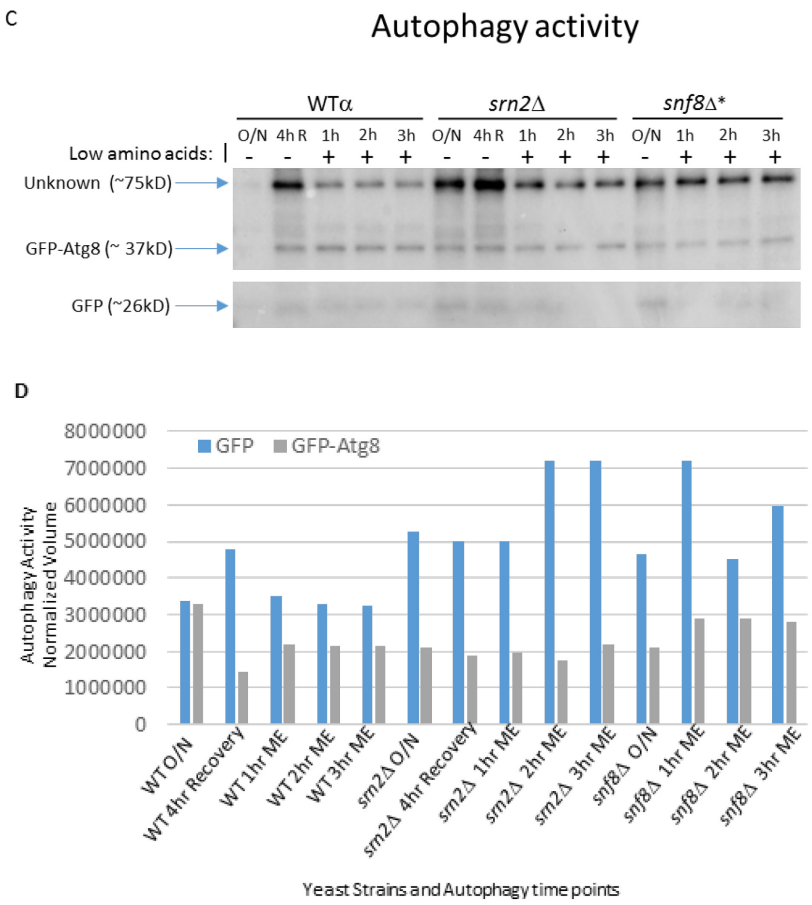

Figure 12 - ESCRT-I and ESCRT-II Tor and autophagy activity.
Unfortunately, not all collected lysates were run due to the limited number of wells per comb, which excluded 4hr recovery sample of Snf8 for both TOR activity and autophagy activity. A) Western blot of TOR activity through phospho-s6 (anti-pS6 1:1000), PGK (anti-PGK 1:5000) loading control. 30 second exposure. Comparison of collected 1OD yeast cell lysates (WTα, *srn2*Δ *(BY MATa)*, and *snf8*Δ *(BY MATa*) transformed with Atg8-GFP plasmid at various time points overnight (O/N), 4hr rich-media recovery, 1hr low amino acids, 2hr low amino acids, 3hr low amino acids. * 4hr recovery time point is excluded due to space of blot. 1-3 hr (ME) time points were gathered after switching to low amino acid medium $SCD_{ME\text{-}URA}$. *srn2*Δ subunit expresses a potential delay in response to a low nutrient condition. B) Quantification of protein expression of WTα , *srn2*Δ (*BY MAT*a), and *snf8*Δ (*BY MAT*a) at normalized volume. n=1. C) Western blot of autophagy activity measuring: Atg8-GFP and GFP. 30 second exposure. Presence of both forms (and large background bands) inhibits concrete data analysis upon autophagy activity; thus, data inconclusive. D) Quantification of autophagy activity.

Figure 13

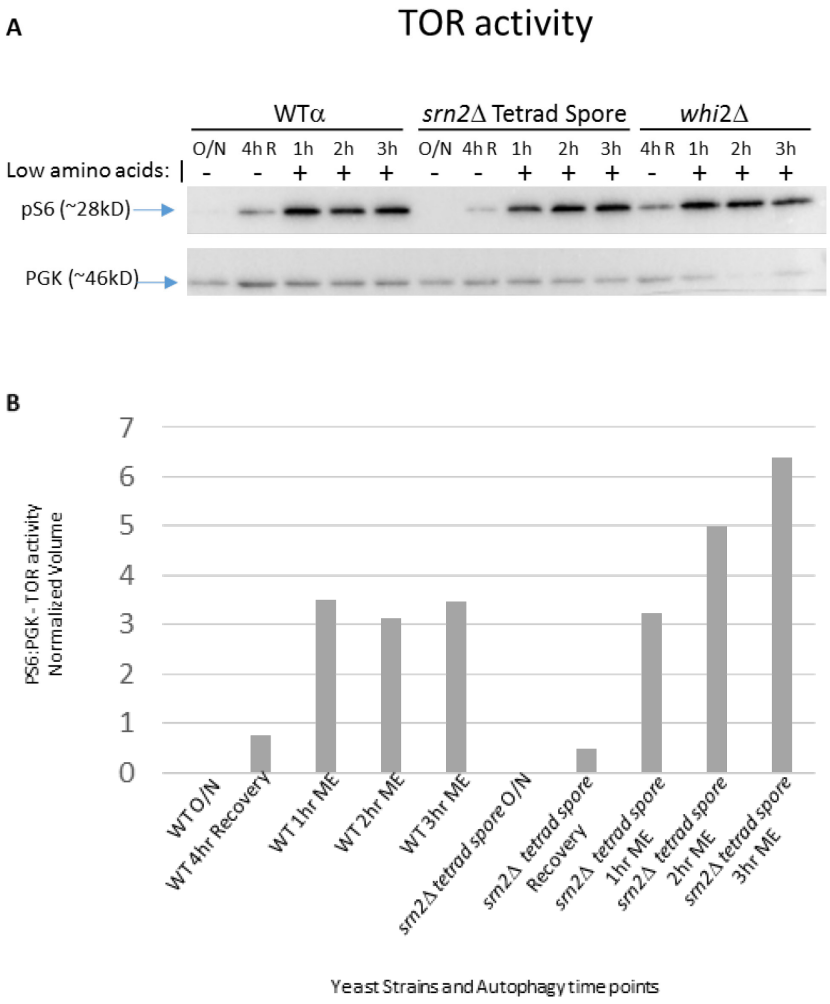
A
TOR activity
WTα
srn2Δ Tetrad Spore
whi2Δ
O/N 4h R 1h 2h 3h O/N 4h R 1h 2h 3h 4h R 1h 2h 3h
Low amino acids: - - + + + - - + + + - + + +
pS6 (~28kD)
PGK (~46kD)
B
PS6:PGK - TOR activity Normalized Volume
0
1
2
3
4
5
6
7
WT O/N
WT 4hr Recovery
WT 1hr ME
WT 2hr ME
WT 3hr ME
srn2Δ tetrad spore O/N
srn2Δ tetrad spore Recovery
srn2Δ tetrad spore 1hr ME
srn2Δ tetrad spore 2hr ME
srn2Δ tetrad spore 3hr ME
Yeast Strains and Autophagy time points

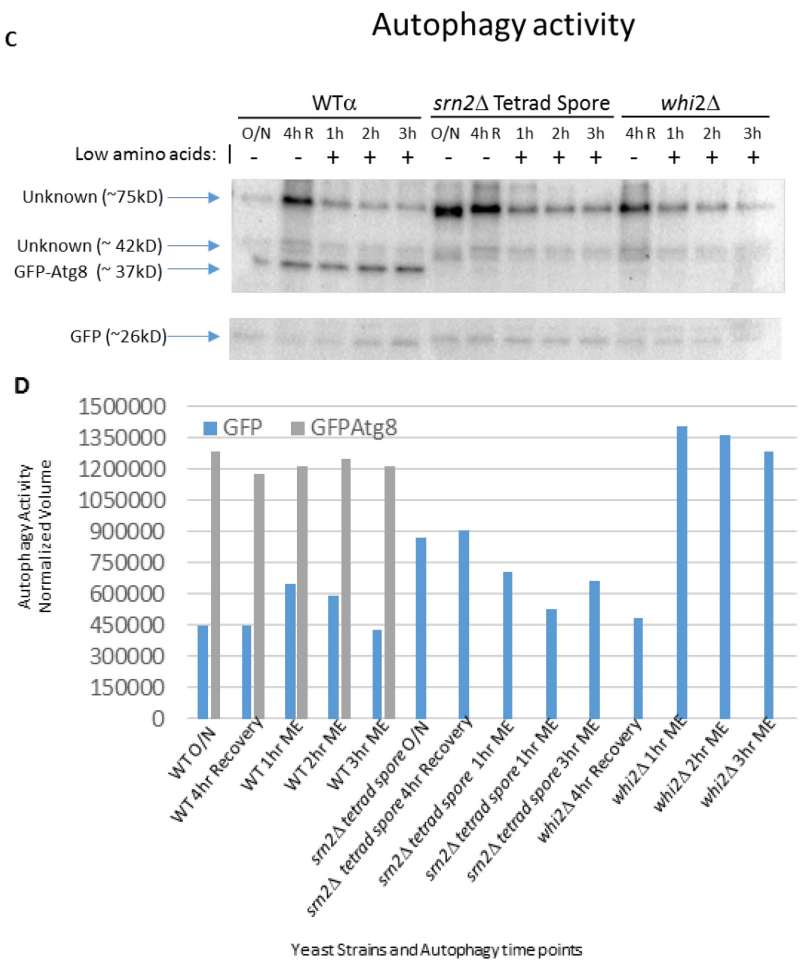

Figure 13 - ESCRT-I (haploid spore) and *WHI2* Tor and autophagy activity
Unfortunately, not all collected lysates were run due to the limited number of wells per comb, excluded 4hr recovery sample of Whi2 for both TOR activity and autophagy activity. A) Western blot of TOR activity through Phospho-serine6 (anti-pS6 1:1000), PGK (anti-PGK 1:5000) loading control. 5 second exposure. Comparison of collected 1OD yeast strains (WTα, *srn2*Δ Tetrad Spore, and *whi2*Δ) transformed with Atg8-GFP plasmid at various time points overnight (O/N), 4hr rich-media recovery, 1hr low amino acids, 2hr low amino acids, 3hr low amino acids. * 4hr recovery time point is excluded due to space of blot. 1-3 hr (ME) time points were gathered after switching to low amino acid medium $SCD_{ME-URA.}$ *srn2*Δ tetrad spore confirms that Srn2 subunit does have a delay in nutrient response. *srn2*Δ *t*etrad spore was taken from my previous tetrad dissection (Kan+, heat resistant, overgrowth, rapamycin resistant). B) Quantification of protein expression of WTα and *srn2*Δ (*BY MAT*a) tetrad spore. n=1. C) Western blot of autophagy activity measuring: Atg8-GFP (anti-GFP 1:5000) and GFP. 2.5 minute exposure. Presence of both forms (and large background bands) inhibits concrete data analysis upon autophagy activity; thus, data inconclusive. D) Quantification of autophagy activity.

Figure 14

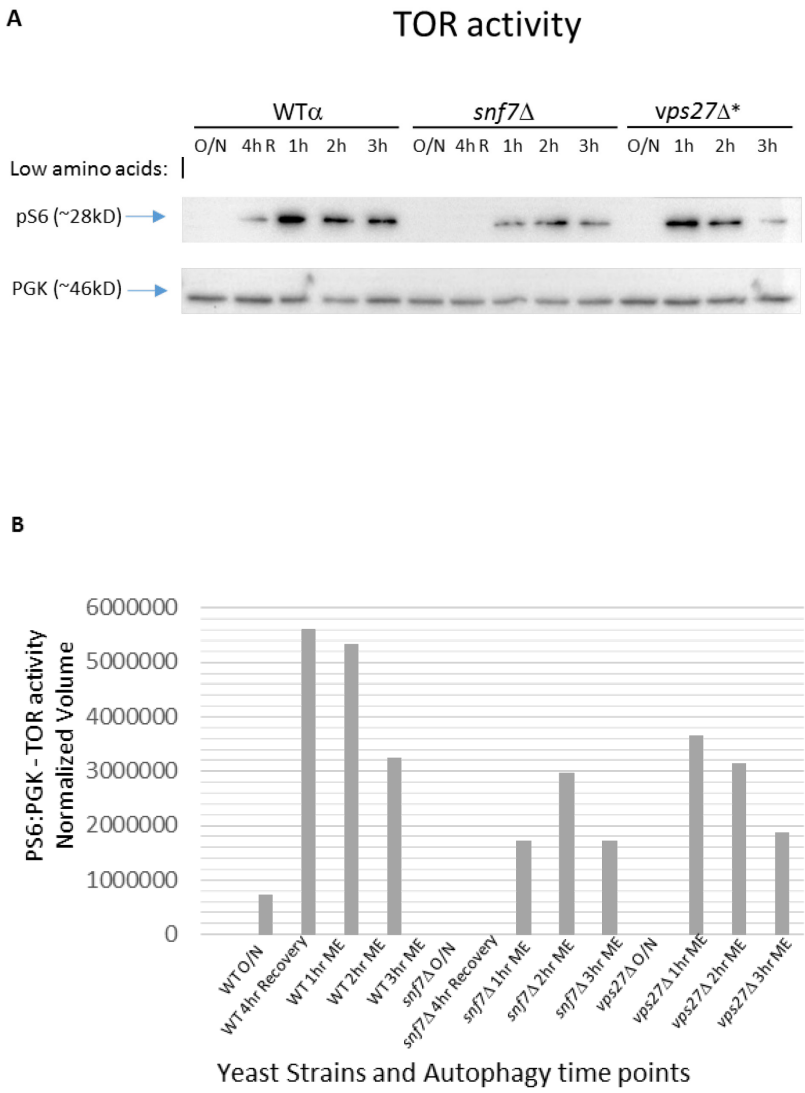
A
TOR activity
WTα
snf7Δ
vps27Δ*
O/N 4h R 1h 2h 3h O/N 4h R 1h 2h 3h O/N 1h 2h 3h
Low amino acids:
pS6 (~28kD)
PGK (~46kD)
B
PS6:PGK - TOR activity Normalized Volume
6000000
5000000
4000000
3000000
2000000
1000000
0
WT O/N
WT 4hr Recovery
WT 1hr ME
WT 2hr ME
WT 3hr ME
snf7Δ O/N
snf7Δ 4hr Recovery
snf7Δ 1hr ME
snf7Δ 2hr ME
snf7Δ 3hr ME
vps27Δ O/N
vps27Δ 1hr ME
vps27Δ 2hr ME
vps27Δ 3hr ME
Yeast Strains and Autophagy time points

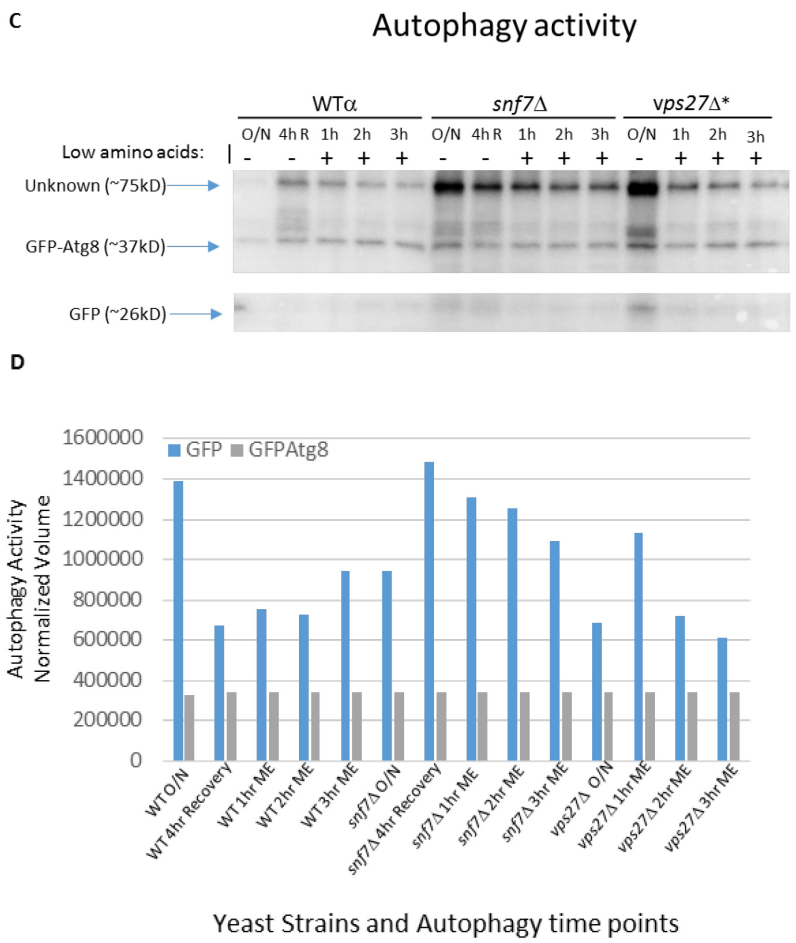

Figure 14 - ESCRT-0 and ESCRT-III Tor and autophagy activity.

Unfortunately, not all collected lysates were run due to the limited number of wells per comb; thus, excluded 4hr recovery sample of Vps27 for both TOR activity and autophagy activity. A) Western blot of TOR activity through Phospho-serine6 (anti-pS6 1:1000), PGK (anti-PGK 1:5000) loading control. 30 second exposure. Comparison of collected 1OD cell lysates of WTα, *snf7*Δ (*BY MAT*a), and *vps27*Δ (*BY MATa*) transformed with Atg8-GFP plasmid at various time points overnight (O/N), 4hr rich-media recovery, 1hr low amino acids, 2hr low amino acids, 3hr low amino acids. * 4hr recovery time point is excluded due to space of blot. 1-3 hr (ME) time points were gathered after switching to low amino acid medium $SCD_{ME\text{-}URA}$. *snf7*Δ subunit expresses a delay in response to a low nutrient condition. B) Quantification of protein expression of WTα , *snf7*Δ (*BY MAT*a), and *vps27*Δ (*BY MATa*) at normalized volume. n=1 C) Western blot of autophagy activity measuring: Atg8-GFP and GFP. 30 second exposure. Presence of both forms (and large background bands) inhibits concrete data analysis upon autophagy activity; thus, data inconclusive. D) Quantification of autophagy activity.

Chapter 3
Discussion and future directions

The cells ability to sense the cellular nutrient status, both externally and internally, in the environment is vital for the cell to sustain life. There is a direct correlation between the nutrient status and cellular proliferation. If the environment is nutrient rich, it cues the cell to initiate and promote cellular growth[1]. On the other hand, if the environment is unfavorable, then it cues the cell to halt proliferation and initiate autophagy[1]. The main nutrient sensor is TOR and is conserved throughout species[2]. TOR is responsible for relaying the nutrient availability to its downstream effectors to control both anabolic and catabolic processes, including inducing the switch from proliferation to degradation by autophagy[3,5]. Although, it still remains a mystery how TOR exactly senses nutrients and how it transduces the signal to its downstream effectors. However, my research may project new insights of possible candidates for the mechanism to sense nutrients, ESCRT complex. This projection is not only based on results, but based on previous findings. In particular, ESCRTs are known to be involved in autophagy[112]. ESCRTs create an alternative autophagy pathway by the formation of amphisomes vesicles (MVB fused with autophagosomes) that later merge with the lysosome for degradation in mammalians, but this was not observed in yeast[112]. In addition, researchers are exploring the idea that ESCRTs are involved in microautophagy[117]. Based on my preliminary results, possible ESCRT interaction with TOR signaling, and previous knowledge in ESCRTs involvement in autophagy might be the link that connects nutrient sensing to autophagy in yeast.

ESCRT involvement

My preliminary data suggest that there is possible involvement of the ESCRT machinery in sensing nutrients and transducing the information to TOR. I made it imperative to subject one subunit from each ESCRT complex to the autophagy assay to test the array of ESCRT complexes activity. Although many ESCRT mutant strains weren't tested, my experiments revealed that not all ESCRT complexes of the canonical pathway may be involved in sensing and relaying nutritional status to TOR. The autophagy experiment provides a dual role. It tracks Tor activity and autophagy activity during nutrient deprived conditions. I created an optimized assay, which constricts yeast to their log phase, excluding any possible outside influence upon the results **(Figure 10)**.

Sustained Tor activity under deprived nutrition conditions and its implications in ESCRT involvement with nutrient sensing

From tetrad dissections all mutant ESCRTs have an overgrowth, relatively heat sensitive, and rapamycin resistant phenotype, which was confirmed to be a result from the gene deletion of the yeast knockout collection. Therefore, all subunits have the potential to have a TOR defect and seem to be position upstream of TOR due it insensitivity to rapamycin. Analyzing the protein expression of these ESCRT strains during starvation time points discovered not all ESCRT components expressed a TOR defect. After completing each time point and blot for Tor activity (pS6) and autophagy activity (GFP-Atg8) revealed that only two ESCRT subunits are potentially involved in relaying information to TOR. Out of the ESCRT strains tested, preliminary results could

reveal not all ESCRT components are required for nutrient signaling. *srn2*Δ and *snf7*Δ express high Tor activity during times of nutrient withdraw, which is in contrast to WTα **(Figure 12, 13, 14)**. Initially, *srn2*Δ only expressed a minimal decrease of TOR activity during nutrient withdraws in comparison to WTα. To further analyze the involvement *srn2*Δ, I tested a haploid spore generated from a previous tetrad dissection against *whi2*Δ as a positive control. Discovered from previous lab members, *whi2*Δ is known to have increasing Tor activity during nutrient withdraw. Blots confirmed the occurrence of a nutrient signaling delay. Protein analysis resulted in a dramatic increase of pS6 expression through all three time points, similar to *whi2*Δ. Therefore, high Tor activity was maintained during nutrient withdrawal. *snf7*Δ blots revealed an increase of pS6 protein expression through the three time points of nutrient withdrawal, contrasting wild type. In conclusion, high Tor activity during nutrient withdrawal in *srn2*Δ *and snf7*Δ might conclude in a TOR defect

It is known that Srn2 subunit of ESCRT-I is involved in sequestering ubiquintinated cargo along with ESCRT-0, but ESCRT-III is typical not known for cargo sequestration. The main responsibility of ESCRT-III is to form the machinery which creates invagination within the membrane to form the ILV of MVB. Perhaps, ESCRT-III does recognize cargo during its process of membrane invagination as a quality control check point. Regardless, *srn2*Δ *and snf7*Δ possible defect projects the possibility of ESCRT-I and ESCRT-III in relaying nutrient status to TOR. I propose two different signaling pathways that require ESCRT machinery to complete its signaling relay to Tor, EGO complex signaling and calcium ER/Golgi signaling via TOR.

ESCRTs relay nutrient signals to TOR through EGO Complex

Starvation conditions induces cell quiescence. When conditions are replenished, exiting G0 stage properly requires a protein complex called EGO[29]. EGO complex interaction with TOR is seen on both levels, EGO alone and in conjunction with the *G*ap1 sorting from endosomes (GSE) complex[37]. Gap1, low specificity transport, is induced in nitrogen-limited environment and is sequestered by MVB when nutrients are replenished[191]. However an additional recycling trafficking step of Gap1 was identified, which competes with MVB sorting, GSE complex and GSE is highly identical with EGO complex[37,192]. Mutants in any components of the GSE/EGO complex fail to recycle Gap1 to plasma membrane and have diminished recovery from rapamycin treatment[37,192]. EGO complex alone presents an interaction with TOR. EGO complex is localized on the vacuolar membrane enabling its sensing of intracellular leucine to TORC1[29]. Leucine starvation results in a reduction of Sch9 dephosphorylation due to the destablization of Gtr1-TORC1[33]. The interaction of EGO with TOR also due to its location and its phosphorylation reduction of Sch9 presents EGO complex as a major upstream regulator of TORC1 **(see Figure 1).** But what remains to be unknown is the mechanism of EGO complex uses to sense amino acid[29].

EGO complex is comprised of Ego1, Ego3, Gtr1, and Gtr2[29]. Gtr1 and Gtr2 belong to a family of Fas-GTPases[193,194]. Gtr1 or Gtr2 is activated when bound to GDP permitting its TORC1-stimulating conformation[33,193–195]. Ego1 is responsible to tether EGO complex to the vacuolar membrane because it is N-terminal and is mryisolated and palmitoylated[28]. Ego3 functions still remains a mystery, but it known to form

homodimers similar to Gtr1 and Gtr2[28]. Gtr1 GTPase activity is negatively regulated by the SEA complex (SEAC), specifically through a subcomplex called SEACIT (SEAC subcomplex Inhibiting TORC1 signaling)[28]. SEACIT is composed of Iml1, Npr2, and Npr3[28]. Leucine deprivation triggers Iml1 to interact with Gtr1 to inhibit TORC1[28]. In addition, experimental data supports SEACIT responds to vesicle trafficking, amino acids, and leucine cues[28]. SEACIT is then negative regulated by SEACAT (SEAC subcomplex Activating TORC1 signaling)[28].

Based off the information previously stated, there are two theories that presents itself. Firstly, since it is know that recycling of Gap1 uses MVB in nitrogen starvation conditions, it could be possible that EGO complexes uses MVB to sense amino acids to relay its information to TOR. Based on the location of EGO complex and Δ*srn2*/Δ*snf7* phenotype, puts both protein complexes upstream of TORC1. Together, EGO complex with their leucine starvation phenotype and *srn2*Δ and *snf7*Δ phenotype, I propose that ESCRT machinery could be the potential mechanism to relay amino acid levels from EGO complex to TOR pathway **(Figure 15a).** Secondly, perhaps it is not a direct interaction between MVBs and the EGO complex, but through SEACIT, since it is the ultimate negatively regulator of TORC1 through Gtr1 **(Figure 15b)**. Alternatively, the loss of ER/Golgi Ca^{2+}/Mn^{2+} ATPase Pmr1 not only increases protein secretion through the secretory pathway, but it is also caused TORC1 activation[188,196].

ESCRTs relaying nutrient signals to TOR correlating with ER/Golgi calcium levels

An alternative pathway that possibly uses ESCRT machinery is the coordination of amino acid levels with calcium levels of ER/Golgi to TOR pathway through Pmr1. Like amino acids, calcium is another essential nutritional factor for organisms, which regulates growth, proliferation, cell death and muscle contraction[187,197,198]. Calcium homeostasis is critical for organisms and maintenance of calcium concentration requires regulation on calcium transporters and sequesters in plasma and organelle membranes[187,199–201]. Transient increase of calcium from induction of vacuolar pump Pmc1, and the ER/Golgi Ca^{2+} pump Pmr1 is a critical stress response that is activated by the calcium/calcineurin signaling[202,203]. A genome-deletion screen of *S. cerevisaie* strains identified Δ*pmr1* as rapamycin resistant, which is a similar phenotype to my ESCRT knockouts **(Table2)** [188]. Pmr1, ER/Golgi Ca^{2+}/Mn^{2+} pump, functions in the secretory pathway for protein glycosylation, protein sorting, and ER protein degradation[188,204]. It was further inferred that due to its rapamycin resistant phenotype in Δ*pmr1*, presents Pmr1 as a negative regulator via opposing Lst9 in TORC1 signaling[188]. Thereby, suggesting Pmr1-dependent Ca^{2+}/Mn^{2+} ion homeostasis is necessary for TOR signaling[188].

Zhao and his colleagues observed ESCRT deletion mutants of ESCRT-I subunits (*stp22*Δ*, vps28*Δ*),* ESCRT-II (*snf8*Δ*, vps25*Δ*,* and *vps36*Δ*)*, and ESCRT-III (*nf7* Δ and *vps20*Δ) renders them calcium-sensitive due to accumulation of intracellular calcium ions in response to calcium stress[187]. Interestingly, they also noticed ESCRT mutants contain a reduced expression of *PMR1* via the reduction of *lacZ* activity by half compared to wild type[187]. Calcium sensitivity in ESCRT mutants was completely suppressed by

overexpression of *PMR1*[187]. It is known that Rim101 is a transcriptional repressor, which is active in its short-length form and inactive in its full-length form[187]. ESCRT mutants only contain Rim101 in its inactive full-length form and this proteolytic defect is responsible for the calcium hypersensitivity in ESCRT mutants[187]. In conclusion, it is surprisingly to see ESCRT mutants with calcium/calcineruin signaling activated (hypersensitivity) have a reduction of *PMR1* because *PMR1* is a positively regulated by calcium/calcineurin signaling, which was due to the defective proteolytic cleaving of Rim101 in ESCRT mutants[187,205]. Therefore, proper ESCRT machinery provides another positive role in signaling transduction within calcium signaling, in addition to its positive influence upon the Wnt signaling[80]. In conclusion, combing evidence of Pmr as a negative TOR regulator and decrease *PMR1* expression in ESCRT mutants, can link Pmr1 with ESCRT components to the expression or modification/sorting in ER/Golgi secretory pathway of nutrient transporters – coordinating calcium signaling with TOR (nutrient sensing) pathway in cells[187].

Since my ESCRTs candidates are also known to be resistance to rapamycin along with Pmr1, it is logical to think that they might interact and maybe also be upstream to TOR. I also investigated the phenotype that was found in our labs yeast screen of Pmr1 to be heat sensitive, overgrowth, and rapamycin resistant. All three of these phenotypes match the substrain ESCRTs phenotypes, which adds additional strength to possibly place the ESCRT candidates in the same pathway as Pmr1-TOR. Next, research just uncovered that ESCRTs have a role in regulating Pmr1 protein expression, presuming leading to negative regulation of TOR[187,188]. However, there was lacking experimental evidence observing the TOR activity within these ESCRT mutants in the study by

Zhao[187]. In fact, it was observed that ESCRT-I (Stp22, Vps28) and ESCRT-II (Snf7, Vps20) mutants to have a decreased Pmr1 expression. Perhaps, my mutant candidates, *srn2*Δ & *snf7*Δ, containing high Tor activity might confirm their Zhao et al. findings in connecting ESCRTs with Tor activity and Pmr1[187,188]. However, not all components of the ESCRT seem to be required to translate to the TOR pathway. Besides this fact, this pathway represents the prime avenue for ESCRT machinery in the relaying of nutrient status to the TOR pathway **(Figure 16)**.

Possible implication of ESCRT involvement based of its autophagy activity

At this point in the investigation, it is hard to definitely conclude any theories based on the occurrence of high background and possible autophagy reflux results. However, the re-occurrence of this autophagy phenotype might speak for itself. It is possible that high background might be due to some cellular dysfunction. During the analysis, when excluding the background bands, the presence of both forms GFP-Atg8 and free GFP might give an insight on autophagy system within the ESCRT mutants. As mentioned earlier, researchers are uncovering ESCRTs involvement in macroautophagy through their involvement in formation of amphisomes in mammalian cells[112]. ESCRT mutants lead to the accumulation of amphisomes and autophagosomes[112]. However, this is not the case for all higher eukaryotic organism, like *C. elegans*. In fact, ESCRT mutants in *C. elegans* express and intact autophagy system, but presents both forms of Atg8; thus, resulting in an autophagy flux rather than accumulation of autophagosomes[112]. Perhaps, this is mimicking what occurs in my ESCRT mutants.

Another explanation for this "reflux" could due to microautophagy rather than macroautophagy. Microautophagy, endosomal microautophagy, involves direct invagination of the vacuolar membrane[29,49]. Research in mammalian cells are uncovering the role of ESCRTs involvement in microautophagy. Current research presents that the endosome microautophagy selectively delivers specific cytosolic proteins to the vesicles of the late endosome during MVB biogenesis[117]. It is easier to comprehend a role for the ESCRTs in microautophagy. ESCRT-III complex will, most likely, be the most important complex in this system due it is responsibility in deforming the membrane to create membrane invaginations. This contradicts current knowledge of endosomal-microautophagy relying on ESCRT-I, ESCRT-II, Vps4 components for MVB formation[117]. However, perhaps, we are not seeing a clean turnover form GFP-Atg8, might be due its possible involvement in microautophagy, rather than macro-autophagy.

Future Direction

The future direction of this project involves the analysis of the rest of the ESCRT components in the autophagy assay in addition to Snf7-stabilizing protein, Bro1. More importantly, the focus of the experiment should shift to protein interaction studies, especially when *snf*7Δ is resulting in a nutrient signaling delay. Is Snf7 sequestering amino acids in addition to its main function of creating membrane invagination? I would then execute immunopercipitate experiments with Snf7. I would want to see if it interacts with Srn2, since that is the other ESCRT subunit that expresses a nutrient signaling delay. Then I would want to test if there is an interaction with Pmr1, since that is a known negative TOR regulator and has the same Hardwick yeast screen phenotype as the

ESCRT mutants, and to observe if there is a direct protein interaction besides its influence upon its negative regulator Rim101/Nrg1 pathway. More importantly, is to test the protein interaction of both Srn2 and Snf7 with Whi2, important strain in discovering the overgrowth phenotype.

Lastly, I would try investigating the specific amino acids are Srn2 and Snf7 are sensitive to and sequesters. In addition, investigation needs to occur on what type of nutrient sensor is being targeted by ESCRTs, whether or not the ESCRTs are sequestering transporters/receptors of amino acid sensing or direct targeting to the amino acid itself. If the end results are true, ESCRTs are involved in nutrient sensing, this will have a dramatic affect in the ESCRT research field and nutrient sensing world. It could potentially reformat the function of the different ESCRT complexes, possible adding the sequestration function to ESCRT-III responsibility. It will open new doors by uncovering more ESCRT involvement in cellular processes along with their implications in the nutrition field and their health impacts.

For instances, the correlation of Pmr1 and its calcium regulation. Calcium is an essential and influential nutrient upon many signaling pathways and is important for many cellular processes. The human homolog of Pmr1 is SPCA2. Recent studies show that dysregulation of SPCA2 along with the discovery of Orai1 (Ca^{2+} channel) mediates store-independent calcium influx constitutively activates this pathway and promotes the activity of tumor cells, specifically the transformation of mammary epithelial cells to cancerous cells[206]. This recent evidence could potential associate the role of ESCRTs and its nutrient sensing potential capabilities with tumor development through its association of Pmr1 (SPCA2). In summary, this irritates the impact that ESCRTs could have on

human health and strengthens the importance of nutrient sensing for proper human development. The links between ESCRTs, nutrient signaling, and human health are only the just beginning to be uncovered.

Figure 15

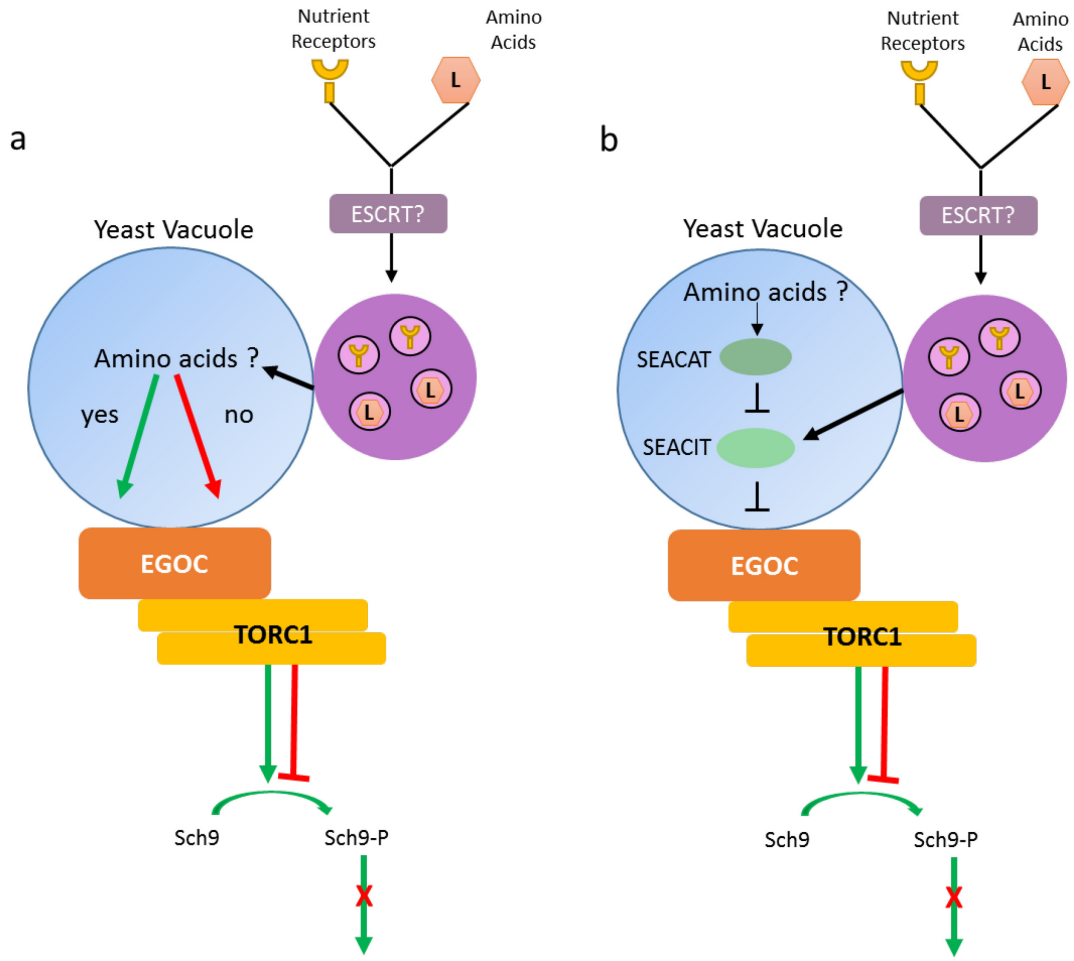

Figure 15 - Schematic depicting possible locations of ESCRT interaction within the EGO pathway communication with TOR.

Schematic depicting possible ESCRT interaction with the EGO complex. A) ESCRT machinery can be the mechanism directly relaying amino acids to the EGO complex to TOR pathway. B) ESCRT machinery, non-direct route, can interact with EGO complex inhibitor, SEACIT, to relaying amino acids to TOR pathway.

Figure 16

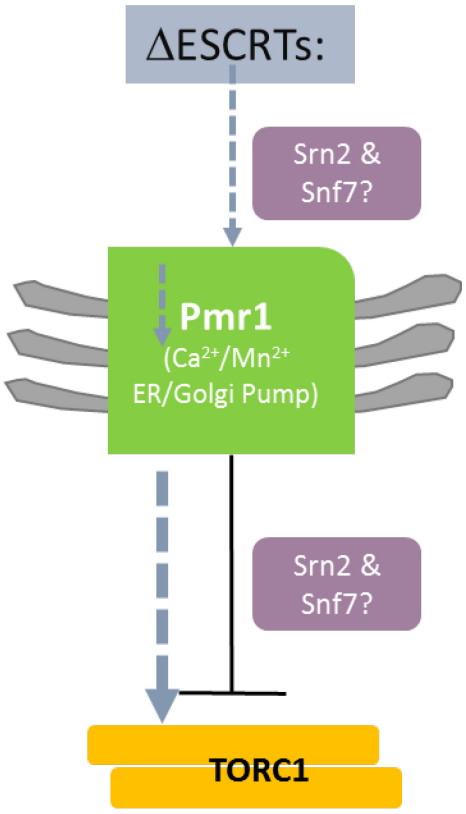

Figure 16 - Schematic depicting possible locations of ESCRT interactions within Pmr1 pathway communication with TOR.
Schematic depicting possible location of ESCRT mutants within the Pmr1 pathway. Srn2 and Snf7 maintaining/increasing high TOR activity results can place them at two positions, upstream and/or downstream of Pmr1. It is already known that the mutants of Srn2 and Snf7, upstream, lead to the decrease expression of *pmr1*, but according to the TOR activity it can also place them downstream of Pmr1 – placing them closer to TOR.

References

1. Zaman, S., Lippman, S. I., Zhao, X. & Broach, J. R. How Saccharomyces responds to nutrients. *Annu. Rev. Genet.* **42,** 27–81 (2008).
2. Dann, S. G. & Thomas, G. The amino acid sensitive TOR pathway from yeast to mammals. *FEBS Lett.* **580,** 2821–2829 (2006).
3. Kapahi, P. *et al.* With TOR, less is more: a key role for the conserved nutrient-sensing TOR pathway in aging. *Cell Metab.* **11,** 453–465 (2010).
4. Heitman, J., Movva, N. R. & Hall, M. N. Targets for cell cycle arrest by the immunosuppressant rapamycin in yeast. *Science* **253,** 905–909 (1991).
5. Wullschleger, S., Loewith, R. & Hall, M. N. TOR signaling in growth and metabolism. *Cell* **124,** 471–484 (2006).
6. Crespo, J. L. & Hall, M. N. Elucidating TOR signaling and rapamycin action: lessons from Saccharomyces cerevisiae. *Microbiol. Mol. Biol. Rev. MMBR* **66,** 579–591, table of contents (2002).
7. Lee, S. *et al.* TOR complex 2 integrates cell movement during chemotaxis and signal relay in Dictyostelium. *Mol. Biol. Cell* **16,** 4572–4583 (2005).
8. Crespo, J. L., Díaz-Troya, S. & Florencio, F. J. Inhibition of target of rapamycin signaling by rapamycin in the unicellular green alga Chlamydomonas reinhardtii. *Plant Physiol.* **139,** 1736–1749 (2005).
9. Helliwell, S. B. *et al.* TOR1 and TOR2 are structurally and functionally similar but not identical phosphatidylinositol kinase homologues in yeast. *Mol. Biol. Cell* **5,** 105–118 (1994).
10. Kunz, J. *et al.* Target of rapamycin in yeast, TOR2, is an essential phosphatidylinositol kinase homolog required for G1 progression. *Cell* **73,** 585–596 (1993).
11. Aronova, S. *et al.* Regulation of ceramide biosynthesis by TOR complex 2. *Cell Metab.* **7,** 148–158 (2008).
12. Schmelzle, T., Helliwell, S. B. & Hall, M. N. Yeast protein kinases and the RHO1 exchange factor TUS1 are novel components of the cell integrity pathway in yeast. *Mol. Cell. Biol.* **22,** 1329–1339 (2002).
13. Wullschleger, S., Loewith, R., Oppliger, W. & Hall, M. N. Molecular organization of target of rapamycin complex 2. *J. Biol. Chem.* **280,** 30697–30704 (2005).
14. Alarcon, C. M., Heitman, J. & Cardenas, M. E. Protein kinase activity and identification of a toxic effector domain of the target of rapamycin TOR proteins in yeast. *Mol. Biol. Cell* **10,** 2531–2546 (1999).
15. Bosotti, R., Isacchi, A. & Sonnhammer, E. L. FAT: a novel domain in PIK-related kinases. *Trends Biochem. Sci.* **25,** 225–227 (2000).
16. Dames, S. A., Mulet, J. M., Rathgeb-Szabo, K., Hall, M. N. & Grzesiek, S. The solution structure of the FATC domain of the protein kinase target of rapamycin suggests a role for redox-dependent structural and cellular stability. *J. Biol. Chem.* **280,** 20558–20564 (2005).
17. Loweith, R. TORC1 signaling in budding yeast. *The Enzymes* 147–176 (2010).
18. Benjamin, D., Colombi, M., Moroni, C. & Hall, M. N. Rapamycin passes the torch: a new generation of mTOR inhibitors. *Nat. Rev. Drug Discov.* **10,** 868–880 (2011).
19. Loewith, R. *et al.* Two TOR complexes, only one of which is rapamycin sensitive, have distinct roles in cell growth control. *Mol. Cell* **10,** 457–468 (2002).
20. Reinke, A. *et al.* TOR complex 1 includes a novel component, Tco89p (YPL180w), and cooperates with Ssd1p to maintain cellular integrity in Saccharomyces cerevisiae. *J. Biol. Chem.* **279,** 14752–14762 (2004).

21. Hara, K. *et al.* Raptor, a binding partner of target of rapamycin (TOR), mediates TOR action. *Cell* **110,** 177–189 (2002).
22. Jacinto, E. *et al.* Mammalian TOR complex 2 controls the actin cytoskeleton and is rapamycin insensitive. *Nat. Cell Biol.* **6,** 1122–1128 (2004).
23. Kim, D.-H. *et al.* mTOR interacts with raptor to form a nutrient-sensitive complex that signals to the cell growth machinery. *Cell* **110,** 163–175 (2002).
24. Sarbassov, D. D. *et al.* Rictor, a novel binding partner of mTOR, defines a rapamycin-insensitive and raptor-independent pathway that regulates the cytoskeleton. *Curr. Biol. CB* **14,** 1296–1302 (2004).
25. Laplante, M. & Sabatini, D. M. Regulation of mTORC1 and its impact on gene expression at a glance. *J. Cell Sci.* **126,** 1713–1719 (2013).
26. Settembre, C. *et al.* A lysosome-to-nucleus signalling mechanism senses and regulates the lysosome via mTOR and TFEB. *EMBO J.* **31,** 1095–1108 (2012).
27. Nicklin, P. *et al.* Bidirectional transport of amino acids regulates mTOR and autophagy. *Cell* **136,** 521–534 (2009).
28. Panchaud, N., Péli-Gulli, M.-P. & De Virgilio, C. SEACing the GAP that nEGOCiates TORC1 activation: evolutionary conservation of Rag GTPase regulation. *Cell Cycle Georget. Tex* **12,** 2948–2952 (2013).
29. Loewith, R. & Hall, M. N. Target of rapamycin (TOR) in nutrient signaling and growth control. *Genetics* **189,** 1177–1201 (2011).
30. Urban, J. *et al.* Sch9 is a major target of TORC1 in Saccharomyces cerevisiae. *Mol. Cell* **26,** 663–674 (2007).
31. Sturgill, T. W. *et al.* TOR1 and TOR2 have distinct locations in live cells. *Eukaryot. Cell* **7,** 1819–1830 (2008).
32. Berchtold, D. & Walther, T. C. TORC2 plasma membrane localization is essential for cell viability and restricted to a distinct domain. *Mol. Biol. Cell* **20,** 1565–1575 (2009).
33. Binda, M. *et al.* The Vam6 GEF controls TORC1 by activating the EGO complex. *Mol. Cell* **35,** 563–573 (2009).
34. Audhya, A. *et al.* Genome-wide lethality screen identifies new PI4,5P2 effectors that regulate the actin cytoskeleton. *EMBO J.* **23,** 3747–3757 (2004).
35. Loewith, R. & Hall, M. N. TOR signaling in yeast: temporal and spatial control of cell growth. *Cell Growth Control Cell Size* 139–166 (2004).
36. Barbet, N. C. *et al.* TOR controls translation initiation and early G1 progression in yeast. *Mol. Biol. Cell* **7,** 25–42 (1996).
37. Dubouloz, F., Deloche, O., Wanke, V., Cameroni, E. & De Virgilio, C. The TOR and EGO protein complexes orchestrate microautophagy in yeast. *Mol. Cell* **19,** 15–26 (2005).
38. Klionsky, D. J. *et al.* A comprehensive glossary of autophagy-related molecules and processes (2nd edition). *Autophagy* **7,** 1273–1294 (2011).
39. Lum, J. J., DeBerardinis, R. J. & Thompson, C. B. Autophagy in metazoans: cell survival in the land of plenty. *Nat. Rev. Mol. Cell Biol.* **6,** 439–448 (2005).
40. Kamada, Y. *et al.* Tor-mediated induction of autophagy via an Apg1 protein kinase complex. *J. Cell Biol.* **150,** 1507–1513 (2000).
41. Kamada, Y. *et al.* Tor directly controls the Atg1 kinase complex to regulate autophagy. *Mol. Cell. Biol.* **30,** 1049–1058 (2010).
42. Yorimitsu, T., He, C., Wang, K. & Klionsky, D. J. Tap42-associated protein phosphatase type 2A negatively regulates induction of autophagy. *Autophagy* **5,** 616–624 (2009).
43. Feng, Y., He, D., Yao, Z. & Klionsky, D. J. The machinery of macroautophagy. *Cell Res.* **24,** 24–41 (2014).

44. Klionsky, D. J. The molecular machinery of autophagy: unanswered questions. *J. Cell Sci.* **118,** 7–18 (2005).
45. Yorimitsu, T. & Klionsky, D. J. Autophagy: molecular machinery for self-eating. *Cell Death Differ.* **12 Suppl 2,** 1542–1552 (2005).
46. Shintani, T. & Klionsky, D. J. Autophagy in health and disease: a double-edged sword. *Science* **306,** 990–995 (2004).
47. Deffieu, M. *et al.* Glutathione participates in the regulation of mitophagy in yeast. *J. Biol. Chem.* **284,** 14828–14837 (2009).
48. Dunn, W. A., Jr *et al.* Pexophagy: the selective autophagy of peroxisomes. *Autophagy* **1,** 75–83 (2005).
49. Kunz, J. B., Schwarz, H. & Mayer, A. Determination of four sequential stages during microautophagy in vitro. *J. Biol. Chem.* **279,** 9987–9996 (2004).
50. Klionsky, D. J. & Eskelinen, E.-L. The vacuole versus the lysosome: when size matters. *Autophagy* **10,** 185–187 (2014).
51. Mehrpour, M., Esclatine, A., Beau, I. & Codogno, P. Overview of macroautophagy regulation in mammalian cells. *Cell Res.* **20,** 748–762 (2010).
52. He, C. & Klionsky, D. J. Atg9 trafficking in autophagy-related pathways. *Autophagy* **3,** 271–274 (2007).
53. Kim, J., Huang, W.-P., Stromhaug, P. E. & Klionsky, D. J. Convergence of multiple autophagy and cytoplasm to vacuole targeting components to a perivacuolar membrane compartment prior to de novo vesicle formation. *J. Biol. Chem.* **277,** 763–773 (2002).
54. Suzuki, K. *et al.* The pre-autophagosomal structure organized by concerted functions of APG genes is essential for autophagosome formation. *EMBO J.* **20,** 5971–5981 (2001).
55. Seglen, P. O., Gordon, P. B. & Holen, I. Non-selective autophagy. *Semin. Cell Biol.* **1,** 441–448 (1990).
56. Dunn, W. A., Jr. Studies on the mechanisms of autophagy: maturation of the autophagic vacuole. *J. Cell Biol.* **110,** 1935–1945 (1990).
57. Fimia, G. M. *et al.* Ambra1 regulates autophagy and development of the nervous system. *Nature* **447,** 1121–1125 (2007).
58. Cheong, H. *et al.* Atg17 regulates the magnitude of the autophagic response. *Mol. Biol. Cell* **16,** 3438–3453 (2005).
59. Kabeya, Y. *et al.* Atg17 functions in cooperation with Atg1 and Atg13 in yeast autophagy. *Mol. Biol. Cell* **16,** 2544–2553 (2005).
60. Kabeya, Y., Kawamata, T., Suzuki, K. & Ohsumi, Y. Cis1/Atg31 is required for autophagosome formation in Saccharomyces cerevisiae. *Biochem. Biophys. Res. Commun.* **356,** 405–410 (2007).
61. Reggiori, F. & Klionsky, D. J. Autophagic processes in yeast: mechanism, machinery and regulation. *Genetics* **194,** 341–361 (2013).
62. Stephan, J. S., Yeh, Y.-Y., Ramachandran, V., Deminoff, S. J. & Herman, P. K. The Tor and PKA signaling pathways independently target the Atg1/Atg13 protein kinase complex to control autophagy. *Proc. Natl. Acad. Sci. U. S. A.* **106,** 17049–17054 (2009).
63. Nair, U. & Klionsky, D. J. Molecular mechanisms and regulation of specific and nonspecific autophagy pathways in yeast. *J. Biol. Chem.* **280,** 41785–41788 (2005).
64. Scott, S. V. *et al.* Apg13p and Vac8p are part of a complex of phosphoproteins that are required for cytoplasm to vacuole targeting. *J. Biol. Chem.* **275,** 25840–25849 (2000).
65. Cheong, H. & Klionsky, D. J. Dual role of Atg1 in regulation of autophagy-specific PAS assembly in Saccharomyces cerevisiae. *Autophagy* **4,** 724–726 (2008).

66. Mao, K. *et al.* Atg29 phosphorylation regulates coordination of the Atg17-Atg31-Atg29 complex with the Atg11 scaffold during autophagy initiation. *Proc. Natl. Acad. Sci. U. S. A.* **110,** E2875–2884 (2013).
67. Reggiori, F., Tucker, K. A., Stromhaug, P. E. & Klionsky, D. J. The Atg1-Atg13 complex regulates Atg9 and Atg23 retrieval transport from the pre-autophagosomal structure. *Dev. Cell* **6,** 79–90 (2004).
68. He, C. *et al.* Recruitment of Atg9 to the preautophagosomal structure by Atg11 is essential for selective autophagy in budding yeast. *J. Cell Biol.* **175,** 925–935 (2006).
69. Legakis, J. E., Yen, W.-L. & Klionsky, D. J. A cycling protein complex required for selective autophagy. *Autophagy* **3,** 422–432 (2007).
70. Yen, W.-L., Legakis, J. E., Nair, U. & Klionsky, D. J. Atg27 is required for autophagy-dependent cycling of Atg9. *Mol. Biol. Cell* **18,** 581–593 (2007).
71. Obara, K., Sekito, T. & Ohsumi, Y. Assortment of phosphatidylinositol 3-kinase complexes--Atg14p directs association of complex I to the pre-autophagosomal structure in Saccharomyces cerevisiae. *Mol. Biol. Cell* **17,** 1527–1539 (2006).
72. Kihara, A., Noda, T., Ishihara, N. & Ohsumi, Y. Two distinct Vps34 phosphatidylinositol 3-kinase complexes function in autophagy and carboxypeptidase Y sorting in Saccharomyces cerevisiae. *J. Cell Biol.* **152,** 519–530 (2001).
73. Araki, Y. *et al.* Atg38 is required for autophagy-specific phosphatidylinositol 3-kinase complex integrity. *J. Cell Biol.* **203,** 299–313 (2013).
74. Shintani, T., Huang, W.-P., Stromhaug, P. E. & Klionsky, D. J. Mechanism of cargo selection in the cytoplasm to vacuole targeting pathway. *Dev. Cell* **3,** 825–837 (2002).
75. Kirisako, T. *et al.* Formation process of autophagosome is traced with Apg8/Aut7p in yeast. *J. Cell Biol.* **147,** 435–446 (1999).
76. Huang, W. P., Scott, S. V., Kim, J. & Klionsky, D. J. The itinerary of a vesicle component, Aut7p/Cvt5p, terminates in the yeast vacuole via the autophagy/Cvt pathways. *J. Biol. Chem.* **275,** 5845–5851 (2000).
77. Xie, Z., Nair, U. & Klionsky, D. J. Atg8 controls phagophore expansion during autophagosome formation. *Mol. Biol. Cell* **19,** 3290–3298 (2008).
78. Hanson, P. I. & Cashikar, A. Multivesicular body morphogenesis. *Annu. Rev. Cell Dev. Biol.* **28,** 337–362 (2012).
79. Wegner, C. S., Rodahl, L. M. W. & Stenmark, H. ESCRT proteins and cell signalling. *Traffic Cph. Den.* **12,** 1291–1297 (2011).
80. Rusten, T. E., Vaccari, T. & Stenmark, H. Shaping development with ESCRTs. *Nat. Cell Biol.* **14,** 38–45 (2012).
81. Katzmann, D. J., Odorizzi, G. & Emr, S. D. Receptor downregulation and multivesicular-body sorting. *Nat. Rev. Mol. Cell Biol.* **3,** 893–905 (2002).
82. McGettrick, A. F. & O'Neill, L. A. J. Localisation and trafficking of Toll-like receptors: an important mode of regulation. *Curr. Opin. Immunol.* **22,** 20–27 (2010).
83. Husebye, H. *et al.* Endocytic pathways regulate Toll-like receptor 4 signaling and link innate and adaptive immunity. *EMBO J.* **25,** 683–692 (2006).
84. Taelman, V. F. *et al.* Wnt signaling requires sequestration of glycogen synthase kinase 3 inside multivesicular endosomes. *Cell* **143,** 1136–1148 (2010).
85. Komada, M. & Soriano, P. Hrs, a FYVE finger protein localized to early endosomes, is implicated in vesicular traffic and required for ventral folding morphogenesis. *Genes Dev.* **13,** 1475–1485 (1999).

86. Krempler, A., Henry, M. D., Triplett, A. A. & Wagner, K.-U. Targeted deletion of the Tsg101 gene results in cell cycle arrest at G1/S and p53-independent cell death. *J. Biol. Chem.* **277,** 43216–43223 (2002).
87. Vaccari, T. & Bilder, D. The Drosophila tumor suppressor vps25 prevents nonautonomous overproliferation by regulating notch trafficking. *Dev. Cell* **9,** 687–698 (2005).
88. Thompson, B. J. *et al.* Tumor suppressor properties of the ESCRT-II complex component Vps25 in Drosophila. *Dev. Cell* **9,** 711–720 (2005).
89. Moberg, K. H., Schelble, S., Burdick, S. K. & Hariharan, I. K. Mutations in erupted, the Drosophila ortholog of mammalian tumor susceptibility gene 101, elicit non-cell-autonomous overgrowth. *Dev. Cell* **9,** 699–710 (2005).
90. Vaccari, T. *et al.* Comparative analysis of ESCRT-I, ESCRT-II and ESCRT-III function in Drosophila by efficient isolation of ESCRT mutants. *J. Cell Sci.* **122,** 2413–2423 (2009).
91. Herz, H.-M. *et al.* vps25 mosaics display non-autonomous cell survival and overgrowth, and autonomous apoptosis. *Dev. Camb. Engl.* **133,** 1871–1880 (2006).
92. Rodahl, L. M. *et al.* Disruption of Vps4 and JNK function in Drosophila causes tumour growth. *PloS One* **4,** e4354 (2009).
93. Théry, C. Exosomes: secreted vesicles and intercellular communications. *F1000 Biol. Rep.* **3,** 15 (2011).
94. Buschow, S. I. *et al.* MHC II in dendritic cells is targeted to lysosomes or T cell-induced exosomes via distinct multivesicular body pathways. *Traffic Cph. Den.* **10,** 1528–1542 (2009).
95. Trajkovic, K. *et al.* Neuron to glia signaling triggers myelin membrane exocytosis from endosomal storage sites. *J. Cell Biol.* **172,** 937–948 (2006).
96. Hurley, J. H. & Hanson, P. I. Membrane budding and scission by the ESCRT machinery: it's all in the neck. *Nat. Rev. Mol. Cell Biol.* **11,** 556–566 (2010).
97. Martin-Serrano, J. & Neil, S. J. D. Host factors involved in retroviral budding and release. *Nat. Rev. Microbiol.* **9,** 519–531 (2011).
98. Garrus, J. E. *et al.* Tsg101 and the vacuolar protein sorting pathway are essential for HIV-1 budding. *Cell* **107,** 55–65 (2001).
99. Martin-Serrano, J., Zang, T. & Bieniasz, P. D. HIV-1 and Ebola virus encode small peptide motifs that recruit Tsg101 to sites of particle assembly to facilitate egress. *Nat. Med.* **7,** 1313–1319 (2001).
100. VerPlank, L. *et al.* Tsg101, a homologue of ubiquitin-conjugating (E2) enzymes, binds the L domain in HIV type 1 Pr55(Gag). *Proc. Natl. Acad. Sci. U. S. A.* **98,** 7724–7729 (2001).
101. Pornillos, O. *et al.* HIV Gag mimics the Tsg101-recruiting activity of the human Hrs protein. *J. Cell Biol.* **162,** 425–434 (2003).
102. Von Schwedler, U. K. *et al.* The protein network of HIV budding. *Cell* **114,** 701–713 (2003).
103. Fisher, R. D. *et al.* Structural and biochemical studies of ALIX/AIP1 and its role in retrovirus budding. *Cell* **128,** 841–852 (2007).
104. Strack, B., Calistri, A., Craig, S., Popova, E. & Göttlinger, H. G. AIP1/ALIX is a binding partner for HIV-1 p6 and EIAV p9 functioning in virus budding. *Cell* **114,** 689–699 (2003).
105. Morita, E. *et al.* ESCRT-III protein requirements for HIV-1 budding. *Cell Host Microbe* **9,** 235–242 (2011).
106. Mueller, M., Adell, M. A. Y. & Teis, D. Membrane abscission: first glimpse at dynamic ESCRTs. *Curr. Biol. CB* **22,** R603–605 (2012).
107. Carlton, J. G. & Martin-Serrano, J. Parallels between cytokinesis and retroviral budding: a role for the ESCRT machinery. *Science* **316,** 1908–1912 (2007).

108. Guizetti, J. *et al.* Cortical constriction during abscission involves helices of ESCRT-III-dependent filaments. *Science* **331,** 1616–1620 (2011).
109. Yang, D. *et al.* Structural basis for midbody targeting of spastin by the ESCRT-III protein CHMP1B. *Nat. Struct. Mol. Biol.* **15,** 1278–1286 (2008).
110. Elia, N., Sougrat, R., Spurlin, T. A., Hurley, J. H. & Lippincott-Schwartz, J. Dynamics of endosomal sorting complex required for transport (ESCRT) machinery during cytokinesis and its role in abscission. *Proc. Natl. Acad. Sci. U. S. A.* **108,** 4846–4851 (2011).
111. Elia, N., Fabrikant, G., Kozlov, M. M. & Lippincott-Schwartz, J. Computational model of cytokinetic abscission driven by ESCRT-III polymerization and remodeling. *Biophys. J.* **102,** 2309–2320 (2012).
112. Manil-Segalén, M., Lefebvre, C., Culetto, E. & Legouis, R. Need an ESCRT for autophagosomal maturation? *Commun. Integr. Biol.* **5,** 566–571 (2012).
113. Parkinson, N. *et al.* ALS phenotypes with mutations in CHMP2B (charged multivesicular body protein 2B). *Neurology* **67,** 1074–1077 (2006).
114. Skibinski, G. *et al.* Mutations in the endosomal ESCRTIII-complex subunit CHMP2B in frontotemporal dementia. *Nat. Genet.* **37,** 806–808 (2005).
115. Talbot, K. & Ansorge, O. Recent advances in the genetics of amyotrophic lateral sclerosis and frontotemporal dementia: common pathways in neurodegenerative disease. *Hum. Mol. Genet.* **15 Spec No 2,** R182–187 (2006).
116. Filimonenko, M. *et al.* Functional multivesicular bodies are required for autophagic clearance of protein aggregates associated with neurodegenerative disease. *J. Cell Biol.* **179,** 485–500 (2007).
117. Jin, M., Liu, X. & Klionsky, D. J. SnapShot: Selective autophagy. *Cell* **152,** 368–368.e2 (2013).
118. Banta, L. M., Robinson, J. S., Klionsky, D. J. & Emr, S. D. Organelle assembly in yeast: characterization of yeast mutants defective in vacuolar biogenesis and protein sorting. *J. Cell Biol.* **107,** 1369–1383 (1988).
119. Raymond, C. K., Howald-Stevenson, I., Vater, C. A. & Stevens, T. H. Morphological classification of the yeast vacuolar protein sorting mutants: evidence for a prevacuolar compartment in class E vps mutants. *Mol. Biol. Cell* **3,** 1389–1402 (1992).
120. Robinson, J. S., Klionsky, D. J., Banta, L. M. & Emr, S. D. Protein sorting in Saccharomyces cerevisiae: isolation of mutants defective in the delivery and processing of multiple vacuolar hydrolases. *Mol. Cell. Biol.* **8,** 4936–4948 (1988).
121. Rothman, J. H., Howald, I. & Stevens, T. H. Characterization of genes required for protein sorting and vacuolar function in the yeast Saccharomyces cerevisiae. *EMBO J.* **8,** 2057–2065 (1989).
122. Rothman, J. H. & Stevens, T. H. Protein sorting in yeast: mutants defective in vacuole biogenesis mislocalize vacuolar proteins into the late secretory pathway. *Cell* **47,** 1041–1051 (1986).
123. Babst, M., Sato, T. K., Banta, L. M. & Emr, S. D. Endosomal transport function in yeast requires a novel AAA-type ATPase, Vps4p. *EMBO J.* **16,** 1820–1831 (1997).
124. Katzmann, D. J., Babst, M. & Emr, S. D. Ubiquitin-dependent sorting into the multivesicular body pathway requires the function of a conserved endosomal protein sorting complex, ESCRT-I. *Cell* **106,** 145–155 (2001).
125. Babst, M., Odorizzi, G., Estepa, E. J. & Emr, S. D. Mammalian tumor susceptibility gene 101 (TSG101) and the yeast homologue, Vps23p, both function in late endosomal trafficking. *Traffic Cph. Den.* **1,** 248–258 (2000).

126. Babst, M., Wendland, B., Estepa, E. J. & Emr, S. D. The Vps4p AAA ATPase regulates membrane association of a Vps protein complex required for normal endosome function. *EMBO J.* **17,** 2982–2993 (1998).
127. Jouvenet, N. Dynamics of ESCRT proteins. *Cell. Mol. Life Sci. CMLS* **69,** 4121–4133 (2012).
128. Schuh, A. L. & Audhya, A. The ESCRT machinery: From the plasma membrane to endosomes and back again. *Crit. Rev. Biochem. Mol. Biol.* (2014). doi:10.3109/10409238.2014.881777
129. Henne, W. M., Buchkovich, N. J. & Emr, S. D. The ESCRT pathway. *Dev. Cell* **21,** 77–91 (2011).
130. Prag, G. *et al.* The Vps27/Hse1 complex is a GAT domain-based scaffold for ubiquitin-dependent sorting. *Dev. Cell* **12,** 973–986 (2007).
131. Ren, X. *et al.* Hybrid structural model of the complete human ESCRT-0 complex. *Struct. Lond. Engl. 1993* **17,** 406–416 (2009).
132. Mayers, J. R. *et al.* ESCRT-0 assembles as a heterotetrameric complex on membranes and binds multiple ubiquitinylated cargoes simultaneously. *J. Biol. Chem.* **286,** 9636–9645 (2011).
133. Hirano, S. *et al.* Double-sided ubiquitin binding of Hrs-UIM in endosomal protein sorting. *Nat. Struct. Mol. Biol.* **13,** 272–277 (2006).
134. Raiborg, C. *et al.* FYVE and coiled-coil domains determine the specific localisation of Hrs to early endosomes. *J. Cell Sci.* **114,** 2255–2263 (2001).
135. Stahelin, R. V. *et al.* Phosphatidylinositol 3-phosphate induces the membrane penetration of the FYVE domains of Vps27p and Hrs. *J. Biol. Chem.* **277,** 26379–26388 (2002).
136. Raiborg, C. *et al.* Hrs sorts ubiquitinated proteins into clathrin-coated microdomains of early endosomes. *Nat. Cell Biol.* **4,** 394–398 (2002).
137. Ren, X. & Hurley, J. H. VHS domains of ESCRT-0 cooperate in high-avidity binding to polyubiquitinated cargo. *EMBO J.* **29,** 1045–1054 (2010).
138. Kato, M., Miyazawa, K. & Kitamura, N. A deubiquitinating enzyme UBPY interacts with the Src homology 3 domain of Hrs-binding protein via a novel binding motif PX(V/I)(D/N)RXXKP. *J. Biol. Chem.* **275,** 37481–37487 (2000).
139. Tanaka, N. *et al.* Possible involvement of a novel STAM-associated molecule 'AMSH' in intracellular signal transduction mediated by cytokines. *J. Biol. Chem.* **274,** 19129–19135 (1999).
140. Chu, T., Sun, J., Saksena, S. & Emr, S. D. New component of ESCRT-I regulates endosomal sorting complex assembly. *J. Cell Biol.* **175,** 815–823 (2006).
141. Curtiss, M., Jones, C. & Babst, M. Efficient cargo sorting by ESCRT-I and the subsequent release of ESCRT-I from multivesicular bodies requires the subunit Mvb12. *Mol. Biol. Cell* **18,** 636–645 (2007).
142. Agromayor, M. *et al.* The UBAP1 subunit of ESCRT-I interacts with ubiquitin via a SOUBA domain. *Struct. Lond. Engl. 1993* **20,** 414–428 (2012).
143. Audhya, A., McLeod, I. X., Yates, J. R. & Oegema, K. MVB-12, a fourth subunit of metazoan ESCRT-I, functions in receptor downregulation. *PloS One* **2,** e956 (2007).
144. Bache, K. G. *et al.* The growth-regulatory protein HCRP1/hVps37A is a subunit of mammalian ESCRT-I and mediates receptor down-regulation. *Mol. Biol. Cell* **15,** 4337–4346 (2004).
145. Bishop, N. & Woodman, P. TSG101/mammalian VPS23 and mammalian VPS28 interact directly and are recruited to VPS4-induced endosomes. *J. Biol. Chem.* **276,** 11735–11742 (2001).

146. Kostelansky, M. S. *et al.* Molecular architecture and functional model of the complete yeast ESCRT-I heterotetramer. *Cell* **129,** 485–498 (2007).
147. Morita, E. *et al.* Identification of human MVB12 proteins as ESCRT-I subunits that function in HIV budding. *Cell Host Microbe* **2,** 41–53 (2007).
148. Pashkova, N. & Piper, R. C. UBAP1: a new ESCRT member joins the cl_Ub. *Struct. Lond. Engl. 1993* **20,** 383–385 (2012).
149. Boura, E. *et al.* Solution structure of the ESCRT-I complex by small-angle X-ray scattering, EPR, and FRET spectroscopy. *Proc. Natl. Acad. Sci. U. S. A.* **108,** 9437–9442 (2011).
150. Bache, K. G., Brech, A., Mehlum, A. & Stenmark, H. Hrs regulates multivesicular body formation via ESCRT recruitment to endosomes. *J. Cell Biol.* **162,** 435–442 (2003).
151. Bilodeau, P. S., Winistorfer, S. C., Kearney, W. R., Robertson, A. D. & Piper, R. C. Vps27-Hse1 and ESCRT-I complexes cooperate to increase efficiency of sorting ubiquitinated proteins at the endosome. *J. Cell Biol.* **163,** 237–243 (2003).
152. Katzmann, D. J., Stefan, C. J., Babst, M. & Emr, S. D. Vps27 recruits ESCRT machinery to endosomes during MVB sorting. *J. Cell Biol.* **162,** 413–423 (2003).
153. Lu, Q., Hope, L. W., Brasch, M., Reinhard, C. & Cohen, S. N. TSG101 interaction with HRS mediates endosomal trafficking and receptor down-regulation. *Proc. Natl. Acad. Sci. U. S. A.* **100,** 7626–7631 (2003).
154. Pornillos, O. *et al.* Structure and functional interactions of the Tsg101 UEV domain. *EMBO J.* **21,** 2397–2406 (2002).
155. Sundquist, W. I. *et al.* Ubiquitin recognition by the human TSG101 protein. *Mol. Cell* **13,** 783–789 (2004).
156. Shields, S. B. *et al.* ESCRT ubiquitin-binding domains function cooperatively during MVB cargo sorting. *J. Cell Biol.* **185,** 213–224 (2009).
157. Stefani, F. *et al.* UBAP1 is a component of an endosome-specific ESCRT-I complex that is essential for MVB sorting. *Curr. Biol. CB* **21,** 1245–1250 (2011).
158. De Souza, R. F. & Aravind, L. UMA and MABP domains throw light on receptor endocytosis and selection of endosomal cargoes. *Bioinforma. Oxf. Engl.* **26,** 1477–1480 (2010).
159. Wollert, T. & Hurley, J. H. Molecular mechanism of multivesicular body biogenesis by ESCRT complexes. *Nature* **464,** 864–869 (2010).
160. Babst, M., Katzmann, D. J., Snyder, W. B., Wendland, B. & Emr, S. D. Endosome-associated complex, ESCRT-II, recruits transport machinery for protein sorting at the multivesicular body. *Dev. Cell* **3,** 283–289 (2002).
161. Im, Y. J. & Hurley, J. H. Integrated structural model and membrane targeting mechanism of the human ESCRT-II complex. *Dev. Cell* **14,** 902–913 (2008).
162. Hierro, A. *et al.* Structure of the ESCRT-II endosomal trafficking complex. *Nature* **431,** 221–225 (2004).
163. Teo, H., Perisic, O., González, B. & Williams, R. L. ESCRT-II, an endosome-associated complex required for protein sorting: crystal structure and interactions with ESCRT-III and membranes. *Dev. Cell* **7,** 559–569 (2004).
164. Henne, W. M., Buchkovich, N. J., Zhao, Y. & Emr, S. D. The endosomal sorting complex ESCRT-II mediates the assembly and architecture of ESCRT-III helices. *Cell* **151,** 356–371 (2012).
165. Slagsvold, T. *et al.* Eap45 in mammalian ESCRT-II binds ubiquitin via a phosphoinositide-interacting GLUE domain. *J. Biol. Chem.* **280,** 19600–19606 (2005).
166. Teo, H. *et al.* ESCRT-I core and ESCRT-II GLUE domain structures reveal role for GLUE in linking to ESCRT-I and membranes. *Cell* **125,** 99–111 (2006).
167. Alam, S. L. *et al.* Ubiquitin interactions of NZF zinc fingers. *EMBO J.* **23,** 1411–1421 (2004).

168. Gill, D. J. *et al.* Structural insight into the ESCRT-I/-II link and its role in MVB trafficking. *EMBO J.* **26,** 600–612 (2007).
169. Babst, M., Katzmann, D. J., Estepa-Sabal, E. J., Meerloo, T. & Emr, S. D. Escrt-III: an endosome-associated heterooligomeric protein complex required for mvb sorting. *Dev. Cell* **3,** 271–282 (2002).
170. Luhtala, N. & Odorizzi, G. Bro1 coordinates deubiquitination in the multivesicular body pathway by recruiting Doa4 to endosomes. *J. Cell Biol.* **166,** 717–729 (2004).
171. Odorizzi, G., Katzmann, D. J., Babst, M., Audhya, A. & Emr, S. D. Bro1 is an endosome-associated protein that functions in the MVB pathway in Saccharomyces cerevisiae. *J. Cell Sci.* **116,** 1893–1903 (2003).
172. Scott, A. *et al.* Structure and ESCRT-III protein interactions of the MIT domain of human VPS4A. *Proc. Natl. Acad. Sci. U. S. A.* **102,** 13813–13818 (2005).
173. Scott, A. *et al.* Structural and mechanistic studies of VPS4 proteins. *EMBO J.* **24,** 3658–3669 (2005).
174. Yu, Z., Gonciarz, M. D., Sundquist, W. I., Hill, C. P. & Jensen, G. J. Cryo-EM structure of dodecameric Vps4p and its 2:1 complex with Vta1p. *J. Mol. Biol.* **377,** 364–377 (2008).
175. Hanson, P. I., Roth, R., Lin, Y. & Heuser, J. E. Plasma membrane deformation by circular arrays of ESCRT-III protein filaments. *J. Cell Biol.* **180,** 389–402 (2008).
176. Muzioł, T. *et al.* Structural basis for budding by the ESCRT-III factor CHMP3. *Dev. Cell* **10,** 821–830 (2006).
177. Teis, D., Saksena, S. & Emr, S. D. Ordered assembly of the ESCRT-III complex on endosomes is required to sequester cargo during MVB formation. *Dev. Cell* **15,** 578–589 (2008).
178. Lata, S. *et al.* Helical structures of ESCRT-III are disassembled by VPS4. *Science* **321,** 1354–1357 (2008).
179. Fabrikant, G. *et al.* Computational model of membrane fission catalyzed by ESCRT-III. *PLoS Comput. Biol.* **5,** e1000575 (2009).
180. Wollert, T., Wunder, C., Lippincott-Schwartz, J. & Hurley, J. H. Membrane scission by the ESCRT-III complex. *Nature* **458,** 172–177 (2009).
181. Saksena, S., Wahlman, J., Teis, D., Johnson, A. E. & Emr, S. D. Functional reconstitution of ESCRT-III assembly and disassembly. *Cell* **136,** 97–109 (2009).
182. Teng, X. *et al.* Genome-wide consequences of deleting any single gene. *Mol. Cell* **52,** 485–494 (2013).
183. Cheng, W.-C. *et al.* Fis1 deficiency selects for compensatory mutations responsible for cell death and growth control defects. *Cell Death Differ.* **15,** 1838–1846 (2008).
184. Teng, X. Unpublished.
185. Dayhoff-Brannigan, M. *Identifying novel genes involved in amino acid sensing*. (2014).
186. Teng, X. *et al.* Gene-dependent cell death in yeast. *Cell Death Dis.* **2,** e188 (2011).
187. Zhao, Y., Du, J., Xiong, B., Xu, H. & Jiang, L. ESCRT components regulate the expression of the ER/Golgi calcium pump gene PMR1 through the Rim101/Nrg1 pathway in budding yeast. *J. Mol. Cell Biol.* **5,** 336–344 (2013).
188. Devasahayam, G., Ritz, D., Helliwell, S. B., Burke, D. J. & Sturgill, T. W. Pmr1, a Golgi Ca2+/Mn2+-ATPase, is a regulator of the target of rapamycin (TOR) signaling pathway in yeast. *Proc. Natl. Acad. Sci. U. S. A.* **103,** 17840–17845 (2006).
189. *Guide to Yeast Genetics and Molecular and Cell Biology - Part B*. **350,** (Elsevier Science (USA), 2002).
190. Graef, M. & Nunnari, J. Mitochondria regulate autophagy by conserved signalling pathways. *EMBO J.* **30,** 2101–2114 (2011).
191. Piper, R. C. Successful transporter gets an EGO boost. *Dev. Cell* **11,** 6–7 (2006).

192. Gao, M. & Kaiser, C. A. A conserved GTPase-containing complex is required for intracellular sorting of the general amino-acid permease in yeast. *Nat. Cell Biol.* **8,** 657–667 (2006).
193. Kim, E., Goraksha-Hicks, P., Li, L., Neufeld, T. P. & Guan, K.-L. Regulation of TORC1 by Rag GTPases in nutrient response. *Nat. Cell Biol.* **10,** 935–945 (2008).
194. Sancak, Y. *et al.* The Rag GTPases bind raptor and mediate amino acid signaling to mTORC1. *Science* **320,** 1496–1501 (2008).
195. Kim, E. & Guan, K.-L. RAG GTPases in nutrient-mediated TOR signaling pathway. *Cell Cycle Georget. Tex* **8,** 1014–1018 (2009).
196. Rudolph, H. K. *et al.* The yeast secretory pathway is perturbed by mutations in PMR1, a member of a Ca2+ ATPase family. *Cell* **58,** 133–145 (1989).
197. Berridge, M. J. Cardiac calcium signalling. *Biochem. Soc. Trans.* **31,** 930–933 (2003).
198. Medler, K. F. Calcium signaling in taste cells: regulation required. *Chem. Senses* **35,** 753–765 (2010).
199. Bonilla, M. & Cunningham, K. W. Calcium release and influx in yeast: TRPC and VGCC rule another kingdom. *Sci. STKE Signal Transduct. Knowl. Environ.* **2002,** pe17 (2002).
200. Cui, J., Kaandorp, J. A., Sloot, P. M. A., Lloyd, C. M. & Filatov, M. V. Calcium homeostasis and signaling in yeast cells and cardiac myocytes. *FEMS Yeast Res.* **9,** 1137–1147 (2009).
201. Cunningham, K. W. Acidic calcium stores of Saccharomyces cerevisiae. *Cell Calcium* **50,** 129–138 (2011).
202. Cunningham, K. W. & Fink, G. R. Calcineurin inhibits VCX1-dependent H+/Ca2+ exchange and induces Ca2+ ATPases in Saccharomyces cerevisiae. *Mol. Cell. Biol.* **16,** 2226–2237 (1996).
203. Stathopoulos, A. M. & Cyert, M. S. Calcineurin acts through the CRZ1/TCN1-encoded transcription factor to regulate gene expression in yeast. *Genes Dev.* **11,** 3432–3444 (1997).
204. Dürr, G. *et al.* The medial-Golgi ion pump Pmr1 supplies the yeast secretory pathway with Ca2+ and Mn2+ required for glycosylation, sorting, and endoplasmic reticulum-associated protein degradation. *Mol. Biol. Cell* **9,** 1149–1162 (1998).
205. Matheos, D. P., Kingsbury, T. J., Ahsan, U. S. & Cunningham, K. W. Tcn1p/Crz1p, a calcineurin-dependent transcription factor that differentially regulates gene expression in Saccharomyces cerevisiae. *Genes Dev.* **11,** 3445–3458 (1997).
206. Feng, M. *et al.* Store-independent activation of Orai1 by SPCA2 in mammary tumors. *Cell* **143,** 84–98 (2010).

Appendix i: Yeast Strains

Contains all strains created and used during any assays and tetrad dissections. This list contains both the parent strains, transformed strains, and the substrains (tetrad spores).
Notes:
*NT – Not True Tetrad
MAT? – mating type can't be distinguished

Name	Background	Genotype
WTa	BY4741	*MATa his3 leu2 ura3 met15*
WTα	BY4742	*MATalpha his3 leu2 ura3 lys2*
Tester a	BY	*MATa lys1D0*
Tester α	BY	*MATα lys1D0*
ΔWhi2_ss1	BY4741	*MATa his3 leu2 ura3 met15*
Δ*vps27_ss1*	BY4741	*MATa his3 leu2 ura3 met15*
Δ*srn2_ss1*	BY4741	*MATa his3 leu2 ura3 met15*
Δ*vps28_ss1*	BY4741	*MATa his3 leu2 ura3 met15*
Δ*mvb12_ss1*	BY4741	*MATa his3 leu2 ura3 met15*
Δ*snf8_ss1*	BY4741	*MATa his3 leu2 ura3 met15*
Δ*vps36_ss1*	BY4741	*MATa his3 leu2 ura3 met15*
Δ*snf7_ss1*	BY4741	*MATa his3 leu2 ura3 met15*
Δ*vps20_ss1*	BY4741	*MATa his3 leu2 ura3 met15*
Δ*did4_ss1*	BY4741	*MATa his3 leu2 ura3 met15*
Δ*vps24_ss1*	BY4741	*MATa his3 leu2 ura3 met15*
Δ*vps60_ss1*	BY4741	*MATa his3 leu2 ura3 met15*
Δ*vps27 prATG8[atg8/GFP]*	BY4741	*MATa his3 leu2 ura3 met15 vps27::KanMX4*
Δ*srn2 prATG8[atg8/GFP]*	BY4741	*MATa his3 leu2 ura3 met15 srn2::KanMX4*
Δ*srn2_6d prATG8[atg8/GFP]*	BY4741	*MATa his3 leu2 ura3 met15 srn2::KanMX4*
Δ*snf8 prATG8[atg8/GFP]*	BY4741	*MATa his3 leu2 ura3 met15 snf8::KanMX4*
Δ*snf7 prATG8[atg8/GFP]*	BY4741	*MATa his3 leu2 ura3 met15 snf7::KanMX4*
WTα *prATG8[atg8/GFP]*	BY4741	*MATa his3 leu2 ura3 met15*
Δ*Whi2 prATG8[atg8/GFP]*	BY4741	*MATa his3 leu2 ura3 met15 Whi2:KanMX4*
Δ*vps27_1a*	sporulated from WT BY4742 x Δ*vps27*	*MATa his3 leu2 ura3 met15*
Δ*vps27_1b*	sporulated from WT BY4742 x Δ*vps27*	*MATalpha his3 leu2 ura3*
Δ*vps27_1c*	sporulated from WT BY4742 x Δ*vps27*	*MATa his3 leu2 ura3 lys2 met15 vps27::KanMX4*
Δ*vps27_1d*	sporulated from WT BY4742 x Δ*vps27*	*MATalpha his3 leu2 ura3 lys2 vps27::KanMX4*

Δ*vps27_2a*	sporulated from WT BY4742 x Δ*vps27*	*MATalpha his3 leu2 ura3 lys2*
Δ*vps27_2b*	sporulated from WT BY4742 x Δ*vps27*	*MATa his3 leu2 ura3*
Δ*vps27_2c*	sporulated from WT BY4742 x Δ*vps27*	*MATalpha his3 leu2 ura3 met15 vps27::KanMX4*
Δ*vps27_2d*	sporulated from WT BY4742 x Δ*vps27*	*MATa his3 leu2 ura3 lys2 met15 vps27::KanMX4*
Δ*vps27_3a*	sporulated from WT BY4742 x Δ*vps27*	*MATa his3 leu2 ura3 lys2*
Δ*vps27_3b*	sporulated from WT BY4742 x Δ*vps27*	*MATa his3 leu2 ura3 met15 vps27::KanMX4*
Δ*vps27_3c*	sporulated from WT BY4742 x Δ*vps27*	*MATalpha his3 leu2 ura3*
Δ*vps27_3d*	sporulated from WT BY4742 x Δ*vps27*	*MATalpha his3 leu2 ura3 lys2 met15 vps27::KanMX4*
Δ*vps27_4a*	sporulated from WT BY4742 x Δ*vps27*	*MATa his3 leu2 ura3 met15*
Δ*vps27_4b*	sporulated from WT BY4742 x Δ*vps27*	*MATalpha his3 leu2 ura3 lys2 vps27::KanMX4*
Δ*vps27_4c*	sporulated from WT BY4742 x Δ*vps27*	*MATalpha his3 leu2 ura3 lys2*
Δ*vps27_4d*	sporulated from WT BY4742 x Δ*vps27*	*MATa his3 leu2 ura3 vps27::KanMX4*
Δ*vps27_5a*	sporulated from WT BY4742 x Δ*vps27*	*MATa his3 leu2 ura3 lys2 met15*
Δ*vps27_5b*	sporulated from WT BY4742 x Δ*vps27*	*MATalpha his3 leu2 ura3 met15*
Δ*vps27_5c*	sporulated from WT BY4742 x Δ*vps27*	*MATa his3 leu2 ura3 vps27::KanMX4*
Δ*vps27_5d*	sporulated from WT BY4742 x Δ*vps27*	*MATalpha his3 leu2 ura3 lys2 vps27::KanMX4*
Δ*vps27_6a*	sporulated from WT BY4742 x Δ*vps27*	*MATa his3 leu2 ura3 lys2*
Δ*vps27_6b*	sporulated from WT BY4742 x Δ*vps27*	*MATa his3 leu2 ura3 vps27::KanMX4*
Δ*vps27_6c*	sporulated from WT BY4742 x Δ*vps27*	*MATalpha his3 leu2 ura3 met15*
Δ*vps27_6d*	sporulated from WT BY4742 x Δ*vps27*	*MATalpha his3 leu2 ura3 lys2 met15 vps27::KanMX4*
Δ*vps27_7a*	sporulated from WT BY4742 x Δ*vps27*	*MATa his3 leu2 ura3 met15 vps27::KanMX4*
Δ*vps27_7b*	sporulated from WT BY4742 x Δ*vps27*	*MATalpha his3 leu2 ura3 lys2*
Δ*vps27_7c*	sporulated from WT BY4742 x Δ*vps27*	*MATa his3 leu2 ura3 vps27::KanMX4*
Δ*vps27_7d*	sporulated from WT BY4742 x Δ*vps27*	*MATalpha his3 leu2 ura3 lys2 met15*
Δ*vps27_8a*	sporulated from WT BY4742 x Δ*vps27*	*MATa his3 leu2 ura3 lys2 met15 vps27::KanMX4*
Δ*vps27_8b*	sporulated from WT BY4742 x Δ*vps27*	*MATalpha his3 leu2 ura3 lys2 met15*
Δ*vps27_8c*	sporulated from WT BY4742 x Δ*vps27*	*MATa his3 leu2 ura3 vps27::KanMX4*
Δ*vps27_8d*	sporulated from WT BY4742 x Δ*vps27*	*MATalpha his3 leu2 ura3*
Δ*vps27_9a*	sporulated from WT BY4742 x Δ*vps27*	*MATa his3 leu2 ura3 lys2*
Δ*vps27_9b*	sporulated from WT BY4742 x Δ*vps27*	*MATalpha his3 leu2 ura3 lys2 met15 vps27::KanMX4*
Δ*vps27_9c*	sporulated from WT BY4742 x Δ*vps27*	*MATa his3 leu2 ura3 met15*
Δ*vps27_9d*	sporulated from WT BY4742 x Δ*vps27*	*MATalpha his3 leu2 ura3 vps27::KanMX4*
Δ*vps27_10a*	sporulated from WT BY4742 x Δ*vps27*	*MATa his3 leu2 ura3 vps27::KanMX4*
Δ*vps27_10b*	sporulated from WT BY4742 x Δ*vps27*	*MATalpha his3 leu2 ura3 met15*
Δ*vps27_10c*	sporulated from WT BY4742 x Δ*vps27*	*his3 leu2 ura3 lys2 met15 vps27::KanMX4*
Δ*vps27_10d*	sporulated from WT BY4742 x Δ*vps27*	*MATalpha his3 leu2 ura3 lys2*

Δ*vps27_11a*	sporulated from WT BY4742 x Δ*vps27*	-
Δ*vps27_11b*	sporulated from WT BY4742 x Δ*vps27*	*MATa his3 leu2 ura3 lys2 met15 vps27::KanMX4*
Δ*vps27_11c*	sporulated from WT BY4742 x Δ*vps27*	*MATalpha his3 leu2 ura3*
Δ*vps27_11d*	sporulated from WT BY4742 x Δ*vps27*	*MATa his3 leu2 ura3 met15*
WTα*_12a*	BY4742	*MATalpha his3 leu2 ura3 met15*
Δ*Whi2_12b*	BY4741	*MATa his3 leu2 ura3 lys2 Whi2::KanMX4*
Δ*vps27_12c*	BY4741	*MATa his3 leu2 ura3 lys2 vps27::KanMX4*
Δ*vps28_1a*	sporulated from WT BY4742 x Δ*vps28*	*MATa his3 leu2 ura3 met15*
Δ*vps28_1b*	sporulated from WT BY4742 x Δ*vps28*	*MATa his3 leu2 ura3 lys2 met15 vps28::KanMX4*
Δ*vps28_1c*	sporulated from WT BY4742 x Δ*vps28*	*MATalpha his3 leu2 ura3 lys2*
Δ*vps28_1d*	sporulated from WT BY4742 x Δ*vps28*	*MATalpha his3 leu2 ura3 vps28::KanMX4*
Δ*vps28_2a*^{*NT}	sporulated from WT BY4742 x Δ*vps28*	*MATa his3 leu2 ura3 vps28::KanMX4*
Δ*vps28_2b*^{*NT}	sporulated from WT BY4742 x Δ*vps28*	*MATa his3 leu2 ura3 lys2 met15 vps28::KanMX4*
Δ*vps28_2c*^{*NT}	sporulated from WT BY4742 x Δ*vps28*	*MATalpha his3 leu2 ura3 lys2 vps28::KanMX4*
Δ*vps28_2d*^{*NT}	sporulated from WT BY4742 x Δ*vps28*	*MATalpha his3 leu2 ura3 lys2 met15*
Δ*vps28_3a*^{*NT}	sporulated from WT BY4742 x Δ*vps28*	*Did not grow, not true tetrad*
Δ*vps28_3b*^{*NT}	sporulated from WT BY4742 x Δ*vps28*	*Did not grow, not true tetrad*
Δ*vps28_3c*^{*NT}	sporulated from WT BY4742 x Δ*vps28*	*Did not grow, not true tetrad*
Δ*vps28_3d*^{*NT}	sporulated from WT BY4742 x Δ*vps28*	*Did not grow, not true tetrad*
Δ*vps28_4a*	sporulated from WT BY4742 x Δ*vps28*	*MATalpha his3 leu2 ura3 met15 vps28::KanMX4*
Δ*vps28_4b*	sporulated from WT BY4742 x Δ*vps28*	*MATa his3 leu2 ura3*
Δ*vps28_4c*	sporulated from WT BY4742 x Δ*vps28*	*MATa his3 leu2 ura3 lys2 met15*
Δ*vps28_4d*	sporulated from WT BY4742 x Δ*vps28*	*MATalpha his3 leu2 ura3 lys2 vps28::KanMX4*
Δ*vps28_5a*^{*NT}	sporulated from WT BY4742 x Δ*vps28*	*MATalpha his3 leu2 ura3 lys2 met15*
Δ*vps28_5b*^{*NT}	sporulated from WT BY4742 x Δ*vps28*	*MAT? his3 leu2 ura3 lys2 met15 vps28::KanMX4*
Δ*vps28_5c*^{*NT}	sporulated from WT BY4742 x Δ*vps28*	*MATalpha his3 leu2 ura3 met15*
Δ*vps28_5d*^{*NT}	sporulated from WT BY4742 x Δ*vps28*	*MAT? his3 leu2 ura3 lys2 vps28::KanMX4*
Δ*vps28_6a*	sporulated from WT BY4742 x Δ*vps28*	*MATalpha his3 leu2 ura3 lys2 vps28::KanMX4*
Δ*vps28_6b*	sporulated from WT BY4742 x ^{*NT} Δ*vps28*	*MATalpha his3 leu2 ura3 lys2 met15*
Δ*vps28_6c*	sporulated from WT BY4742 x Δ*vps28*	*MATa his3 leu2 ura3 vps28::KanMX4*
Δ*vps28_6d*	sporulated from WT BY4742 x Δ*vps28*	*MATa his3 leu2 ura3 met15*
Δ*vps28_7a*^{*NT}	sporulated from WT BY4742 x Δ*vps28*	*MAT? his3 leu2 ura3 lys2 met15 vps28::KanMX4*
Δ*vps28_7b*^{*NT}	sporulated from WT BY4742 x Δ*vps28*	*MATalpha his3 leu2 ura3 lys2*
Δ*vps28_7c*^{*NT}	sporulated from WT BY4742 x Δ*vps28*	*MATa his3 leu2 ura3 met15*
Δ*vps28_7d*^{*NT}	sporulated from WT BY4742 x Δ*vps28*	*MATa his3 leu2 ura3 met15 vps28::KanMX4*
Δ*vps28_8a*	sporulated from WT BY4742 x Δ*vps28*	*MATa his3 leu2 ura3*

Δ*vps28_8b*	sporulated from WT BY4742 x Δ*vps28*	*MATalpha his3 leu2 ura3 met15 vps28::KanMX4*
Δ*vps28_8c*	sporulated from WT BY4742 x Δ*vps28*	*MATa his3 leu2 ura3 lys2*
Δ*vps28_8d*	sporulated from WT BY4742 x Δ*vps28*	*MATalpha his3 leu2 ura3 lys2 met15 vps28::KanMX4*
Δ*vps28_9a*	sporulated from WT BY4742 x Δ*vps28*	*MATa his3 leu2 ura3 lys2 met15 vps28::KanMX4*
Δ*vps28_9b*	sporulated from WT BY4742 x Δ*vps28*	*MATa his3 leu2 ura3 vps28::KanMX4*
Δ*vps28_9c*	sporulated from WT BY4742 x Δ*vps28*	*MATalpha his3 leu2 ura3*
Δ*vps28_9d*	sporulated from WT BY4742 x Δ*vps28*	*MATalpha his3 leu2 ura3 lys2 met15*
Δ*vps28_10a*	sporulated from WT BY4742 x Δ*vps28*	*MATalpha his3 leu2 ura3 lys2 vps28::KanMX4*
Δ*vps28_10b*	sporulated from WT BY4742 x Δ*vps28*	*MATa his3 leu2 ura3 lys2 vps28::KanMX4*
Δ*vps28_10c*	sporulated from WT BY4742 x Δ*vps28*	*MATalpha his3 leu2 ura3 met15*
Δ*vps28_10d*	sporulated from WT BY4742 x Δ*vps28*	*MATa his3 leu2 ura3 met15*
Δ*vps28_11a*^{*NT}	sporulated from WT BY4742 x Δ*vps28*	*MAT? his3 leu2 ura3 lys2 met15 vps28::KanMX4**
Δ*vps28_11b*^{*NT}	sporulated from WT BY4742 x Δ*vps28*	*MATalpha his3 leu2 ura3 lys2*
Δ*vps28_11c*^{*NT}	sporulated from WT BY4742 x Δ*vps28*	*MATalpha his3 leu2 ura3 met15*
Δ*vps28_11d*^{*NT}	sporulated from WT BY4742 x Δ*vps28*	*MATa his3 leu2 ura3 met15 vps28::KanMX4*
WTα*_12a*	BY4742	*MATalpha his3 leu2 ura3 met15*
Δ*Whi2_12b*	BY4741	*MATa his3 leu2 ura3 lys2 Whi2::KanMX4*
Δ*vps28_12c*	BY4741	*MATaxMATalpha his3 leu2 ura3 lys2 met15 vps28::KanMx4*
Δ*srn2_1a*	sporulated from WT BY4742 x Δ*srn2*	*MATa his3 leu2 ura3 T*
Δ*srn2_1b*	sporulated from WT BY4742 x Δ*srn2*	*MATalpha his3 leu2 ura3 lys2 met15 srn2::KanMX4T*
Δ*srn2_1c*	sporulated from WT BY4742 x Δ*srn2*	*MATalpha his3 leu2 ura3 lys2T*
Δ*srn2_1d*	sporulated from WT BY4742 x Δ*srn2*	*MATa his3 leu2 ura3 met15 srn2::KanMX4T*
Δ*srn2_2a*^{*NT}	sporulated from WT BY4742 x Δ*srn2*	*MATa his3 leu2 ura3 met15 srn2::KanMX4*
Δ*srn2_2b*^{*NT}	sporulated from WT BY4742 x Δ*srn2*	*MATalpha his3 leu2 ura3 lys2 met15 srn2::KanMX4*
Δ*srn2_2c*^{*NT}	sporulated from WT BY4742 x Δ*srn2*	*MATalpha his3 leu2 ura3 lys2 met15*
Δ*srn2_2d*^{*NT}	sporulated from WT BY4742 x Δ*srn2*	*MATa his3 leu2 ura3 lys2*
Δ*srn2_3a*^{*NT}	sporulated from WT BY4742 x Δ*srn2*	*MATa his3 leu2 ura3 met15*
Δ*srn2_3b*^{*NT}	sporulated from WT BY4742 x Δ*srn2*	*MATalpha his3 leu2 ura3 lys2 met15 srn2::KanMX4*
Δ*srn2_3c*^{*NT}	sporulated from WT BY4742 x Δ*srn2*	*MAT? his3 leu2 ura3*
Δ*srn2_3d*^{*NT}	sporulated from WT BY4742 x Δ*srn2*	*MATa his3 leu2 ura3 lys2 srn2::KanMX4*
Δ*srn2_4a*^{*NT}	sporulated from WT BY4742 x Δ*srn2*	*MATalpha met15*
Δ*srn2_4b*^{*NT}	sporulated from WT BY4742 x Δ*srn2*	*MAT? his3 leu2 ura3 lys2 srn2::KanMX4*
Δ*srn2_4c*^{*NT}	sporulated from WT BY4742 x Δ*srn2*	*MAT? his3 leu2 ura3 lys2 met15*
Δ*srn2_4d*^{*NT}	sporulated from WT BY4742 x Δ*srn2*	*MATa his3 leu2 ura3*
Δ*srn2_5a*^{*NT}	sporulated from WT BY4742 x Δ*srn2*	*MATalpha his3 leu2 ura3 met15*
Δ*srn2_5b*^{*NT}	sporulated from WT BY4742 x Δ*srn2*	*MATa his3 leu2 ura3 lys2*

Δ*srn2_5c*^{*NT}	sporulated from WT BY4742 x Δ*srn2*	*MATa his3 leu2 ura3 met15 srn2::KanMX4*
Δ*srn2_5d*^{*NT}	sporulated from WT BY4742 x Δ*srn2*	*MAT? his3 leu2 ura3 lys2 srn2::KanMX4*
Δ*srn2_6a*	sporulated from WT BY4742 x Δ*srn2*	*MATa his3 leu2 ura3 lys2 met15 T*
Δ*srn2_6b*	sporulated from WT BY4742 x Δ*srn2*	*MATalpha his3 leu2 ura3 srn2::KanMX4 T*
Δ*srn2_6c*	sporulated from WT BY4742 x Δ*srn2*	*MATalpha his3 leu2 ura3 lys2 met15 T*
Δ*srn2_6d*	sporulated from WT BY4742 x Δ*srn2*	*MATa his3 leu2 ura3 srn2::KanMX4 T*
Δ*srn2_7a*	sporulated from WT BY4742 x Δ*srn2*	*MATalpha his3 leu2 ura3 met15 T*
Δ*srn2_7b*	sporulated from WT BY4742 x Δ*srn2*	*MATalpha his3 leu2 ura3 srn2::KanMX4 T*
Δ*srn2_7c*	sporulated from WT BY4742 x Δ*srn2*	*MATa his3 leu2 ura3 lys2 met15 srn2::KanMX4 T*
Δ*srn2_7d*	sporulated from WT BY4742 x Δ*srn2*	*MATa his3 leu2 ura3 lys2 T*
Δ*srn2_8a*^{*NT}	sporulated from WT BY4742 x Δ*srn2*	*MAT? his3 leu2 ura3 met15 srn2::KanMX4**NT*
Δ*srn2_8b*^{*NT}	sporulated from WT BY4742 x Δ*srn2*	*MAT? his3 leu2 ura3 srn2::KanMX4*
Δ*srn2_8c*^{*NT}	sporulated from WT BY4742 x Δ*srn2*	*MAT? his3 leu2 ura3 lys2 met15*
Δ*srn2_8d*^{*NT}	sporulated from WT BY4742 x Δ*srn2*	*MAT? his3 leu2 ura3 lys2*
Δ*srn2_9a*^{*NT}	sporulated from WT BY4742 x Δ*srn2*	*MAT? his3 leu2 ura3 lys2 met15 srn2::KanMX4*
Δ*srn2_9b*^{*NT}	sporulated from WT BY4742 x Δ*srn2*	*MATalpha his3 leu2 ura3 srn2::KanMX4*
Δ*srn2_9c*^{*NT}	sporulated from WT BY4742 x Δ*srn2*	*MATa his3 leu2 ura3 lys2 met15*
Δ*srn2_9d*^{*NT}	sporulated from WT BY4742 x Δ*srn2*	*MAT? his3 leu2 ura3 lys3 met15 srn2::KanMX4*
Δ*srn2_10a*^{*NT}	sporulated from WT BY4742 x Δ*srn2*	*MAT? his3 leu2 ura3 lys2 met15 srn2::KanMX4*
Δ*srn2_10b*^{*NT}	sporulated from WT BY4742 x Δ*srn2*	*MAT? his3 leu2 ura3*
Δ*srn2_10c*^{*NT}	sporulated from WT BY4742 x Δ*srn2*	*MATa his3 leu2 ura3 lys2 srn2::KanMX4*
Δ*srn2_10d*^{*NT}	sporulated from WT BY4742 x Δ*srn2*	*MATalpha his3 leu2 ura3 lys2 met15*
Δ*srn2_11a*	sporulated from WT BY4742 x Δ*srn2*	*MATalpha his3 leu2 ura3 srn2::KanMX4 T*
Δ*srn2_11b*	sporulated from WT BY4742 x Δ*srn2*	*MATa his3 leu2 ura3 lys2 met15 srn2::KanMX4 T*
Δ*srn2_11c*	sporulated from WT BY4742 x Δ*srn2*	*MATalpha his3 leu2 ura3 lys2 met15*
Δ*srn2_11d*	sporulated from WT BY4742 x Δ*srn2*	*MATa his3 leu2 ura3*
WTα_*12a*	BY4742	*MATalpha his3 leu2 ura3 met15*
Δ*Whi2_12b*	BY4741	*MATa his3 leu2 ura3 lys2 Whi2::KanMX4*
Δ*srn2_12c*	BY4741	*MATa his3 leu2 ura3 lys2 srn2::KanMX4*
Δ*mvb12_1a*	sporulated from WT BY4742 x Δ*mvb12*	*MATalpha his3 leu2 ura3 lys2 met15*
Δ*mvb12_1b*	sporulated from WT BY4742 x Δ*mvb12*	*MATalpha his3 leu2 ura3 met15 mvb12::KanMX4*
Δ*mvb12_1c*	sporulated from WT BY4742 x Δ*mvb12*	*MATa his3 leu2 ura3 lys2 mvb12::KanMX4*
Δmvb12_*1d*	sporulated from WT BY4742 x Δ*mvb12*	*MATa his3 leu2 ura3*
Δmvb12_*2a*	sporulated from WT BY4742 x Δ*mvb12*	*MATalpha his3 leu2 ura3 lys2 met15 mvb12::KanMX4*
Δmvb12_*2b*	sporulated from WT BY4742 x Δ*mvb12*	*MATa his3 leu2 ura3*

Δ*mvb12_2c*	sporulated from WT BY4742 x Δ*mvb12*	*MATa his3 leu2 ura3 mvb12::KanMX4*
Δ*mvb12_2d*	sporulated from WT BY4742 x Δ*mvb12*	*MATalpha his3 leu2 ura3 lys2 met15*
Δ*mvb12_3a*	sporulated from WT BY4742 x Δ*mvb12*	*MATalpha his3 leu2 ura3 lys2 mvb12::KanMX4*
Δ*mvb12_3b*	sporulated from WT BY4742 x Δ*mvb12*	*MATalpha his3 leu2 ura3 lys2*
Δ*mvb12_3c*	sporulated from WT BY4742 x Δ*mvb12*	*MATa his3 leu2 ura3 met15 mvb::KanMX4*
Δ*mvb12_3d*	sporulated from WT BY4742 x Δ*mvb12*	*MATa his3 leu2 ura3 met15*
Δ*mvb12_4a*	sporulated from WT BY4742 x Δ*mvb12*	*MATalpha his3 leu2 ura3*
Δ*mvb12_4b*	sporulated from WT BY4742 x Δ*mvb12*	*MATa his3 leu2 ura3 lys2 met15*
Δ*mvb12_4c*	sporulated from WT BY4742 x Δ*mvb12*	*MATa his3 leu2 ura3 lys2 met15 mvb12::KanMX4*
Δ*mvb12_4d*	sporulated from WT BY4742 x Δ*mvb12*	*MATalpha his3 leu2 ura3 mvb12::KanMX4*
Δ*mvb12_5a*	sporulated from WT BY4742 x Δ*mvb12*	*MATalpha his3 leu2 ura3 met15*
Δ*mvb12_5b*	sporulated from WT BY4742 x Δ*mvb12*	*MATa his3 leu2 ura3 lys2 met15 mvb12::KanMX4*
Δ*mvb12_5c*	sporulated from WT BY4742 x Δ*mvb12*	*MATa his3 leu2 ura3*
Δ*mvb12_5d*	sporulated from WT BY4742 x Δ*mvb12*	*MATalpha his3 leu2 ura3 lys2 mvb12::KanMX4*
Δ*mvb12_6a*	sporulated from WT BY4742 x Δ*mvb12*	*MATalpha his3 leu2 ura3 lys2 met15 mvb12::KanMX4*
Δ*mvb12_6b*	sporulated from WT BY4742 x Δ*mvb12*	*MATa his3 leu2 ura3 met15*
Δ*mvb12_6c*	sporulated from WT BY4742 x Δ*mvb12*	*MATa his3 leu2 ura3*
Δ*mvb12_6d*	sporulated from WT BY4742 x Δ*mvb12*	*MATalpha his3 leu2 ura3 lys2 mvb12::KanMX4*
Δ*mvb12_7a*	sporulated from WT BY4742 x Δ*mvb12*	*MATa his3 leu2 ura3*
Δ*mvb12_7b*	sporulated from WT BY4742 x Δ*mvb12*	*MATalpha his3 leu2 ura3 lys2 mvb12::KanMX4*
Δ*mvb12_7c*	sporulated from WT BY4742 x Δ*mvb12*	*MATalpha his3 leu2 ura3 met15 mvb12::KanMX4*
Δ*mvb12_7d*	sporulated from WT BY4742 x Δ*mvb12*	*MATa his3 leu2 ura3 lys2 met15*
Δ*mvb12_8a*^{*NT}	sporulated from WT BY4742 x Δ*mvb12*	*MATa his3 leu2 ura3 lys2 met15 mvb12::KanMX4*
Δ*mvb12_8b*^{*NT}	sporulated from WT BY4742 x Δ*mvb12*	*MATalpha his3 leu2 ura3 lys2 met15 mvb12::KanMX4*
Δ*mvb12_8c*^{*NT}	sporulated from WT BY4742 x Δ*mvb12*	*MATa his3 leu2 ura3 mvb12::KanMX4*
Δ*mvb12_8d*^{*NT}	sporulated from WT BY4742 x Δ*mvb12*	*MATalpha his3 leu2 ura3*
Δ*mvb12_9a*^{*NT}	sporulated from WT BY4742 x	*MATa his3 leu2 ura3*

	Δ*mvb12*	
Δ*mvb12_9b*^{*NT}	sporulated from WT BY4742 x Δ*mvb12*	*MAT? his3 leu2 ura3 lys2 met15*
Δ*mvb12_9c*^{*NT}	sporulated from WT BY4742 x Δ*mvb12*	*MATa his3 leu2 ura3 mvb12::KanMX4*
Δ*mvb12_9d*^{*NT}	sporulated from WT BY4742 x Δ*mvb12*	*Did not grow*
Δ*mvb12_10a*	sporulated from WT BY4742 x Δ*mvb12*	*MATa his3 leu2 ura3 lys2 met15 mvb12::KanMX4*
Δ*mvb12_10b*	sporulated from WT BY4742 x Δ*mvb12*	*MATa his3 leu2 ura3*
Δ*mvb12_10c*	sporulated from WT BY4742 x Δ*mvb12*	*MATalpha his3 leu2 ura3 lys2 mvb12::KanMX4*
Δ*mvb12_10d*	sporulated from WT BY4742 x Δ*mvb12*	*MATalpha his3 leu2 ura3 met15 mvb12::KanMX4*
Δ*mvb12_11a*	sporulated from WT BY4742 x Δ*mvb12*	*MATa his3 leu2 ura3 met15*
Δ*mvb12_11b*	sporulated from WT BY4742 x Δ*mvb12*	*MATa his3 leu2 ura3 lys2 mvb12::KanMX4*
Δ*mvb12_11c*	sporulated from WT BY4742 x Δ*mvb12*	*MATalpha his3 leu2 ura3 lys2 mvb12::KanMX4*
Δ*mvb12_11d*	sporulated from WT BY4742 x Δ*mvb12*	*MATalpha his3 leu2 ura3 met15*
WTα_*12a*	BY4742	*MATalpha his3 leu2 ura3 met15*
Δ*Whi2_12b*	BY4741	*MATa his3 leu2 ura3 lys2 Whi2::KanMX4*
Δ*mvb12_12c*	BY4741	*MATa his3 leu2 ura3 lys2 mvb12::KanMX4*
Δ*snf8_1a*	sporulated from WT BY4742 x Δ*snf8*	*MATalpha his3 leu2 ura3 met15 snf8::KanMX4*
Δ*snf8_1b*	sporulated from WT BY4742 x Δ*snf8*	*MATalpha his3 leu2 ura3 lys2 snf8:: KanMX4*
Δ*snf8_1c*	sporulated from WT BY4742 x Δ*snf8*	*MATa his3 leu2 ura2 lys2 met15*
Δ*snf8_1d*	sporulated from WT BY4742 x Δ*snf8*	*MATa his3 leu2 ura2*
Δ*snf8_2a*	sporulated from WT BY4742 x Δ*snf8*	*MAT? his3 leu2 ura3 lys2*
Δ*snf8_2b*	sporulated from WT BY4742 x Δ*snf8*	*MATa his3 leu2 ura3 met15 snf8:: KanMX4*
Δ*snf8_2c*	sporulated from WT BY4742 x Δ*snf8*	*MATalpha his3 leu2 ura3 met15*
Δ*snf8_2d*	sporulated from WT BY4742 x Δ*snf8*	*MATa his3 leu2 ura3 lys2 snf8:: KanMX4*
Δ*snf8_3a*	sporulated from WT BY4742 x Δ*snf8*	*MATa his3 leu2 ura3 snf8:: KanMX4*
Δ*snf8_3b*	sporulated from WT BY4742 x Δ*snf8*	*MATa his3 leu2 ura3 lys2 met15*
Δ*snf8_3c*	sporulated from WT BY4742 x Δ*snf8*	*MATalpha his3 leu2 ura3 lys2 snf8:: KanMX4*
Δ*snf8_3d*	sporulated from WT BY4742 x Δ*snf8*	*MATalpha his3 leu2 ura3 met15*
Δ*snf8_4a*	sporulated from WT BY4742 x Δ*snf8*	*MATa his3 leu2 ura3 lys2 met15 snf8:: KanMX4*
Δ*snf8_4b*	sporulated from WT BY4742 x Δ*snf8*	*MATalpha his3 leu2 ura3*
Δ*snf8_4c*	sporulated from WT BY4742 x Δ*snf8*	*MATa his3 leu2 ura3 met15 snf8:: KanMX4*
Δ*snf8_4d*	sporulated from WT BY4742 x Δ*snf8*	*MATalpha his3 leu2 ura3 lys2*
Δ*snf8_5a*	sporulated from WT BY4742 x Δ*snf8*	*MATa his3 leu2 ura3 met15 snf8:: KanMX4*
Δ*snf8_5b*	sporulated from WT BY4742 x Δ*snf8*	*MATa his3 leu2 ura3 snf8:: KanMX4*

Δ*snf8_5c*	sporulated from WT BY4742 x Δ*snf8*	*MATalpha his3 leu2 ura3 lys2*
Δ*snf8_5d*	sporulated from WT BY4742 x Δ*snf8*	*MATalpha his3 leu2 ura3 lys2 met15*
Δ*snf8_6a*	sporulated from WT BY4742 x Δ*snf8*	*MATalpha his3 leu2 ura3 lys2 met15*
Δ*snf8_6b*	sporulated from WT BY4742 x Δ*snf8*	*MATa his3 leu2 ura3 met15*
Δ*snf8_6c*	sporulated from WT BY4742 x Δ*snf8*	*MATalpha his3 leu2 ura3 snf8:: KanMX4*
Δ*snf8_6d*	sporulated from WT BY4742 x Δ*snf8*	*MATalpha his3 leu2 ura3 lys2 snf8:: KanMX4*
Δ*snf8_7a*	sporulated from WT BY4742 x Δ*snf8*	*MATalpha his3 leu2 ura3*
Δ*snf8_7b*	sporulated from WT BY4742 x Δ*snf8*	*MATalpha his3 leu2 ura3 lys2 met15*
Δ*snf8_7c*	sporulated from WT BY4742 x Δ*snf8*	*MATa his3 leu2 ura3 snf8:: KanMX4*
Δ*snf8_7d*	sporulated from WT BY4742 x Δ*snf8*	*Mata his3 leu2 ura3 lys2 met15 snf8:: KanMX4*
Δ*snf8_8a*	sporulated from WT BY4742 x Δ*snf8*	*MATa his3 leu2 ura3 lys2 met15 snf8:: KanMX4*
Δ*snf8_8b*	sporulated from WT BY4742 x Δ*snf8*	*MATalpha his3 leu2 ura3*
Δ*snf8_8c*	sporulated from WT BY4742 x Δ*snf8*	*MATa his3 leu2 ura3 lys2 met15 snf8:: KanMX4*
Δ*snf8_8d*	sporulated from WT BY4742 x Δ*snf8*	*MATalpha his3 leu2 ura3 met15 snf8:: KanMX4*
Δ*snf8_9a*	sporulated from WT BY4742 x Δ*snf8*	*MATalpha his3 leu2 ura3 lys2 met15*
Δ*snf8_9b*	sporulated from WT BY4742 x Δ*snf8*	*MATalpha his3 leu2 ura3 met15 snf8:: KanMX4*
Δ*snf8_9c*	sporulated from WT BY4742 x Δ*snf8*	*MATa his3 leu2 ura3 lys2 snf8:: KanMX4*
Δ*snf8_9d*	sporulated from WT BY4742 x Δ*snf8*	*MATa his3 leu2 ura3*
Δ*snf8_10a*	sporulated from WT BY4742 x Δ*snf8*	*MATalpha his3 leu2 ura3 met15*
Δ*snf8_10b*	sporulated from WT BY4742 x Δ*snf8*	*MATa his3 leu2 ura3 lys2 snf8:: KanMX4*
Δ*snf8_10c*	sporulated from WT BY4742 x Δ*snf8*	*MATalpha his3 leu2 ura3 met15 snf8:: KanMX4*
Δ*snf8_10d*	sporulated from WT BY4742 x Δ*snf8*	*MATa his3 leu2 ura3 lys2*
Δ*snf8_11a*	sporulated from WT BY4742 x Δ*snf8*	*MATa his3 leu2 ura3 lys2 met15*
Δ*snf8_11b*	sporulated from WT BY4742 x Δ*snf8*	*MATa his3 leu2 ura3 met15*
Δ*snf8_11c*	sporulated from WT BY4742 x Δ*snf8*	*MATalpha his3 leu2 ura3 lys2 snf8:: KanMX4*
Δ*snf8_11d*	sporulated from WT BY4742 x Δ*snf8*	*MATalpha his3 leu2 ura3 snf8:: KanMX4*
WTa_*12a*	BY4741	*MATa his3 leu2 ura3 lys2*
Δ*Whi2_12b*	BY4741	*MATa his3 leu2 ura3 lys2 whi2:: KanMX4*
Δ*snf8_12c*	BY4742 x BY4741	*MATaXMATalpha his3 leu2 ura3 lys2 met15 snf8::KanMX4*
Δ*snf7_1a*	sporulated from WT BY4742 x Δ*snf7*	*MATalpha his3 leu2 ura3 lys2 met15*
Δ*snf7_1b*	sporulated from WT BY4742 x Δ*snf7*	*MATa his3 leu2 ura3 met15*
Δ*snf7_1c*	sporulated from WT BY4742 x Δ*snf7*	*MATa his3 leu2 ura3 lys2 snf7::KanMX4*
Δ*snf7_1d*	sporulated from WT BY4742 x Δ*snf7*	*MATalpha his3 leu2 ura3 snf7::KanMX4*
Δ*snf7_2a*	sporulated from WT BY4742 x Δ*snf7*	*MATalpha his3 leu2 ura3 lys2 snf7::KanMX4*
Δ*snf7_2b*	sporulated from WT BY4742 x Δ*snf7*	*MATa his3 leu2 ura3 lys2 met15*
Δ*snf7_2c*	sporulated from WT BY4742 x Δ*snf7*	*MATalpha his3 leu2 ura3 met15 snf7::KanMX4*

Δ*snf7_2d*	sporulated from WT BY4742 x Δ*snf7*	*MATa his3 leu2 ura3*
Δ*snf7_3a*	sporulated from WT BY4742 x Δ*snf7*	*MATa his3 leu2 ura3*
Δ*snf7_3b*	sporulated from WT BY4742 x Δ*snf7*	*MATalpha his3 leu2 ura3 lys2 snf7::KanMX4*
Δ*snf7_3c*	sporulated from WT BY4742 x Δ*snf7*	*MATa his3 leu2 ura3 lys3 met15*
Δ*snf7_3d*	sporulated from WT BY4742 x Δ*snf7*	*MATalpha his3 leu2 ura3 met15 snf7::KanMX4*
Δ*snf7_4a*	sporulated from WT BY4742 x Δ*snf7*	*MATalpha his3 leu2 ura3 lys2*
Δ*snf7_4b*	sporulated from WT BY4742 x Δ*snf7*	*MATa his3 leu2 ura3 snf7::KanMX4*
Δ*snf7_4c*	sporulated from WT BY4742 x Δ*snf7*	*MATa his3 leu2 ura3 lys2 met15 snf7::KanMX4*
Δ*snf7_4d*	sporulated from WT BY4742 x Δ*snf7*	*MATalpha his3 leu2 ura3 met15*
Δ*snf7_5a*	sporulated from WT BY4742 x Δ*snf7*	*MATa his3 leu2 ura3 lys2*
Δ*snf7_5b*	sporulated from WT BY4742 x Δ*snf7*	*MATalpha his3 leu2 ura3 lys2*
Δ*snf7_5c*	sporulated from WT BY4742 x Δ*snf7*	*MAT? His3 leu2 ura3 lys2 met15 snf7::KanMX4*
Δ*snf7_5d*	sporulated from WT BY4742 x Δ*snf7*	*MATalpha his3 leu2 ura3 met15 snf7::KanMX4*
Δ*snf7_6a*	sporulated from WT BY4742 x Δ*snf7*	*MATa his3 leu2 ura3 snf7::KanMX4*
Δ*snf7_6b*	sporulated from WT BY4742 x Δ*snf7*	*MATa his3 leu2 ura3 met15*
Δ*snf7_6c*	sporulated from WT BY4742 x Δ*snf7*	*MATalpha his3 leu2 ura3 lys2 snf7::KanMX4*
Δ*snf7_6d*	sporulated from WT BY4742 x Δ*snf7*	*MATalpha his3 leu2 ura3 lys2 met15*
Δ*snf7_7a*^{*NT}	sporulated from WT BY4742 x Δ*snf7*	*MAT? his3 leu2 ura3 lys2 met15 snf7::KanMX4*
Δ*snf7_7b*^{*NT}	sporulated from WT BY4742 x Δ*snf7*	*MATalpha his3 leu2 snf7::KanMX4*
Δ*snf7_7c*^{*NT}	sporulated from WT BY4742 x Δ*snf7*	*MATa his3 leu2 ura3 met15*
Δ*snf7_7d*^{*NT}	sporulated from WT BY4742 x Δ*snf7*	*MATa his3 leu2 ura3 lys2 met15 snf7::KanMX4*
Δ*snf7_8a*	sporulated from WT BY4742 x Δ*snf7*	*MATalpa his3 leu2 ura3 met15 snf7::KanMX4*
Δ*snf7_8b*	sporulated from WT BY4742 x Δ*snf7*	*MATa his3 leu2 ura3*
Δ*snf7_8c*	sporulated from WT BY4742 x Δ*snf7*	*MATalpha his3 lue2 ura3 met15 snf7::KanMX4*
Δ*snf7_8d*	sporulated from WT BY4742 x Δ*snf7*	*MATa his3 leu2 ura3 lys2*
Δ*snf7_9a*	sporulated from WT BY4742 x Δ*snf7*	*MATa his3 leu2 ura3 snf7::KanMX4*
Δ*snf7_9b*	sporulated from WT BY4742 x Δ*snf7*	*MATa his3 leu2 ura3 lys2 met15 snf7::KanMX4*
Δ*snf7_9c*	sporulated from WT BY4742 x Δ*snf7*	*MATalpha his3 leu2 ura3 lys2 met15*
Δ*snf7_9d*	sporulated from WT BY4742 x Δ*snf7*	*MATalpha his3 leu2 ura3*
WTα*_10a**	BY4742	*MATa his3 leu2 ura3 lys2**
Δ*Whi2_10b*	BY4741	*MATa his3 leu2 ura3 lys2 Whi2::KanMX4*
Δ*snf7_10c*	BY4742 x BY4741	*MATaxMATalpha his3 leu2 ura3 lys2 met15 snf7::KanMX4*
WTα*_11b*	BY4742	*MATalpha his3 leu2 ura3 met15*
Δ*Whi2_11a*	BY4741	*MATa his3 leu2 ura3 lys2 Whi2::KanMX4*
Δ*did4_1a*^{*NT}	sporulated from WT BY4742 x Δdid4	*MATalpha his3 leu2 ura3 lys2 met15 did4::KanMX4*

Δ*did4_1b*^{*NT}	sporulated from WT BY4742 x Δdid4	*MATa his3 leu2 ura3 lys2*
Δ*did4_1c*^{*NT}	sporulated from WT BY4742 x Δdid4	*MATalpha his3 leu2 ura3 lys2 did4::KanMX4*
Δ*did4_1d*^{*NT}	sporulated from WT BY4742 x Δdid4	*MATa his3 leu2 ura3 met15*
Δ*did4_2a*	sporulated from WT BY4742 x Δdid4	*MATa his3 leu2 ura3 lys2*
Δ*did4_2b*	sporulated from WT BY4742 x Δdid4	*MATalpha his3 leu2 ura3 lys2 met15 did4:KanMX4*
Δ*did4_2c*	sporulated from WT BY4742 x Δdid4	*MATa his3 leu2 ura3 did4:KanMX4*
Δ*did4_2d*	sporulated from WT BY4742 x Δdid4	*MATalpha his3 leu2 ura3 met15*
Δ*did4_3a*^{*NT}	sporulated from WT BY4742 x Δdid4	*MATa his3 leu2 ura3 lys2 met15 did4::KanMX4*
Δ*did4_3b*^{*NT}	sporulated from WT BY4742 x Δdid4	*MATalpha his3 leu2 ura3 lys2 did4::KanMX4*
Δ*did4_3c*^{*NT}	sporulated from WT BY4742 x Δdid4	*MATa his3 leu2 ura3 lys2 met15 did4::KanMX4*
Δ*did4_3d*^{*NT}	sporulated from WT BY4742 x Δdid4	*MATalpha his3 leu2 ura3 met15*
Δ*did4_4a*^{*NT}	sporulated from WT BY4742 x Δdid4	*MATalpha his3 leu2 ura3 did4::KanMX4*
Δ*did4_4b*^{*NT}	sporulated from WT BY4742 x Δdid4	*MATalpha his3 leu2 ura3 lys2 met15 did4::KanMX4*
Δ*did4_4c*^{*NT}	sporulated from WT BY4742 x Δdid4	*MATa his3 leu2 ura3 lys2 met15 did4::KanMX4*
Δ*did4_4d*^{*NT}	sporulated from WT BY4742 x Δdid4	*MATa his3 leu2 ura3 lys2*
Δ*did4_5a*	sporulated from WT BY4742 x Δdid4	*MATa his3 leu2 ura3 lys2*
Δ*did4_5b*	sporulated from WT BY4742 x Δdid4	*MATalpha his3 leu2 ura3 met15 did4::KanMX4*
Δ*did4_5c*	sporulated from WT BY4742 x Δdid4	*MATa his3 leu2 ura3*
Δ*did4_5d*	sporulated from WT BY4742 x Δdid4	*MATalpha his3 leu2 ura3 lys2 met15 did::KanMX4*
Δ*did4_6a*	sporulated from WT BY4742 x Δdid4	*MATalpha his3 leu2 ura3*
Δ*did4_6b*	sporulated from WT BY4742 x Δdid4	*MATalpha his3 leu2 ura3 lys2 did4::KanMX4*
Δ*did4_6c*	sporulated from WT BY4742 x Δdid4	*MATa his3 leu2 ura3 met15*
Δ*did4_6d*	sporulated from WT BY4742 x Δdid4	*MATa his3 leu2 ura3 lys2 met15 did4::KanMX4*
Δ*did4_7a*	sporulated from WT BY4742 x Δdid4	*MATa his3 leu2 ura3 met15*
Δ*did4_7b*	sporulated from WT BY4742 x Δdid4	*MATalpha his3 leu2 ura3 did4::KanMX4*
Δ*did4_7c*	sporulated from WT BY4742 x Δdid4	*MATa his3 leu2 ura3 lys2 met15*

Δ*did4_7d*	sporulated from WT BY4742 x Δdid4	*MATalpha his3 leu2 ura3 lys2 did4::KanMX4*
Δ*did4_8a*	sporulated from WT BY4742 x Δdid4	*MATa his3 leu2 ura3*
Δ*did4_8b*	sporulated from WT BY4742 x Δdid4	*MATalpha his3 leu2 ura3 did4::KanMX4*
Δ*did4_8c*	sporulated from WT BY4742 x Δdid4	*MATalpha his3 leu2 ura3 lys2 met15 did4::KanMX4*
Δ*did4_8d*	sporulated from WT BY4742 x Δdid4	*MATa his3 leu2 ura3 lys2 met15*
WTα*_9a*	BY4742	*MATa his3 leu2 ura3 lys2*
Δ*Whi2_9b*	BY4741	*MATa his3 leu2 ura3 lys2 whi2::KanMX4*
Δ*did4_9c*	BY4742 x BY4741	*MATaXMATalpha his2 leu2 ura3 lys2 met15 did4::KanMX4*
WTα*_10a*	BY4742	*MATalpha his3 leu2 ura3 met15*
Δ*Whi2_10b*	BY4741	*MATa his3 leu2 ura3 lys2 whi2::KanMX4*
Δ*vps4_1a*	sporulated from WT BY4742 x Δ*vps28*	*MATa his3 leu2 ura3 met15*
Δ*vps4_1b*	sporulated from WT BY4742 x Δ*vps28*	*MATalpha his3 leu2 ura3 lys2 vps4::KanMX4*
Δ*vps4_1c*	sporulated from WT BY4742 x Δ*vps28*	*MATalpha his3 leu2 ura3 lys2 vps4::KanMX4*
Δ*vps4_1d*	sporulated from WT BY4742 x Δ*vps28*	*MATa his3 leu2 ura3 lys2 met15*
Δ*vps4_2a*	sporulated from WT BY4742 x Δ*vps28*	*MATalpha his3 leu2 ura3*
Δ*vps4_2b*	sporulated from WT BY4742 x Δ*vps28*	*MATalpha his3 leu2 ura3 met15 vps4::KanMX4*
Δ*vps4_2c*	sporulated from WT BY4742 x Δ*vps28*	*MATa his3 leu2 ura3 lys2*
Δ*vps4_2d*	sporulated from WT BY4742 x Δ*vps28*	*MATa his3 leu2 ura3 lys2 met15 vps4::KanMX4*
Δ*vps4_3a*	sporulated from WT BY4742 x Δ*vps28*	*MATalpha his3 leu2 ura3 lys2*
Δ*vps4_3b*	sporulated from WT BY4742 x Δ*vps28*	*MATa his3 leu2 ura3*
Δ*vps4_3c*	sporulated from WT BY4742 x Δ*vps28*	*MATalpha his3 leu2 ura3 lys2 met15 vps4::KanMX4*
Δ*vps4_3d*	sporulated from WT BY4742 x Δ*vps28*	*MATa his3 leu2 ura3 met15 vps4::KanMX4*
Δ*vps4_4a*	sporulated from WT BY4742 x Δ*vps28*	*MATa his3 leu2 ura3 met15 vps4:KanMX4*
Δ*vps4_4b*	sporulated from WT BY4742 x Δ*vps28*	*MATalpha his3 leu2 ura3 lys2 met15 vps4:KanMX4*
Δ*vps4_4c*	sporulated from WT BY4742 x Δ*vps28*	*MATalpha his3 leu2 ura3*
Δ*vps4_4d*	sporulated from WT BY4742 x Δ*vps28*	*MATa his3 leu2 ura3 lys2*
Δ*vps4_5a*	sporulated from WT BY4742 x Δ*vps28*	*MATa his3 leu2 ura3 lys2*
Δ*vps4_5b*	sporulated from WT BY4742 x Δ*vps28*	*MATalpha his3 leu2 ura3 met15 vps4::KanMX4*
Δ*vps4_5c*	sporulated from WT BY4742 x Δ*vps28*	*MATalphs his3 leu2 ura3 lys2*
Δ*vps4_5d*	sporulated from WT BY4742 x Δ*vps28*	*MATa his3 leu2 ura3 met15 vps4::KanMX4*
Δ*vps4_6a*	sporulated from WT BY4742 x Δ*vps28*	*MATa his3 leu2 ura3 lys2*
Δ*vps4_6b*	sporulated from WT BY4742 x Δ*vps28*	*MATalpha his3 leu2 ura3 vps4::KanMX4*

Δ*vps4_6c*	sporulated from WT BY4742 x Δ*vps28*	*MATa his3 leu2 ura3 met15 vsp4::KanMX4*
Δ*vps4_6d*	sporulated from WT BY4742 x Δ*vps28*	*MATalpha his3 leu2 ura3 lys2 met15*
Δ*vps4_7a*^{*NT}	sporulated from WT BY4742 x Δ*vps28*	*MAT? his3 leu2 ura3 lys2 met15 vps4::KanMX4*
Δ*vps4_7b*^{*NT}	sporulated from WT BY4742 x Δ*vps28*	*MATalpha his3 leu2 ura3 lys2 met15 vps4:KanMX4*
Δ*vps4_7c*^{*NT}	sporulated from WT BY4742 x Δ*vps28*	*MATa his3 leu2 ura3 lys2 vps4::KanMX4*
Δ*vps4_7d*^{*NT}	sporulated from WT BY4742 x Δ*vps28*	*MATalpha his3 leu2 ura3*
Δ*vps4_8a*	sporulated from WT BY4742 x Δ*vps28*	*MATalpha his3 leu2 ura3 lys2 vps4::KanMX4*
Δ*vps4_8b*	sporulated from WT BY4742 x Δ*vps28*	*MATa his3 leu2 uar3 lys2 met15*
Δ*vps4_8c*	sporulated from WT BY4742 x Δ*vps28*	*MATalpha his3 leu2 ura3 met15*
Δ*vps4_8d*	sporulated from WT BY4742 x Δ*vps28*	*MATa his3 leu2 ura3 vps4::KanMX4*
Δ*vps4_9a*	sporulated from WT BY4742 x Δ*vps28*	*MATa his3 leu2 ura3 vps4::KanMX4*
Δ*vps4_9b*	sporulated from WT BY4742 x Δ*vps28*	*MATalpha his3 leu2 ura3 lys2*
Δ*vps4_9c*	sporulated from WT BY4742 x Δ*vps28*	*MATalpha his3 leu2 ura3 met15 vps4::KanMX4*
Δ*vps4_9d*	sporulated from WT BY4742 x Δ*vps28*	*MATa his3 leu2 ura3 lys2 met15*
Δ*vps4_10a*	sporulated from WT BY4742 x Δ*vps28*	*MATa his3 leu2 ura3 lys2 met15 vps4::KanMX4*
Δ*vps4_10b*	sporulated from WT BY4742 x Δ*vps28*	*MATa his3 leu2 ura3 vps4::KanMX4*
Δ*vps4_10c*	sporulated from WT BY4742 x Δ*vps28*	*MATalpha his3 leu2 ura3 lys2*
Δ*vps4_10d*	sporulated from WT BY4742 x Δ*vps28*	*MATalpha his3 leu2 ura3 met15*
Δ*vps4_11a*^{*NT}	sporulated from WT BY4742 x Δ*vps28*	*MATa his3 leu2 ura3 lys2 vps4::KanMX4*
Δ*vps4_11b*^{*NT}	sporulated from WT BY4742 x Δ*vps28*	*MATalpha his3 leu2 ura3 met15*
Δ*vps4_11c*^{*NT}	sporulated from WT BY4742 x Δ*vps28*	*did not grow*
Δ*vps4_11d*^{*NT}	sporulated from WT BY4742 x Δ*vps28*	*MATa his3 leu2 ura3 met15*
WTα*_12a*	BY4742	*MATalpha his3 leu2 ura3 met15*
Δ*Whi2_12b*	BY4741	*MATa his3 leu2 ura3 lys2 Whi2::KanMX4*
Δ*vps4_12c*	BY4741	*MATa his3 leu2 ura3 lys2 vps4::KanMX4*

Appendix ii: Raw Tetrad Data

Contains raw tetrad data of the characteristic analysis and phenotype analysis compiled from this study. Tetrad dissection methods can be found in Chapter 2 (Methods) and the abbreviations are listed below. Tetrads were performed backcrossing with wild type α (*BY4742 MATα*). Controls for each tetrad analysis are WT (*BY4741 MATa*) or WT (28B) (*BY4742 MATα*), Δ*whi2,* and parental strain (haploid or diploid).

Abbreviation	
MAT	Mating type
LYS2	Presence of *LYS2*
MAT15	Presence of *MET15*
KAN	Presence of KanMX knockout indicator
HR	Heat ramp assay (Cell death)
LAA	Low amino acid assay
LAA + (5nM or 2.5nM) Rap	Rapamycin assay
OD	48hr OD_{600}

Δvps27
Notes:
LAA+5nMRap* - analysis discrepancies based on poor growth on 5nM concentration of rapamycin
*NT - not true tetrad

tetrad	spore	viability	MAT	LYS2	MET15	KAN	HR	LAA	LAA+2.5nMRap	OD
1	a	m	a		+		++++	+	+	0.745
	b	m	alpha				++++	+	+	0.731
	c	m	a	+	+	+	+++	++++	++++	0.751
	d	m	alpha	+		+	+++	++++	++++	0.743
2	a	m	alpha	+			++++	+	+	0.856
	b	m	a				++++	+	+	0.771
	c	m	alpha		+	+	+++	++++	++++	0.889
	d	m	a	+	+	+	+++	++++	++++	0.846
3	a	m	a	+			++++	+	+	0.718
	b	m	a		+	+	+++	++++	++++	0.773
	c	m	alpha				++++	+	+	0.743
	d	m	alpha	+	+	+	+++	++++	++++	0.745
4	a	m	a		+		++++	+	+	0.764
	b	m	alpha	+		+	+++	++++	++++	0.722
	c	m	alpha	+			++++	+	+	0.802
	d	m	a			+	+++	++++	++++	0.736
5	a	m	a	+	+		++++	+	+	0.791
	b	m	alpha		+		++++	+	+	0.920
	c	m	a			+	+++	++++	++++	0.835
	d	m	alpha	+		+	+++	++++	++++	0.811
6	a	m	a	+			++++	+	+	0.734
	b	m	a			+	+++	++++	++++	0.784
	c	m	alpha		+		++++	+	+	0.781

	d	m	alpha	+	+	+	+++	++++	++++	1.133
7	a	m	a		+	+	+++	++++	++++	0.857
	b	m	alpha	+			++++	+	+	0.715
	c	m	a			+	+++	++++	++++	0.913
	d	m	alpha	+	+		++++	+	+	0.721
8	a	m	a	+	+	+	+++	++++	++++	0.765
	b	m	alpha	+	+		++++	+	+	0.699
	c	m	a			+	+++	++++	++++	0.882
	d	m	alpha				++++	+	+	0.654
9	a	m	a	+			++++	+	+	0.827
	b	m	alpha	+	+	+	+++	++++	++++	0.711
	c	m	a		+		++++	+	+	0.904
	d	m	alpha			+	+++	++++	++++	0.717
10*NT	a	Not recorded	a			+	-	+++	-	0.465
	b	Not recorded	alpha		+		++++	-	+	0.721
	c	Not recorded	-	+	+	+	+++	+	+++	0.841
	d	Not recorded	alpha	+			++++	++	+	0.754
11*NT	a	Not recorded	-				-	-	-	-0.007
	b	Not recorded	a	+	+	+	++++	++++	++++	0.067
	c	Not recorded	alpha				++++	+	++	0.928
	d	Not recorded	a		+		++++	+	+++	1.011
C	a	WT 28B	alpha		+		++++	+	+	0.779
	b	whi2	a	+		+	+	++++	-	0.698
	c	gene of I	a	+		+	+++	++++	++++	0.842
		*	*	*	*	*	*	*	*	

Δmvb12

Notes:

viability* - not recorded

LAA+5nMRap* - analysis discrepancies based on poor growth on 5nM concentration of rapamycin

*NT - not true tetrad

tetrad	spore	viability*	MAT	LYS2	MET15	KAN	HR	LAA	LAA+5nMRap*	
1	a		alpha	+	+		++++	+	-	
	b		alpha		+	+	++	+++	+	
	c		a	+		+	++	+++	+	
	d		a				++++	+	-	
2	a		alpha	+	+	+	+	+++	+	
	b		a				++	-	-	
	c		a			+	+	+++	+	
	d		alpha	+	+		++	-	-	
3	a		alpha	+		+	++	+++	+	
	b		alpha	+			+++	+++	-	
	c		a		+	+	++	+++	+	
	d		a		+		+++	+	-	
4	a		alpha				+++	+	?	

OD Not available at this time

	b		a	+	+		+++	+		?
	c		a	+	+	+	++	+++		?
	d		alpha			+	++	+++		?
5	a		alpha		+		++++	+		-
	b		a	+	+	+	++	+++		+
	c		a				+++	+		-
	d		alpha	+		+	++	+++		+
6	a		alpha	+	+	+	+++	+++		+
	b		a		+		++++	+		-
	c		a				++++	+		-
	d		alpha	+		+	++	+++		+
7	a		a				++++	+		-
	b		alpha	+		+	+++	++		+
	c		alpha		+	+	+++	++		+
	d		a	+	+		++++	+		-
8*NT	a		a	+	+	+	+	+		-
	b		alpha	+	+	+	++	+++		+
	c		a			+	++	+++		+
	d		alpha				+	+		-
9*NT	a		alpha				++++	+		-
	b		alpha	+	+		++++	+		-
	c		a			+	+++	+++		+
	d		both				-	_		-
10	a		a	+	+	+	++	+++		?
	b		a				+++	+		?
	c		alpha	+		+	++	+++		?
	d		alpha		+		+++	+		?
11	a		a		+		++++	+		?
	b		a	+		+	+++	+++		?
	c		alpha	+		+	+++	+++		?
	d		alpha		+		++++	+		?
C	a	WT 28B	alpha		+		++++	+		+
	b	whi2	a	+		+	+	++++		-
	c	gene of I	a	+		+	+++	+++		+
	d									
		*	*	*	*	*	*	*		*

Δsrn2

Notes:

viability* - not recorded

LAA+5nMRap* - analysis discrepancies based on poor growth on 5nM concentration of rapamycin

*NT - not true tetrad

tetrad	spore	viability*	MAT	LYS2	MET15	KAN	HR	LAA	LAA+5nMRap*	OD

1	a		a				++++	+	-	1.133
	b		alpha	+	+	+	++++	+++	+	1.006
	c		alpha	+			++++	+	-	1.003
	d		a		+	+	++++	+++	+	1.140
2 *NT	a		a		+	+	+++/+	+++	+	0.977
	b		alpha	+	+	+	+	+	-	0.964
	c		alpha	+	+		++++	+	+	1.019
	d		a	+			+++/+	+	-	1.039
3*NT	a		a		+		++++	+	-	1.013
	b		alpha	+	+	+	+++	+++	+	0.993
	c		a/alpha				++++	+	-	1.019
	d		a	+		+	+++	+++	+	1.034
4*NT	a		alpha		+		++++	+	+	1.027
	b		a/alpha	+		+	+++	+++	-	1.083
	c		a/alpha	+	+		++++	+	-	1.027
	d		a				++++	+	+	1.064
5*NT	a		alpha		+		++++	+	-	1.166
	b		a	+			+++	+	-	1.043
	c		a		+	+	+++	+++	-	1.062
	d		a?/alpha	+		+	++	+++	+	0.985
6	a		a	+	+		++++	+	-	1.035
	b		alpha			+	++	+++	+	0.981
	c		alpha	+	+		++++	+	-	0.993
	d		a			+	++	+++	+	1.021
7	a		alpha		+		++++	+	-	0.990
	b		alpha			+	+++	+++	+	1.014
	c		a	+	+	+	++++	+++	+	1.000
	d		a	+			++++	+	-	1.059
8*NT	a		a/alpha		+	+	++++	+++	-	1.042
	b		a			+	+++	+++	+	1.015
	c		alpha	+	+		++++	+	-	1.026
	d		a	+			++++	++	+	1.038
9*NT	a		alpha	+	+	+	++	+	+	0.991
	b		alpha			+	+++	+++	+	0.961
	c		a	+	+		++++	+	-	1.065
	d		a/alpha	+	+	+	+++	+++	-	1.080
10*NT	a		alpha/a	+	+	+	++	+	+	1.031
	b		a/alpha				++++	+	+	1.075
	c		a	+		+	+++	+++	-	1.066
	d		alpha	+	+		++++	+	-	1.033
11	a		alpha			+	+++	+++	+	1.040
	b		a	+	+	+	++++	+++	+	1.008
	c		alpha	+	+		++++	+	-	1.027
	d		a				++++	+	-	1.082
C	a	WT 28B	alpha		+		++++	+	-	1.049

	b	whi2	a	+		+	-	++++	-	1.168
	c	gene of I	a	+		+	++	+++	+	0.984
		*	*	*	*	*	*	*	*	

Δvps28

Notes:

LAA + 5nMRap* - analysis discrepancies based on poor growth on 5nM concentration of rapamycin

*NT – not a true tetrad

tetrad	spore	viability	MAT	LYS2	MET15	KAN	HR	LAA	LAA+5nMRap*	OD
1	a	m	a		+		+++	+	-	0.948
	b	s	a	+	+	+	+++	++++	+	0.992
	c	m	alpha	+			++++	+	-	0.983
	d	s	alpha			+	+++	+++	+	0.911
2	a	s	a			+	++++	++++	+	0.923
	b	m	a	+	+	+	++++	+	-	0.972
	c	s	alpha	+		+	+++	++++	-	0.967
	d	m	alpha	+	+		++++	+	+	0.924
3	a	dot	a	-	-	-	-	-	-	0.009
	b	dot	alpha	-	-	-	-	+	+	0.126
	c	dot	n/a	-	-	-	-	-	-	0.002
	d	dot	n/a	-	-	-	-	-	+	0.000
4	a	s	alpha		+	+	+++	++++	+	0.869
	b	m	a				++++	+	-	0.915
	c	m	a	+	+		++++	+	-	0.898
	d	s	alpha	+		+	+++	++++	+	0.945
5*NT	a	m	alpha	+	+		++++	+	+	0.909
	b	L	?	+	+	+	++++	+	-	0.963
	c	m	alpha		+		++++	+	-	0.924
	d	s	a	+		+	+++	++++	+	1.115
6	a	s	alpha	+		+	+++	++++	+	0.933
	b	m	alpha	+	+		++++	+	-	0.909
	c	s	a			+	+++	++++	+	0.882
	d	m	a		+		++++		-	0.942
7*NT	a	m	n/a	+	+	+	+++	-	-	0.893
	b	s	alpha	+			+++	+	-	0.934
	c	m	a		+		++++	+	-	0.913
	d	s	a		+	+	++++	+++	+	0.965
8	a	m	a				++++	+	-	1.015
	b	s	alpha		+	+	+++	++++	+	0.914
	c	m	a	+			++++	+	-	0.936
	d	s	alpha	+	+	+	+++	++++	+	0.968
9	a	s	a	+	+	+	+++	++++	+	0.944
	b	s	a			+	+++	++++	+	0.912
	c	m	alpha				++++	-	-	0.915
	d	m	alpha	+	+		++++	-	-	0.956

10	a	s	alpha	+		+	+++	++++	+	0.964
	b	s	a	+		+	+++	++++	+	0.912
	c	m	alpha		+		++++	+	-	0.907
	d	m	a		+		++++	+	-	1.090
11*NT	a	m	n/a	+	+	+	++++	?	-	0.958
	b	s	alpha	+			++++	+	-	0.886
	c	s	alpha		+		+++	++++	+	0.904
	d	m	a		+	+	++++	+	-	1.117
C	a	WT 28B	alpha		+		+++	+	?	
	b	whi2	a	+		+	+	++++	?	
diploid	c	gene of I	both	+	+	+	-	+	?	
	d									
		*	*	*	*	*	*	*	*	

Δsnf8

Notes:

LAA + 5nMRap* - analysis discrepancies based on poor growth on 5nM concentration of rapamycin

*NT – not a true tetrad

tetrad	spore	viability	MAT	LYS2	MET15	KAN	HR	LAA	LAA+5nMRap	OD
1	a	s	alpha		+	+	+++	++++	+	0.945
	b	s	alpha	+		+	+++	++++	+	0.926
	c	m	a	+	+		++++	+	-	1.029
	d	m	a				++++	+	-	1.041
2	a	m	-	+			++++	+	-	1.011
	b	s	a		+	+	+++	++++	+	0.923
	c	m	alpha		+		++++	+	-	1.023
	d	s	a	+		+	+++	++++	+	1.013
3	a	s	a			+	+++	++++	+	0.9
	b	m	a	+	+		++++	+	-	0.926
	c	s	alpha	+		+	+++	++++	+	0.893
	d	m	alpha		+		++++	+	-	1.052
4	a	m	a (very faint)	+	+	+	++++	+	-	0.995
	b	m	alpha				++++	+	-	1.022
	c	s	a		+	+	+++	++++	+	0.943
	d	s	alpha	+			+++	+	+	1.004
5	a	s	a		+	+	+++	++++	+	0.97
	b	s	a			+	+++	++++	+	0.959
	c	m	alpha	+			++++	+	-	1.009
	d	m	alpha	+	+		++++	+	-	1.037
6	a	m	alpha	+	+		++++	+	-	0.978
	b	m	a		+		++++	+	-	0.976
	c	s	alpha			+	+++	++++	+	1
	d	s	alpha	+		+	+++	++++	+	0.987
7	a	m	alpha				++++	+	-	0.933
	b	m	alpha	+	+		++++	+	-	1

	c	s	a			+	+++	++++	+	0.95
	d	s	a	+	+	+	+++	++++	+	1.126
8	a	m	a	+	+	+	+++	++++	+	1.042
	b	m	alpha				++++	+	-	0.998
	c	m	a	+			++++	+	-	1.061
	d	s	alpha		+	+	+++	++++	+	1.045
9	a	m	alpha	+	+		++++	+	-	1.042
	b	s	alpha		+	+	+++	++++	+	0.983
	c	s	a	+		+	+++	++++	+	1.047
	d	m	a				++++	+	-	1.061
10	a	m	alpha		+		++++	+	-	1.006
	b	s	a	+		+	+++	++++	+	1.001
	c	s	alpha		+	+	+++	++++	+	1.019
	d	m	a	+			++++	+	-	1.099
11	a	m	a	+	+		++++	+	-	1.048
	b	m	a		+		++++	+	-	1.015
	c	s	alpha	+		+	+++	++++	+	1.043
	d	s	alpha			+	+++	++++	+	1.067
C	a	WT a	a	+			++++	+	?	1.009
	b	whi2	a	+		+	+++	++++	?	1.031
	c	snf8	a	+	+	+	+++	+	?	0.969
		*	*	*	*	*	*	*	*	

Δsnf7

Notes:

LAA + 5nMRap* - analysis discrepancies based on poor growth on 5nM concentration of rapamycin

*NT – not a true tetrad

tetrad	spore	viability	MAT	LYS2	MET15	KAN	HR	LAA	LAA+5nMRap*	OD
1	a	m	alpha	+	+		++++	+	-	0.889
	b	L	a		+		++++	+	-	0.881
	c	s	a	+		+	+++	+++	+	0.882
	d	s	alpha			+	+++	+++	+	0.816
2	a	s	alpha	+		+	+++	+++	+	0.937
	b	m	a	+	+		++++	+	-	0.989
	c	s	alpha		+	+	+++	+++	+	0.945
	d	m	a				++++	+	-	0.992
3	a	m	a				++++	+	-	1.030
	b	s	alpha	+		+	+++	++++	+	1.100
	c	m	a	+	+		++++	+	-	1.267
	d	s	alpha		+	+	+++	++++	+	0.943
4	a	m	alpha	+			++++	+	-	1.156
	b	s	a			+	+++	++++	+	0.948
	c	s	a	+	+	+	+++	++++	+	1.051
	d	m	alpha		+		++++	+	-	0.932

5	a	m	a	+			++++	+	-	1.034
	b	m	alpha	+			++++	+	-	0.950
	c	m	-	+	+	+	+++	+	-	1.002
	d	s	alpha		+	+	+++	++++	+	0.940
6	a	s	a			+	+++	++++	+	1.007
	b	m	a		+		++++	+	-	0.975
	c	s	alpha	+		+	+++	++++	+	0.963
	d	m	alpha	+	+		++++	+	-	1.077
7	a	L	-	+	+	+	++++	+	-	0.860
	b	s	alpha			+	+++	++++	+	1.022
	c	L	a		+		++++	+	-	0.954
	d	s	a	+	+	+	+++	++++	+	1.056
8	a	s	alpha		+	+	+++	++++	+	1.081
	b	m	a	+			++++	+	-	1.012
	c	s	alpha		+	+	+++	++++	+	0.977
	d	m	a	+			++++	+	-	1.164
9	a	s	a			+	+++	++++	+	1.023
	b	s	a	+	+	+	+++	++++	+	1.102
	c	m	alpha	+	+		++++	+	-	1.211
	d	m	alpha				++++	+	-	1.160
C	a	WT a	a	+			++++	+	-	1.036
	b	whi2	a	+		+	+++	++++	-	0.993
	c	gene of I	n/a	+	+	+	++	+	-	0.952
									-	0.000
C	b	WT 28B	alpha		+		++++	+	-	1.166
	a	whi2	a	+		+	+++	++++	-	0.949
		*	*	*	*	*	*	*	*	

Δdid4

Notes:

LAA + 5nMRap* - analysis discrepancies based on poor growth on 5nM concentration of rapamycin

*NT – not a true tetrad

did4 analysis

tetrad		viability	MAT	LYS2	MET15	KAN	HR	LAA	LAA+2.5nMRap	OD
1*NT	a	m	alpha	+	+	+	+++	+	-	0.737
	b	s	a	+			++++	+	-	0.800
	c	s	alpha	+		+	+++	++++	+	0.885
	d	m	a		+		++++	+	-	0.824
2	a	m	a	+			++++	+	-	0.816
	b	xs	alpha	+	+	+	+++	++++	+	1.037
	c	s	a			+	+++	++++	+	0.935
	d	m	alpha		+		++++	+	-	0.862
3*NT	a	m	a	+	+	+	+++	+	-	0.825

	b	s	alpha	+		+	+++	++++	+	0.922
	c	m	a	+	+	+	+++	++++	+	0.907
	d	m	alpha		+		++++	+	-	0.819
4*NT	a	s	alpha			+	+++	++++	+	0.896
	b	m	alpha	+	+	+	++++	+	-	0.877
	c	s	a	+	+	+	+++	++++	+	0.927
	d	m	a	+			++++	+	-	0.832
5	a	m	a	+			++++	+	-	1.071
	b	xs	alpha		+	+	+++	++++	+	1.080
	c	m	a				+++	++++	+	1.095
	d	s	alpha	+	+	+	++++	+	-	0.841
6	a	m	alpha				++++	+	-	0.807
	b	xs	alpha	+		+	+++	++++	+	0.874
	c	m	a		+		++++	+	-	0.846
	d	s	a	+	+	+	+++	++++	+	1.082
7	a	s	a		+		++++	+	-	0.955
	b	xs	alpha			+	+++	++++	+	0.881
	c	m	a	+	+		++++	+	-	0.810
	d	s	alpha	+		+	+++	++++	+	1.072
8	a	m	a				++++	+	-	0.903
	b	xs	alpha			+	+++	++++	+	0.863
	c	xs	alpha	+	+	+	+++	++++	+	0.941
	d	m	a	+	+		++++	+	-	0.977
C1	a	WT a	a	+			++++	+	-	0.794
	b	whi2	a	+		+	++	++++	-	0.899
	c	did4 (diploid)	a/alpha	+	+	+	+++	+	-	0.936
C2	a	WT a	alpha		+		++++	+	-	0.854
	b	whi2	a	+		+	+++	++++	-	1.113
		*	*	*	*	*	*	*	*	

Δvps4 analysis

Notes:

LAA + 5nMRap* - analysis discrepancies based on poor growth on 5nM concentration of rapamycin

*NT – not a true tetrad

tetrad	spore	viability	MAT	LYS2	MET15	KAN	HR	LAA	LAA+2.5nMRap	OD
1	a	m	a		+		++++	+	+	0.705
	b	m	alpha			+	+++	++++	++++	0.708
	c	m	alpha	+		+	+++	++++	++++	0.690
	d	m	a	+	+		++++	+	+	0.672
2	a	m	alpha				++++	++	+	0.707
	b	m	alpha		+	+	+++	++++	++++	0.695
	c	m	a	+			++++	+	+	0.715
	d	m	a	+	+	+	+++	++++	++++	0.761
3	a	m	alpha	+			++++	+	+	0.745
	b	m	a				++++	+	+	0.734
	c	m	alpha	+	+	+	+++	++++	++++	0.724
	d	m	a		+	+	+++	++++	++++	0.757
							1:50 dilution			
4	a	m	a		+	+	+++	++++	++++	0.745
	b	m	alpha	+	+	+	++	++++	++++	0.729
	c	m	alpha				++	+	+	0.714
	d	m	a	+			+++	+	+	0.737
5	a	m	a	+			++++	+	+	0.775
	b	s	alpha		+	+	+++	++++	++++	0.688
	c	m	alpha	+			++++	+	+	0.718
	d	m	a		+	+	+++	++++	++++	0.694
6	a	m	a	+			++++	+	+	0.731
	b	m	alpha			+	+++	++++	++++	0.700
	c	m	a		+	+	+++	++++	++++	0.698
	d	m	alpha	+	+		++++	+	+	0.772
7*NT	a	m	a/alpha	+	+	+	++	+	-	0.621
	b	m	alpha	+	+	+	++++	++++	++++	0.614
	c	m	a	+		+	++++	++++	++++	0.638
	d	m	alpha				++++	+	+	0.691
8	a	m	alpha	+		+	++	++++	++++	0.701
	b	m	a	+	+		++++	+	+	0.713
	c	m	alpha		+		++++	+	+	0.700
	d	m	a			+	++++	++++	++++	0.730
9	a	m	a			+	++++	++++	++++	0.766
	b	m	alpha	+			+++	+	+	0.751
	c	m	alpha		+	+	+++	++++	++++	0.731
	d	m	a	+	+		++++	+	+	0.746
							1:50 dilution			
10	a	m	a	+	+	+	+++	++++	++++	0.728
	b	m	a			+	+++	++++	++++	0.731
	c	m	alpha	+			++++	+	+	0.734
	d	m	alpha		+		++++	+	+	0.706
11*NT	a	m	a	+		+	+++	++++	++++	0.771
	b	m	alpha		+		++++	+	+	0.737

	c	-	n/a				-	-	-	- 0.004
	d	m	a		+		++++	+	++	0.800
C	a	WT	alpha		+		++++	+	+	0.830
	b	whi2	a	+		+	+	++++	+	0.747
	c	vps4	a	+		+	+++	++++	+++	0.618
		*	*	*	*	*	*	*	*	

Appendix iii: Tetrad Plate Images

Vps27

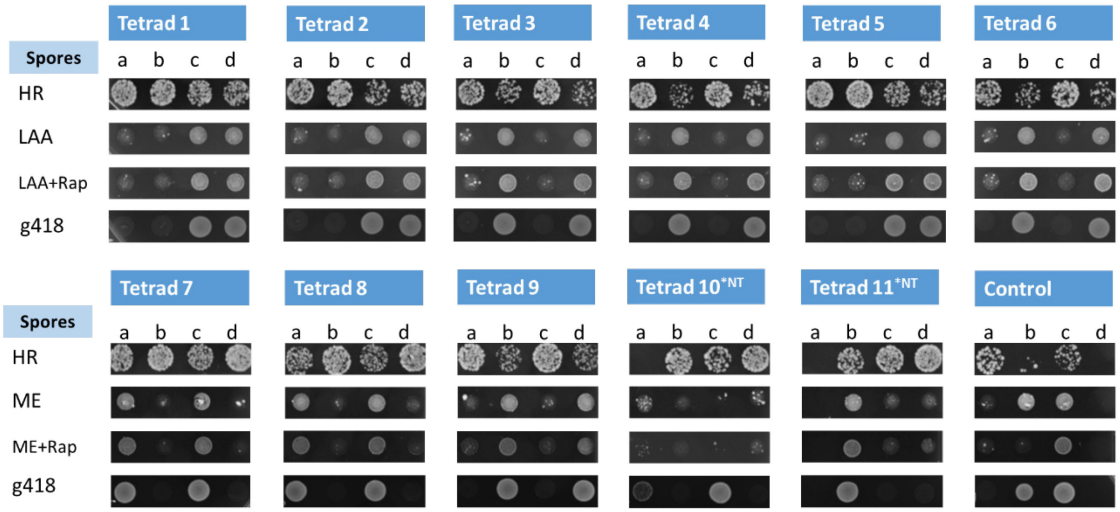

Vps28

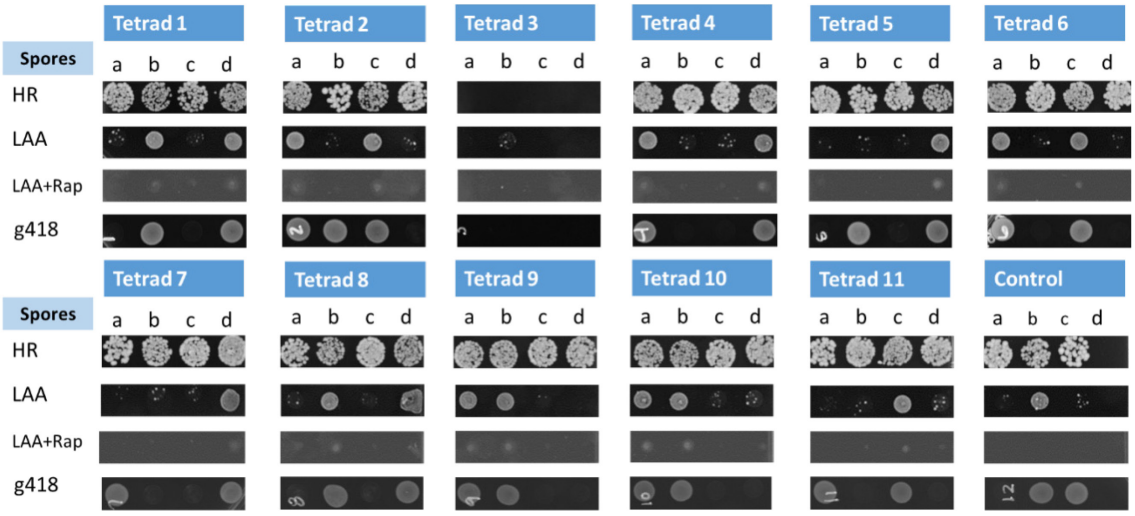

Snf8

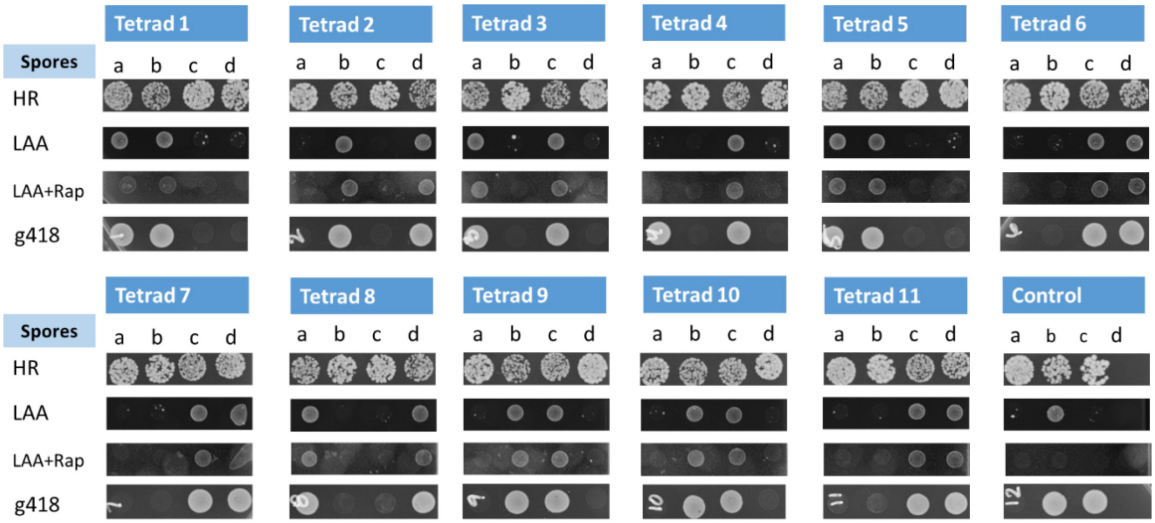
Tetrad 1
Tetrad 2
Tetrad 3
Tetrad 4
Tetrad 5
Tetrad 6
Spores
a b c d
HR
LAA
LAA+Rap
g418
Tetrad 7
Tetrad 8
Tetrad 9
Tetrad 10
Tetrad 11
Control

Snf7

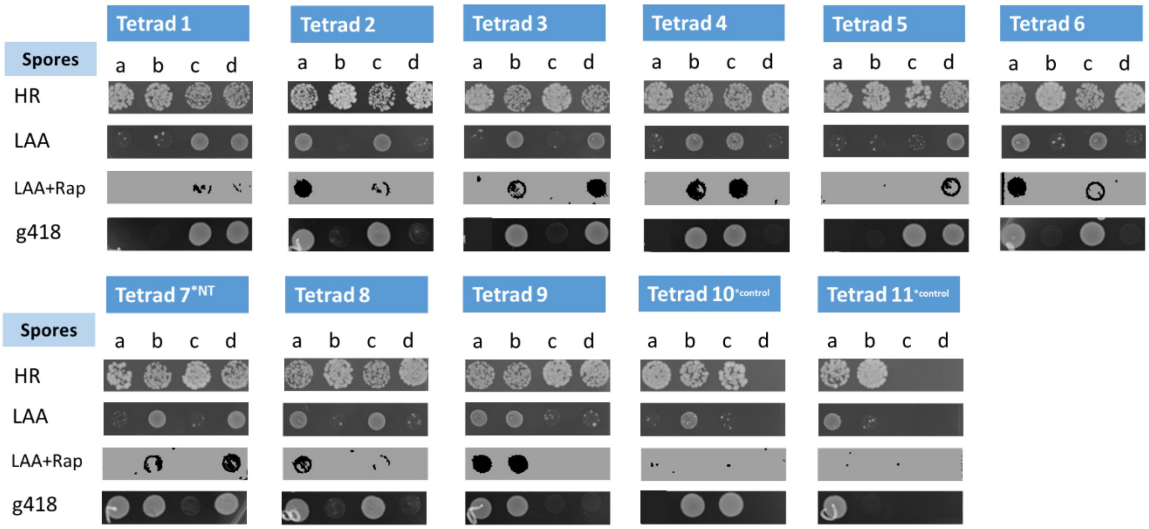
Tetrad 1
Tetrad 2
Tetrad 3
Tetrad 4
Tetrad 5
Tetrad 6
Spores
a b c d
HR
LAA
LAA+Rap
g418
Tetrad 7*NT
Tetrad 8
Tetrad 9
Tetrad 10*control
Tetrad 11*control

Did4

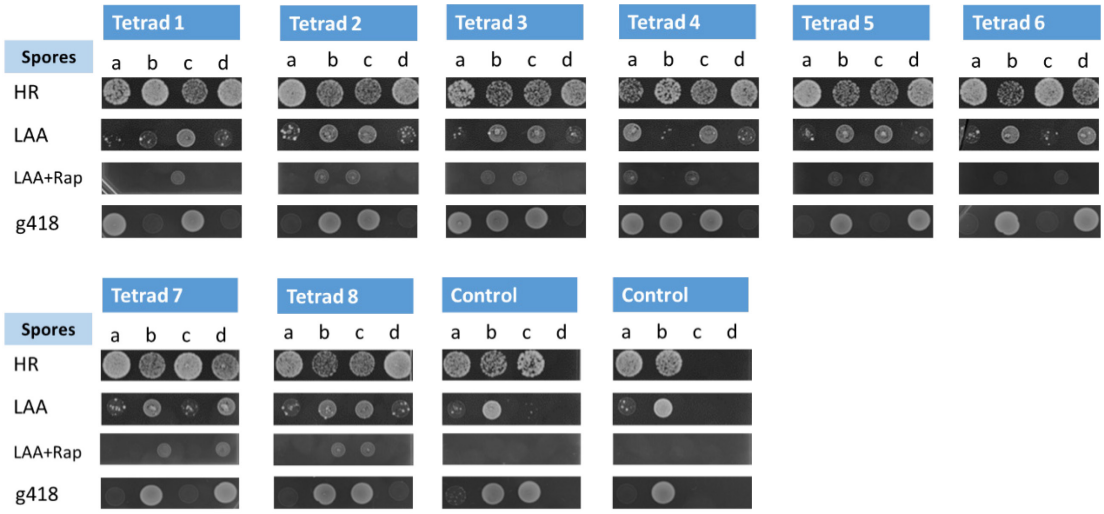
Tetrad 1
Tetrad 2
Tetrad 3
Tetrad 4
Tetrad 5
Tetrad 6
Spores
a b c d
HR
LAA
LAA+Rap
g418
Tetrad 7
Tetrad 8
Control
Control

Vps4

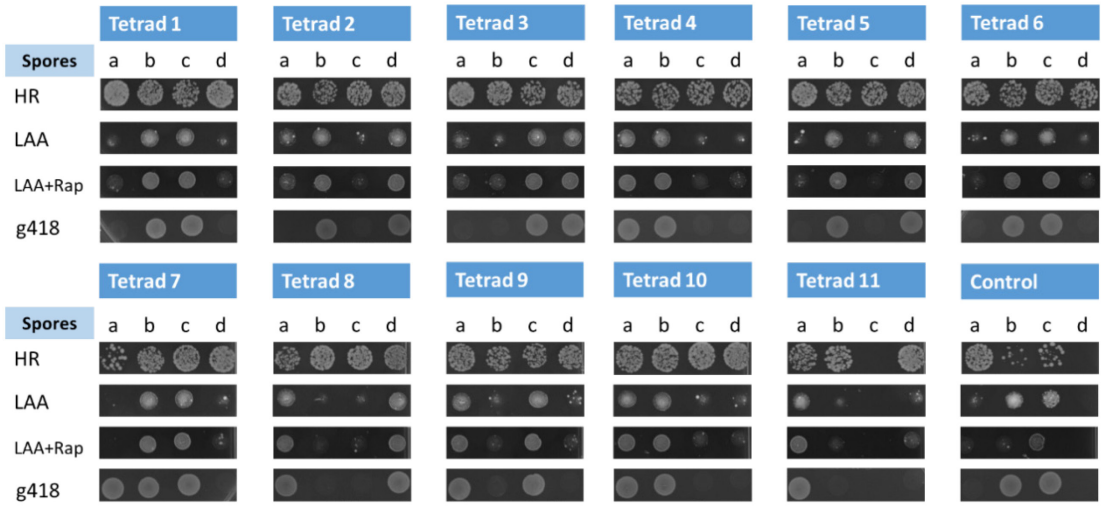
Tetrad 1
Tetrad 2
Tetrad 3
Tetrad 4
Tetrad 5
Tetrad 6
Spores
a b c d
HR
LAA
LAA+Rap
g418
Tetrad 7
Tetrad 8
Tetrad 9
Tetrad 10
Tetrad 11
Control

Cierra Sing

July 14, 1987 - Santa Clara, CA
c.sing1418@gmail.com • (408) 368-9539

EDUCATION

Master of Science in Molecular Microbiology & Immunology
Expected May 2014
Johns Hopkins Bloomberg School of Public Health, Baltimore, MD
Thesis: *Understanding the relationship between autophagy and nutrients in an ESCRT protein complex perspective in Saccharomyces cerevisiae*

Bachelor of Arts in Biochemistry & Molecular Cell Biology
May 2009
Mills College, Oakland, CA
Thesis: *Control of Cell Division by the Metabolic Cycle in Saccharomyces cerevisiae*

RESEARCH EXPERIENCE

ScM Graduate Student Researcher, Molecular Microbiology and Immunology Dept., Johns Hopkins School of Public Health, Baltimore, MD
November 2012 - Current

- Conducting thesis research in *Saccharomyces cerevisiae* investigating the ESCRT's complex role in relation to nutrient sensing and autophagy processes
- Thesis project design extrapolated from current literature research knowledge and the unknown factors of ESCRT's role in autophagy and nutrient sensing
- Perform a genetic technique, tetrad dissections, on ESCRT protein complex verifying mutant deletion gives rise to the overgrowth phenotype in low amino acid conditions
- Transformed Atg 8 tagged with GFP plasmid into ESCRT mutants to observe its interaction with autophagy process
- Perform western blotting to determine the protein expression during autophagy process and nutrient starvation by measuring TOR activity
- Optimizing Autophagy assay to: reduce incubation time, increase efficiency, maintain yeast in growth log phase
- Laboratory maintenance routinely conducted composes of: media, butter solutions, and western gel preparation
- Participate in weekly: lab meetings, journal clubs, and PI meetings

Research Assistant, International Health Dept., Johns Hopkins School of Public Health, Baltimore, MD
September 2013 - Current

- Participate in MAL-ED nutrient research project, a multi-country study, funded by the Gate's foundation
- Help MAL-ED project to assess and track nutritional deficiencies of neonatal/childhood development to understand nutritional impact upon childhood diseases
- Run ELISAs to detect Transferrin Receptors for iron levels in serum samples collected in MAL-ED project
- Prepare assay reagents and conduct lab maintenance tasks
- Assessing quality of data output and compile data
- Daily report of data samples to project manager

Research Associate I, MedImmune, Mountain View, CA
March 2011 – Dec 2011

- Conducted routine daily lab maintenance, which consisted of: changing charts, temperature recording, cleaning equipment, and reviewing equipment excursions
- Operated daily testing service in a team oriented work environment
- Effectively executed Fluorescent Focus Assay and cell-based assays for live attenuated viruses of Influenza & Respiratory Syncytial Virus (RSV)
- Managed all of RSV development samples & development stability projects tested by ELISA assays
- Communicated test results to appropriate departments before assay deadline
- Efficiently orchestrated and assembled assay reagents & media to optimize assay time
- Completed each assay with fine detail to testing operation, analyzing results, and documented to GMP standards
- Consistently used automated fluorescent microscopy plate reader and fluorescent microscopes to generate potency titers

Barrett Research Scholar, Mills College, CA
Jan 2009 – Aug 2009

- Developed and executed a collaborated research project based on classifying the protein characteristics of YPR015C in *Saccharomyces cerevisiae*
- Designed two-part primers of YPR015C in *S. cerevisiae* to generate a knockout strain via PCR homologous recombination to study its effect on cell cycle progression under various stress conditions
- Generated a GFP tagged knockout strain via PCR homologous recombination for the purpose of isolating cellular locations of YPR015C

REU–Microbiology Intern, University of Wisconsin at Madison
May 2008 – Aug 2008

- Conducted independent research in laboratory of Dr. Diana Downs, studying metabolic integration by substituting an equivalent enzyme used in B1 synthesis pathway from *Bacillus subtilis* to *Salmonella enterica*
- Isolated B1 auxotroph mutants from transduction mutant hunt to acquire knowledge of components needed to support B1 synthesis in the substituted strain
- Synthesized construct with a promoter mutation to increase expression to restore growth of the B1 auxotroph strain in anaerobic conditions
- Sequestered Valine and Leucine as amino acids to restore growth in both respiring and fermenting anaerobic conditions
- Presented research findings in symposium to the REU-Microbiology program and departments

WORK EXPERIENCE

Principles of Bacterial Infection Teaching Assistant, JHSPH, MD
March 2013 – May 2013

- Maintained communication between professor and students
- Organized and maintained incoming lectures from guest speakers on student's electronic data base

- Responsible for copying documents and distribution to students
- Compiled recommended book list for the class
- Accompanied each class to upload guest speaker presentation and observe materials taught during class sessions

PUBLICATIONS

X. Teng, M. Dayhoff-Brannigan, W. Cheng, C. Gilbert, **C. Sing,** N.L. Diny, M.J. Dunham, S.J. Wheelan, J.D. Boeke, F.J. Pineda, and J.M. Hardwick. "Genome-wide consequences of deleting any single gene." *Molecular Cell.* 21 November 2013.

CERTIFICATES

Good Clinical Practice Certificate, JHSPH, MD May 2013
Vaccine Certificate, JHSPH, MD Expected May 2014